WATER-ROCK INTERACTIONS AND DEVELOPMENT OF HYDROGEOCHEMICAL FACIES IN HARD-ROCK ASSOCIATED AQUIFER SYSTEM, SOUTHERN INDIA: STABLE ISOTOPES, GEOCHEMICAL, HYDRAULIC CONSTRAINTS

Thesis submitted to

THE UNIVERSITY OF CALICUT

For the award of the Degree of

DOCTOR OF PHILOSOPHY

in

GEOLOGY

By

C. AJITH KUMAR

Under the Supervision of

Dr. V.A. AYISHA

Department of PG Studies and Research in Geology
MES Ponnani College, Ponnani

(UNIVERSITY OF CALICUT)

August 2017

DEPARTMENT OF P.G. STUDIES AND RESEARCH IN GEOLOGY
M.E.S. PONNANI COLLEGE, PONNANI
(NAAC Accredited and Affiliated to the University of Calicut)

Ponnani South–PO · Malappuram–District · Kerala 697586 · INDIA
Phone: +91 494 266 6077 · Fax: +91 494 266 9788 · E-mail: geology.mes@gmail.com
Website: www.mesponnanicollege.com

Dr. V.A. Ayisha
Associate Professor& Head

March 31, 2018

CERTIFICATE

This is to certify that the thesis entitled "Water-rock interactions and development of hydrogeochemical facies in hard-rock associated aquifer system, southern India: stable isotopes, geochemical, hydraulic constraints" submitted by Mr. C. Ajith Kumar to the University of Calicut, for the award of the degree of Doctor of Philosophy is a bonafide record of the research work carried out by him under my supervision and guidance. the content of the thesis, in full or parts have not been submitted to any other institute or university for the award of any degree or diploma.
The corrections / suggestions from the adjudicators have been incorporated

Dr. V.A. Ayisha

"Haritha", Edapal–PO, Malappuram District, Kerala–679576
Tel: +91 494 2680570 Mob: +91 944 6154720 E-mail: ayishaabdulla@gmail.com

Ponnani
August 22, 2017

DECLARATION

I hereby declare that the work in this thesis entitled **"Water-rock interactions and development of hydrogeochemical facies in hard-rock associated aquifer system, southern India: stable isotopes, geochemical, hydraulic constraints"** is based on the original work done by me under the supervision of Dr. V.A Ayisha, Associate Professor and Head, Department of PG Studies and Research in Geology, MES Ponani College, Ponani, Kerala, India. The subject matter presented in the thesis has not previously been formed the basis of award of any degree, diploma, associateship, fellowship or any other similar title except where the due acknowledgement has been made in the text.

C. Ajith Kumar

Acknowledgements

First and foremost I would like to thank my supervisor **Dr. V.A. Ayisha,** Associate professor and Head, Dept. of PG Studies and Research in Geology, MES Ponani College, Ponani, University of Calicut. It has been an honour to be her first Ph.D. student. I acknowledge all her contributions to make my PhD experience productive and stimulating.

This work was possible only because of the unconditional support provided by my friend and senior **Dr. Sajeev Krishnan**, Associate Professor, Centre for Earth Sciences, Indian Institute of Science (IISc), Bangalore. A person with an amicable and positive disposition, he has always made himself available to clarify my doubts despite his busy schedules and I consider it as a great opportunity to do my doctoral programme under his expertise. My thanks are due to him and also for the facilities and services rendered to me by his department. Without his efforts my job would have undoubtedly been very difficult.

I wish to express my sincere and heartfelt gratitude to **Dr. K. Gopalakrishna**, Former HoD, Dept.of PG Studies and Research in Geology, MES Ponani College, Ponani, University of Calicut for his unstinting moral support and encouragement during my work.

It is with great pleasure and immense gratitude that I wish to acknowledge **Prof. Jean Riotte**, Indo-French cell, IISc Bangalore who gave access to the laboratory and research facilities for water chemistry analysis.

I am grateful to **Dr. M Satish–Kumar**, Professor in Geology, Niigata University Japan for providing me with Walayar marble samples and isotope data which was very helpful in the last phase of my work.

I am very grateful to **Dr. Prosenjith Ghosh**, Associate Professor, Centre for Earth Sciences, Indian Institute of Science (IISc), who graciously allowed me to utilise the isotope analysis facilities in his lab and for his support on isotope analysis and data processing.

I would like to thank **Dr. Ramananda Chakrabarti**, Assistant Professor, Centre for Earth Sciences, Indian Institute of Science (IISc), for providing me the facilities to do REE analysis of water samples in his laboratory.

I am also indebted to **Dr Iswar-Kumar, C**, Post-Doctoral Fellow IISc Bangalore (currently at IIT Kanpur), who deserves the credit for creating GIS maps for my thesis.

I am immensely grateful to **Dr. George Paul Mathews** (NW University, Xian, China) and **Dr. Vinod Ommen Samuel** (Yonsei University, South Korea) for their insightful comments and encouragement and also for the difficult questions which incented me to widen my research from various perspectives.

My sincere gratitude to **Ms Durgalakshmi** (ANU, Australia) for providing a friendly and co-operative atmosphere at work and also for her useful feed backs and insightful comments on my work.

I must also acknowledge **Mr. Prakash Arya** for the suggestions and his help regarding WQI preparation.

My thanks are due to **Mr. Shreyas** for the help extended during thin section preparation.

A special thanks to my brother **Dr. C Sreejith**, Assistant Professor, MES Ponani College for his ideas and concepts which had a remarkable influence on my entire work in the field.

I also thank **Dr. V.K. Brijesh**, Assistant Professor, MES Ponani College, for inspirational discussions regarding my work.

I am very much thankful to **Mr. Abdul Nafih, P.K,** Assistant Professor MES Ponani College and **Mr. Shabeer Ahammed** for helping me to collect rock and water samples from the field. I enjoyed their company during the field work.

I sincerely admire the contribution of all **petrology team members** of CEaS, IISc, Bangalore **Mr. Jaseem, Mr. Thamam Mubarish, Mr. Kiran, Mr. Rajkumar, Mr. Sreehari Lakshman, Mr. Vinod P.G., Mrs. Athira P.G., Mrs. Thanooja and Ms. Veni Sudarsan** for extending their unstinted support, timely motivation and unfailing help during the course of entire work.

My heartfelt thanks to District Hydro Geologist, State ground water department, Palakkad for permitting the use of data collected by the department and for suggestions in the present work.

I express my sincere gratitude to **Team CES** for the help during the conveyances of rock and water samples.

This work would not have been accomplished without the timely help rendered by my wife **Radhika** and the support of my kids, **Aadarsh and Avanish.**

I would also like to thank my ***parents and siblings*** who were always supporting me and encouraging me with their best wishes.

C. AJITH KUMAR

Contents

Chapter	Title	Page
	Acknowledgements	
	List of Tables	
	List of Figures	
	Abstract	
1.	**Introduction**	**1-4**
	Objectives	3
	Outline and organisation of the Thesis	4-5
2.	**Literature Review**	**5-12**
3.	**Methodology**	**13-28**
	Thin-Section Making	14-15
	Petrological Microscope	15-16
	EPMA Analysis	17-18
	XRF Analysis	18-21
	Map making	21-24
	Water Sample collection	24-28
4.	**Geological Setting**	**29-38**
	Southern Granulite Terrain	30-33
	Geology of the study area	33-38
5.	**Petrology and Geochemistry**	**39-55**
	Petrography	40-48
	Geochemistry	48-51
	Mineral Chemistry	51-54
6.	**Hydrogeochemistry**	**56-77**
	Thematic maps and Interpretation	57=59
	pH	59
	Electrical conductivity (EC)	59-60
	Calcium	60
	Magnesium	61
	Sodium	61
	Potassium	62
	Silica	62-63
	Chloride	63
	Nitrate	63
	Sulphate	63
	Fluoride	63
	Carbonates and bicarbonates	64
	Alkalinity	64

	Salinity	65
	Total dissolved solids (TDS)	65-66
	Piper-Hill Diagram	66-67
	Pie charts	67-68
	Water quality of the area	68-69
	WQI determination	69-73
	Oxygen Isotopic Analysis	74-76
	Rare Earth Elements (REE) in ground water analyses	76-77
7.	**Discussion and Conclusions**	**78-85**
	Hydrogeochemical facies and Geochemical equilibria	83-84
	Conclusions	84-85
	References	**86-94**
	Appendix 1	95-109
	Appendix 2	110-123
	Appendix 3	124-125

List of Tables

Table No.	Caption	Page
4.1.	Rock sampling location and rock types	34
5.1.	Petrological summary of all the samples from the study area	41
5.2.	Major and trace element data for all the samples collected from the study area	55
6.1.	Chemical analysis for the collected water samples	58
6.2.	Oxygen isotope data for seasonal water samples	76
6.3.	REE chemistry data for water samples	77

List of Figures

Fig. No.	Caption	Page No.
1.1.	Flowchart showing various steps in this study	4
3.1.	Petrological microscope at CEaS, IISc	16
3.2.	Schematic diagram of EPMA with JEOL JXA-8230 EPMA housed at AFMM, IISc	18
3.3.	Steps for XRF sample preparation	19
3.4	Steps for XRF sample preparation	20
3.5	XRF machine at Niigata University, Japan and sample channel of XRF	21
3.6	ASTER DEM overlapped with the digitized structural lineaments of the study area	22
3.7	Drainage map of the study area	23
3.8	Water sample collection in the field	24
4.1	Tectonic framework of southern India with major shear zones	31
4.2	Geological map of the study area with water and rock sample locations	33
4.3	Field exposures for foliated and massive charnockite and hornblende-biotite gneiss and biotite gneiss from the study area	36
4.4	Structural lineament map of study area overlapped with ASTER DEM with sample locations.	37
4.5	Geological cross-section drawn across A-B along the eastern side of the study area.	38
5.1	Photomicrograph of charnockite (A) and hornblende-biotite gneiss (B) from the study area	40
5.2	Representative photomicrographs of samples AJ-1 and 3.	42
5.3	Representative photomicrographs of samples AJ-4 and 5.	43
5.4	Representative photomicrographs of samples AJ-9A,B, 10 and 11A, B.	45
5.5	Representative photomicrographs of samples AJ-13A, B, 14, and 16A.	47
5.6	Harker variation diagrams for the major elements of charnockite and gneiss samples	49
5.7	Spider diagram showing Trace and Rare Earth Element (REE) chemistry analyses normalized to Upper Continental Crust values.	50

5.8	Geochemical plots using the charnockite and gneissic samples from the study area	5153
5.9	Amphibole chemistry for all the studied thin-sections	53
5.10	Feldspar chemistry for all the studied thin-sections	59
6.1	pH variation map for the study area	59
6.2	Calcium variation map for the study area	60
6.3	Magnesium variation map for the study area	61
6.4	Sodium variation map for the study area	61
6.5	Potassium variation map for the study area	62
6.6	Silica variation map for the study area	63
6.7	Alkalinity variation map for the study area	64
6.8	Salinity variation map for the study area	65
6.9	Piper plot for 66 groundwater samples from the study area	67
6.10	Cation and anion composition plotted on geological map of the study area	68
6.11	WQI diagram for all the water samples	72
6.12	Gibbs (A, B) and Wilcox (C) plot for the water samples studied.	73
6.13	Oxygen isotope data for the seasonal water samples	75
6.14	Relation between ΣREE and pH of analysed water samples	76
7.1	Comparison of Salinity and alkalinity of water samples from the study area	80
7.2	Comparison for silica and alkali content in local rock and the water samples	81
7.3	Cross section of the study area with comparison to salinity and oxygen isotope results	82
7.4	A comparison of water REE normalized to local rock REE	83
7.5	Distribution of different water type in the study area	84

List of Publications

C. AjithKumar, V.A. Ayisha, V.O. Samuel, P.M. George, V. Jaseem, K. Sajeev (2015) Geology of Palakkad Shear System Tectonic Implications. Extended Abstract Published in Kerala Science Congress 2015 held at University of Calicut.

C. AjithKumar, V.A. Ayisha, S. Veni, K. Sajeev (2017) Metamorphic and tectonic evolution of Palakkad region within Palakkad Shear system. UGC seminar Kerala University.

C. Ajith Kumar, A. Prakash, V.A. Ayisha, K. Sajeev Metamorphism of high grade rocks from Palakkad gap: Inferences Archean-Neoproterozoic terrane boundary. Geological Journal (accepted)

C. Ajith Kumar, A. Prakash, V.A. Ayisha, K. Sajeev Degradation of water quality from East to West of Palakkad district, Kerela. Science of the Total Environment (under review)

Chapter 1

Introduction

This chapter introduces the research problem with its importance. The chapter also lists out the major objectives of this thesis with outline and organization of the thesis.

Chapter 1
Introduction

Chemistry of groundwater is an important factor in determining its use for domestic, irrigational and industrial purposes. It is well understood that the groundwater chemically evolves by its interaction with minerals and other chemical components within the aquifer and host rock or by the intermixing among the different groundwater reservoirs along flow path in the subsurface. The geochemical processes are responsible for seasonal and spatial variations in groundwater quality. Hence it is significantly important to study hydro-geochemical characteristics of aquifer from different seasons. It is also important to look at the possible sources, especially the geology of the surrounding area, which could influence the groundwater chemistry.

The geochemical processes occurring within the groundwater system, dissolved minerals have a profound effect on water chemistry. Thus, the hydro-geochemistry of an aquifer system can provide information on the reactions and/or interactions taking place with the hard rock system. Such approaches in research are not very common from southern India. However, recently many attempts towards this direction to simulate the shallow groundwater aquifer using hydrogeochemical models were carried out (e.g., Subramani and Elango, 2010).

Water quality is a term used to describe the physical, chemical and the biological characteristics of water. The chemical composition of the groundwater can influence chemical composition of the rocks through which its flows, depending upon the mineral dissolution, mineral solubility, ion exchange, oxidation reduction and so on.

In the present study an attempt has been made to understand the chemical behaviour of groundwater by understanding the geochemistry and mineralogy of the

surrounding area through which the groundwater resides and flows by different means (Fig. 1.1A).

Rock-water interaction study can reveal the ionic exchanges between minerals and groundwater; thereby we can understand the geochemical facies developed in a particular area. It can be achieved by thoroughly knowing the rock as well as groundwater chemistry.

Detailed investigation and analyses were carried out to understand the rocks chemistry and its effects on quality of the water from the area under study (Palakkad, Kerala, southern India) (Fig. 1.1B). Aquifer associated with different rock types was selected, which differ in chemistry as we can delineate the influence clearly. The major objectives of the present study are:

- ***To understand the quality of groundwater in terms of geochemical and isotopic compositions.***
- ***Systematically analyse and document the water–rock ionic exchange reactions***
- ***To characterise the hydro geochemical facies in different rock units.***

Outline and organisation of the Thesis

The thesis presents Hydrogeochemical, Petrological, and isotopic data and proposes a new hydro geochemical facies in different rock units of Palakkad district, Kerala. Including the chapter 1 Introduction, a total number of seven chapters are presented in this thesis. Each chapter focuses on separate aspects to look into the main problem of Water–rock interaction.

Chapter 2 presents a detailed review on previous works on this field, titled as review of literature. This chapter deals the major available publication regarding the water rock interaction with special reference to southern India.

Chapter 3 summarize various analytical methods utilized in this study.

Chapter 4 presents the general geological setting of southern India. The chapter documents the general geological features of Palakkad Cauvery Shear Zone (PCSZ).

Chapter 5 tries to describe the petrology, mineral chemistry and whole rock chemistry of the collected rock samples.

Chapter 6 attempts to give the clear idea about the chemistry of water samples.

The final chapter 7 summarises and discuss the results before concluding the finds.

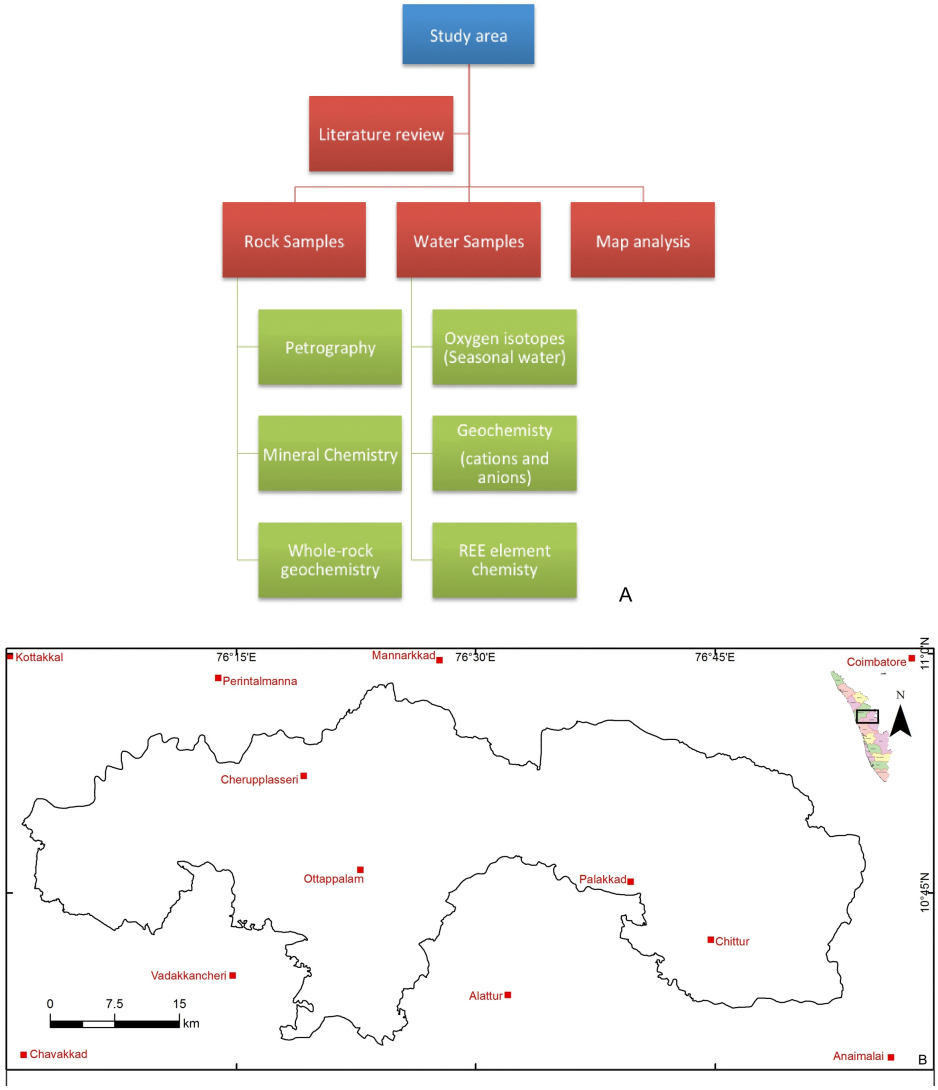

***Fig. 1.1**: A) Flowchart showing various steps in this study. B) Study area around Palakkad region, Kerala, southern India*

Chapter 2

Literature Review

Previous studies and related research results which helps to formulate the present objectives and research plan is summarised in this chapter.

Chapter 2
Literature Review

Groundwater is the most accessible and exploited freshwater resource available on the Earth. Therefore, groundwater quality has been a subject of great interest in the past few decades. The quality of groundwater and the variation in its chemistry is controlled by various factors which are both natural or geological and anthropogenic. It is quintessential to study the geological processes and setting that control the chemical parameters of groundwater in order to comprehend the factors influencing groundwater quality. Rock-water interaction allows diffusion of ions into the groundwater system and thus is a major aspect of hydro geochemistry. Though there are several hydro geochemical studies done around the globe, the documentation of the same in southern India is limited. Palakkad, in Kerala, southern India is a terrain facing immense stress on groundwater resource mainly due to issues related to groundwater quality. Hence it is very important to study and understand the different hydro geochemical characteristics of aquifers in different geological setting in this area to evaluate the groundwater chemistry and delineate various hydro geochemical processes that are involved in the evolution of groundwater quality by adopting various graphical methods and interpreting different indices attempted by many workers in the recent past.

The geochemical properties of groundwater depend on the chemistry of water in the recharge area as well as on different geochemical processes that are taking place in the subsurface. The quality of water along the course of its underground movement is therefore dependent on the chemical and physical properties of surrounding rocks, the quantitative and qualitative properties of the flowing water bodies, and the products of human activity (Matthess, 1982). The previous studies explain the influences of geology, hydrogeology, climate and human activities on groundwater chemical composition. Hence it has become imperative to evaluate their effects on groundwater quality. A detailed rock water interaction studies has not

been attempted before in the present study area. Hence it is difficult to follow some literature.

The Palakkad district lies in the northern side of the state, India, where groundwater is one of the major sources of fresh water. The region has a low elevation and is bounded by the mountains in the northern and southern side; these mountains are a part of Western Ghats. The low elevation is known as the "Palakkad Gap", which is a mountainous low pass in the Western Ghats from Palakkad, to Coimbatore, Tamil Nadu. The region is one of the most populated regions of having a population density of 627 according to the district census handbook Palakkad, (Census of India, 2011). The main factors contributing to the pollution of groundwater is increasing anthropogenic waste in the cities, runoff from rural regions, dumping areas, open defections and industrial waste; other than anthropogenic contribution there are some natural causes of groundwater contaminations such as high levels of fluorine in granitic and meta-igneous rocks. The heavy metals leach out into the groundwater from the mineralized zones and contribute towards groundwater pollution, which is very common in mine areas; the water near the mines are highly acidic and rich in heavy metals (Zeng B. et, al., 2017). Since Dharwar craton is one of the major metallogenic terrains of Indian subcontinent, the groundwater in this region shows a signature of both natural and man-made contamination. In humans about 80% of the diseases are caused by drinking water (WHO 2004, CPCB, 2007, 2015). For a densely populated country like India, water scarcity can cause political instability, economic problems and social imbalance. The availability of freshwater is the backbone of a healthy ecosystem. The World Health Organisation (WHO) has acknowledged this and included availability of sustainable and clean drinking water in the Millennium Development Goals (WHO, 2004). However fresh water does not exist everywhere due to which in some parts of the world people are suffering from problems of scarcity and contaminated water. In some of the studies a high fluoride concentration has been found in the ground water of the Palakkad region (Shaji E et., al. 2007). WQI is a well-known indicator of water quality proposed by Horton in 1965. Since then WQI of rivers as well as groundwater from several parts of the world has been

reported. The water quality index is based on the strong logic that some of the selected parameters can give a good indication of the overall water quality (Sharma et. al., 2014, Cade, 2011). It also allows us to infer the bulk quality of water (Zhenghui et al., 2012). Water quality can be measured through different methods depending on the aim of the study (Sharma et. al., Simeonov et. al., 2002, Boyacioglu et. al., 2007). WQI can be calculated most by using suitable indices (Dwivedi S. L. and Pathak V., 2007). Selection of indices is based on the physico-chemical parameters and biological parameters present in the water sample. Indices value is helpful in long monitoring programs of watersheds, lakes, rivers groundwater and soils. It provides useful information to the people and the decision makers about the health of the ecosystem (Simoes et. al., 2008). The Q_i values of a parameter become negatives when a parameter shifts from its given range. The higher shift from range, higher the negative values. The water quality index with large negative values is considered unfit for drinking purposes (Stoner J., D., 1978). The present study provides detailed information on the variation of water quality index in the Palakkad region of state, India.

A few earlier studies in this area conducted by state and central government agencies (CGWB and State Groundwater Department) focused only on the quality of groundwater. Some noticeable work in southern India on the evolution of groundwater chemistry with reference to ionic exchanges, by adopting various graphical methods and interpreting different indices were attempted by many workers in the recent past. Elango et al (2003); Kumar et al.(2006); Singh et al.(2006); Subbarao(2006); Raju(2007); Rashid and Izrar(2007); Apadaca et al.(2007); Pophare and Dewalkar(2007); Pandian and Sankar (2007) have observed that host rocks are the main source of dissolved solids in the groundwater of Viappar river basin, Tamil Nadu by adopting various methods like Gibbs plots, Kelley's indices, and chloro-alkali indices (CAI). Brijraj and Kaur (2007) have concluded that the chemical quality of surface and groundwater of Rawalsar Lake, Mandi district, Himachal Pradesh was controlled by weathering of rocks, which supplied most of the dissolved constituents to the water. Gowd (2005) and Reddy and Prasad (2005) have studied and delineated the hydro geochemistry of the Peddavanka watershed

and the Tadpatri area of Anantapur district, Andhra Pradesh, India. Rajmohan and Elango (2004); gives a detailed account on identifying the hydro geochemical processes and its relation to the chemical composition of groundwater by mathematical and graphical approaches in Palar and Cheyyar River basins. Rock water interaction studies use detailed geochemical analysis to find out the strong influence of rock composition in groundwater.

Subramani, et al. (2009) thoroughly evaluated the hydro geochemical processes that regulate groundwater chemistry in Chithar River basin, Tamilnadu, by using primary and secondary sets data to compile the groundwater chemistry. Different ion concentrations reveal the hydro geochemical processes involved. A similar study was attempted by Sridhar et al. (2013) and presented the spatial distribution of different ions during post-monsoon and pre-monsoon. The plots were fixed to categorize water on the basis of chemistry and had concluded that chemistry of water was a result of rock water interaction. SubbaRao, et al. (2011) studied Varaha River basin for geo chemical characteristics where groundwater is brackish and very hard, due to geologic, anthropogenic and marine sources. The observed data was compared with WHO and BIS values. An experimental water rock interaction study carried out by Saxena and Ahmed (2011) in Pattabellam village in Krishna district of Andhrapradesh to evaluate the fluoride dissolution concluded that aqueous ionic species and concentrations, as well as their interaction with fluoride - enriched minerals and their residence time are important in controlling the fluoride dissociation process. An integrated approach of Groundwater Quality Assessment in the hard rock terrain of Ranchi district, Jharkhand, India, by BinduKumari et al. (2015) shows that the spatial distribution of various chemical parameters enables us to categorize groundwater by WQI calculation and the possible sources of contamination and the remedies can be substantiated. Reddy and Niranjan Kumar (2009) studied the Penna-Chitravathi river basins to identify and delineate the important geochemical processes which were responsible for the evolution of chemical composition of groundwater. It is an attempt to explain the groundwater chemistry influenced by water-rock interaction followed by evapotranspiration process. The groundwater in Penna–Chithravathi river sub basins exhibited marginal

variations in its chemical parameters between pre-and post–monsoon, but distinct change in water chemistry was noticed in different hydro geological environments. Significant variations in hydrochemistry of different rock types are influenced by water-rock interaction and aquifer material mineralogy, whereas the aquifer hydraulics play limited role in hydro geochemical processes.

The study of groundwater chemistry of aquifers along the coastal zone of central Kerala by Laluraj et al. (2005)analyzed the major ionic distribution by using standard procedures and the microbiological quality of samples were also analysed in this study. The chemical analysis revealed that the groundwater present in the shallow aquifers of some of the stations were poor quality and beyond the potable limit as per the standards set by WHO and ISI. Srinivasamoorthy et al. (2008) studied the Archean crystalline rocks of Salem district, Tamilnadu, to identify the major sources controlling groundwater chemistry in a hard rock terrain. They concluded that generally water chemistry is guided by lithological influences and the chemical composition of groundwater of the study area is strongly influenced by rock water interaction, dissolution and deposition of silicates group of minerals. Chan-Ho –Jeong (2000) assessed the hydro chemical and mineralogical effects on the fate of radionuclides along groundwater pathways in Samkwang mine area of Korea.

Pacheco and Weijden, (1996) attempted to study the contributions made by chemical weathering and anthropogenic inputs to the groundwater composition in a granitoid area in Fundao, Central Portugal by using a combination of grouping algorithms and weathering algorithm to assess the contributions.

The present study concentrates on the western part of the extensively studied Palghat-Cauvery shear zone where petrological and geochronological evolutions are established. Nishimiya et al. (2008) attempts to establish the pressure temperature conditions of the rocks present and suggest a prograde–high pressure metamorphism due to continent–continent collision during the amalgamation of Gondwana super continent. Sajeev et al. (2009) reveals the type and nature of metamorphism of the area and provides the exact tectonic scenario of the Palghat-Cauvery suture zone.

Thomson et al. (2012) established the crustal residence age of Charnockite orthogenesis and presented a large data set of major, trace element Rb-Sr and Sm-Nd isotopic composition. Nair and Prasnnakumar (2000), studied the characteristic features of Palghat gap being a shear zone by interpreting the petrography and structural analysis results. It was concluded that the Palghat gap topography is a combined effect of shearing and erosion.

Very few works have been attempted on the characterization of hard-rock aquifers based on geochemical and isotopic analyses, which indicates that water rock interaction has not been fully investigated yet. Present study tries to propose a comprehensive investigation of stable isotope geochemistry in a hard rock aquifer system. Bhattacharya et al. (1985) analysed oxygen and hydrogen isotopes in groundwater to provide a clear scenario of these isotope measurements in different seasons. Lambs et al. (2011) has efficiently used stable isotopes to understand the isotope systematic during weathering and other surface processes. Many of the Rare Earth Elements in groundwater would have been enhanced due to the weathering of minerals in the rocks. Weathering processes release these metals to the groundwater. Present study of Palakkad area also focuses on the REE distribution in groundwater as well as the rock samples. Renie and Verweij (2003) have tried to understand the behaviour of REE in groundwater by calculation of the speciation. They showed that the pH is by far the most significant groundwater characteristic, which contributes to the variation in REE concentrations. Tweed et al. (2006) investigates the processes controlling REE concentrations at different stages along groundwater flow paths in different fractured rock aquifers, and the effectiveness of using REE as tracers of regional flow. Gob et al. (2013) analysed water samples from different stratigraphic units of SW Germany for major and trace elements. It showed that the chemical composition of water depends on several clearly distinguishable factors, which provides information about water rock interaction. These are the major element composition of water, which is determined by the enclosing rock type, but also trace elements like Rb and Cs can give information about alteration processes due to their different affinities for absorption of clay minerals.

The previous studies regarding hydro geochemistry of hard rock aquifers of southern India provides a good research path to the present study area. Many have attempted to simulate different hard-rock aquifers using hydro geochemical and isotopic models. They have widely applied stable isotopes and major chemical constituents in relating the chemical evolution of groundwater through different geological column, and interpreted and rectified by different models. Hard-rock aquifer characterizations by means of detailed petrological, geochemical, and isotopic means have not been fully investigated so far.

Chapter 3

Methodology

This chapter summarise versions analytical protocols and methods used in this study to attain the results. Various analytical equipment like EPMA, XRF, ICPMS, IRMS, Chromatographs and sample preparations units were utilized in this work and it analytical set up is explained here.

Chapter 3
Methodology

Detailed geochemical analyses were carried out on all collected rock and water samples from the study area. A total of 16 thin sections, 17 whole-rock geochemistry and 16 samples mineral chemical analysis were carried out on rock samples. 66 water samples were analysis for major anion and cations, 17 samples were analysed for REE analysis. Apart from this 96 seasonally (32 per season) collected samples were used for oxygen isotope analysis, which is later compared with 4 marble samples from the study area. Results were synthesised in the map of the study area using GIS software. Detailed description of sample preparation and analytical protocol is described in this chapter.

THIN-SECTION MAKING

Petrological thin-section is a 0.03mm thick slice of rock attached to a glass slide using epoxy for petrographic observations. It is used to identify the minerals by observing their optical properties and to study the textural settings.

Cutting the rock to chip:

Break the rock samples to ample sizes to be cut on the diamond cutter. Using the diamond cutter the rock is cut perpendicular to the foliation into a chip of uniform thickness (~ 2-3 cm) and dimension close to that of the glass slide.

Grinding the chip:

One side of the chip is ground and flattened using silicon carbide abrasive powders of mesh sizes 80, 120, 220, 400, 600, and 800 microns on a rock grinder. Fine polishing should be done on a glass plate using 1200-micron mesh silicon carbide powder. This is done to make the surface smooth and flat so as to stick it to the glass slide on top of

it properly.

Heating and Mounting:

Clean the polished rock chip in running water and dry it with Kim wipers. It is important to make sure that there is no dust or foreign particles on the top of the polished surface of the chip. Set a hotplate at 150°C and place the sample on the hotplate with the polished side facing up. Heat the sample for at least two hours and make sure that no moisture remains in the sample after heating. Clean the sample surface again using a dust free Kim-wiper. Clean the glass slide using ethanol and heat the glass slide for about 3 minutes before sticking it to the polished surface using epoxy. After fixing the glass slide without air trapping, keep the chip on hotplate for at least 20 minutes to 2 hours, until the epoxy gets cured. Switch off the hotplate and allow the chip to cool down slowly.

Preparation of epoxy:

Epoxy is prepared by mixing resin and curing agent (in the present study Petropoxy 154) in 1:9 ratio in a mixing jar and stir it with a rod and keep the mix for more than 20 minutes to avoid air bubbles generated while mixing.

Precision cutting:

Cut the rock chip attached to the glass slide to a thickness close to few millimeters or thinner after it is cooled properly using a second precision cutter.

Grinding and polishing:

The final grinding of the chip to 0.03mm thickness is done on the same rock grinders using silicon carbide powders of mesh size 80, 120, 220, 400, 600, 800 microns. The sample is then ground to thin-section thickness by grinding it on a glass plate using fine-grained (1200-micron mesh or smaller) silicon carbide powder. The thin-section is finally polished using diamond paste of 1 and 3 micron size on a woven 100% wool cloth using solvent. The mirror polished sections are used for petrographical

observations and for further analysis using EPMA.

PETROLOGICAL MICROSCOPE

Petrographical observations are carried out using a petrological microscope (*OLYMPUS* BX51) with fluorite grade 2X, 5X, 10X, 20X and 50X objectives. Images of potential reaction textures are captured using a CCD camera (DP 20) attached to the microscope. Generally, the parts of a microscope are- Illuminator, sub-stage assembly, aperture, diaphragm, condensing lens, stage, objectives, upper polarizer and eyepiece. The BX51 microscope set-up housed at IISc has additional components like- two illuminators, one providing transmitted light and other providing reflected light (Fig. 3.1). Various types of filters are used to filter-in required wavelengths of light. Focus knob at the base helps to the focus the image and the diaphragm adjusts the diameter of the light ray passing through it. The condenser and auxiliary condenser system is used for orthoscopic and conoscopic vision. The stage consists of vernier scale, rotating knobs in X-Y rotating planes. Above the stage where the thin-section is placed are the objectives of varying magnification. The nicol prism between the objective and the eyepiece is inserted to observe the samples under crossed and open conditions. Using this microscope the minerals and mineral reactions in the thin-sections are identified based on their optical properties in open and crossed nicol.

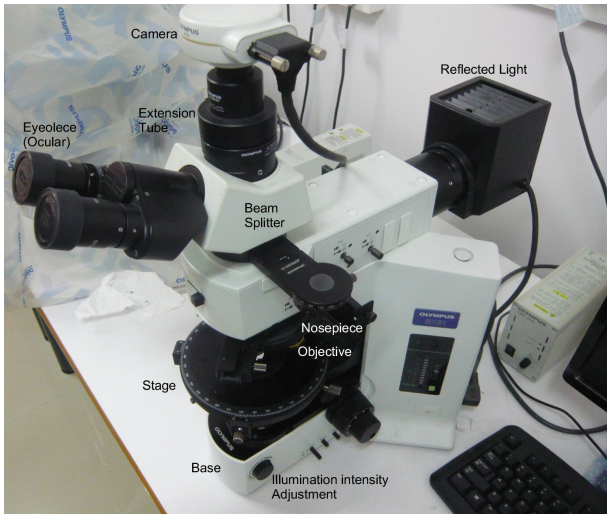

Fig. 3.1: Petrological microscope at CEaS, IISc

EPMA ANALYSIS

Electron Probe Micro-Analysis is a non-destructive elemental analytical technique giving quantitative and qualitative measurements of elements. EPMA works on the principle of Bragg's diffraction $n\lambda=2d\sin\theta$. Electrons impinging on solid materials undergo inelastic and elastic interactions with atomic electrons and atomic nuclei. The 'backscattered' and 'secondary' electrons deflected and dislodged from the sample surface are used for imaging. A 'continuous' 'characteristic' X-ray spectrum produced by electron transition between the inner atomic shells helps to analyze the elements quantitatively and qualitatively. The Wavelength-Dispersive Spectrometer and Energy-Dispersive Spectrometer function complementarily for quantitative and qualitative measurements. All the elements between Beryllium (Z=4) to Uranium (Z=92) can be measured in EPMA with an accuracy of ±1% with a spatial resolution of few microns (1 microns). The oxides of the desirable elements are measured in weight percentages that are later re-calculated for cations. The Electron Probe Micro probe housed at AFMM, IISc (JEOL JXA-8230 EPMA) (Fig. 3.2) is the fifth generation super probe that has high resolution, highly stable SEM with five spectrometers with multiple LIF, TAP and PET crystals with two gas flow detectors on a 100 mm Rowland circle. The machine is settled up to a working distance of 11mm, operating with an accelerating voltage of 15 kV and beam current of 12 nA. Natural and synthetic silicates and oxides standards are supplied by JEOL and Astimex 53 Mineral mount standards are used for calibration. Mineral chemical data are obtained for all the major minerals present in the rocks examined in this study. SiO_2, TiO_2, Cr_2O_3, Al_2O_3, FeO, MgO, MnO, CaO, Na_2O, K_2O and ZnO were analysed for all minerals. The data are reduced using ZAF correction procedures. $Fe^{3+}$is calculated by normalising analyses to respective cation total through charge balance considerations (Droop, 1989).

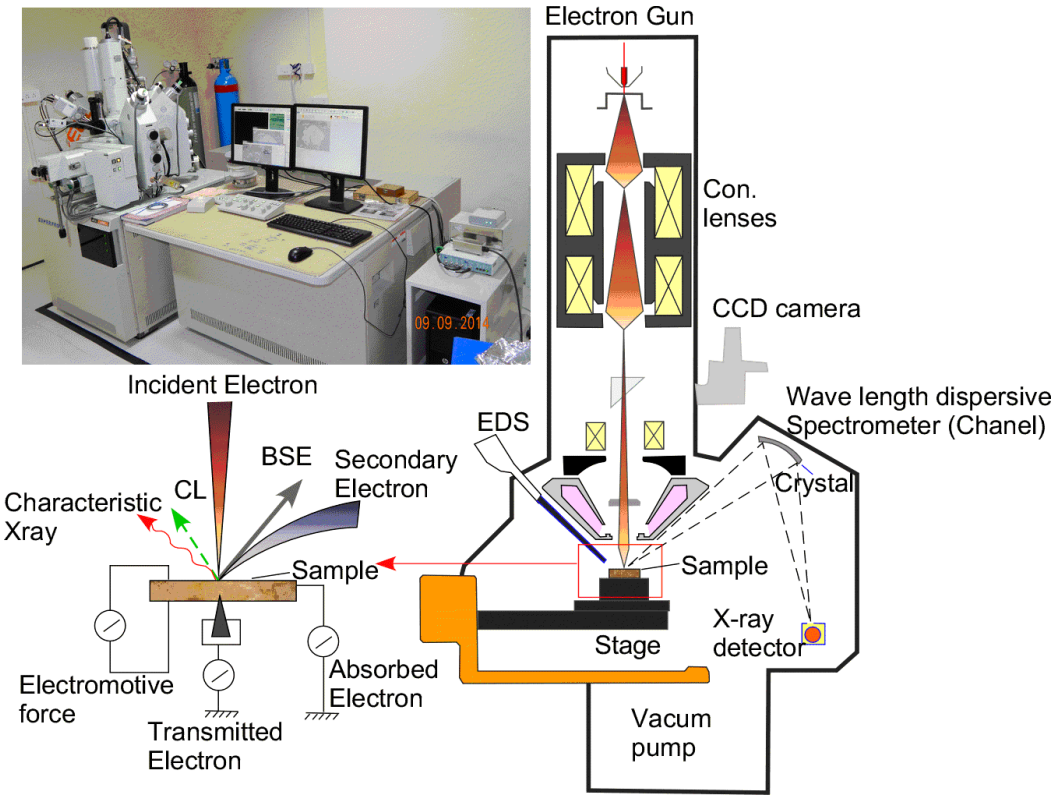

***Fig. 3.2: Schematic diagram of EPMA with* JEOL JXA-8230 EPMA housed at AFMM, IISc**

XRF ANALYSIS

X-Ray fluorescence (XRF) analysis is helpful to understand the elemental composition of the rock samples. Samples analysed and results are listed chapter 5.

Procedure for Sample preparation

The rock samples are cut into small chips of approximately 8cm length, 4cm width and 2cm height using first cutter (Fig.3.3A). Take care to avoid the weathered surface and cracks. The samples should be a homogenous representation of the mineral assemblage. After grinding the rock chips (up to 600 mesh size) to obtain smooth and curved surfaces, they are cut into small pieces (around $1cm^3$) with the help of crushing machine (Fig.3.3B). These crushed samples should be washed well in an

ultrasonic bath (Fig.3.3C) and transferred into a crucible. The samples are then heated for about6 hours at 110°C in a hot air oven (Fig.3.3D). The dried samples should be crushed by using tungsten mortar and then powdered well with agate mortar and ball mill (Powdering time – 40mnt). This will help to mix the sample thoroughly and make it homogenous.

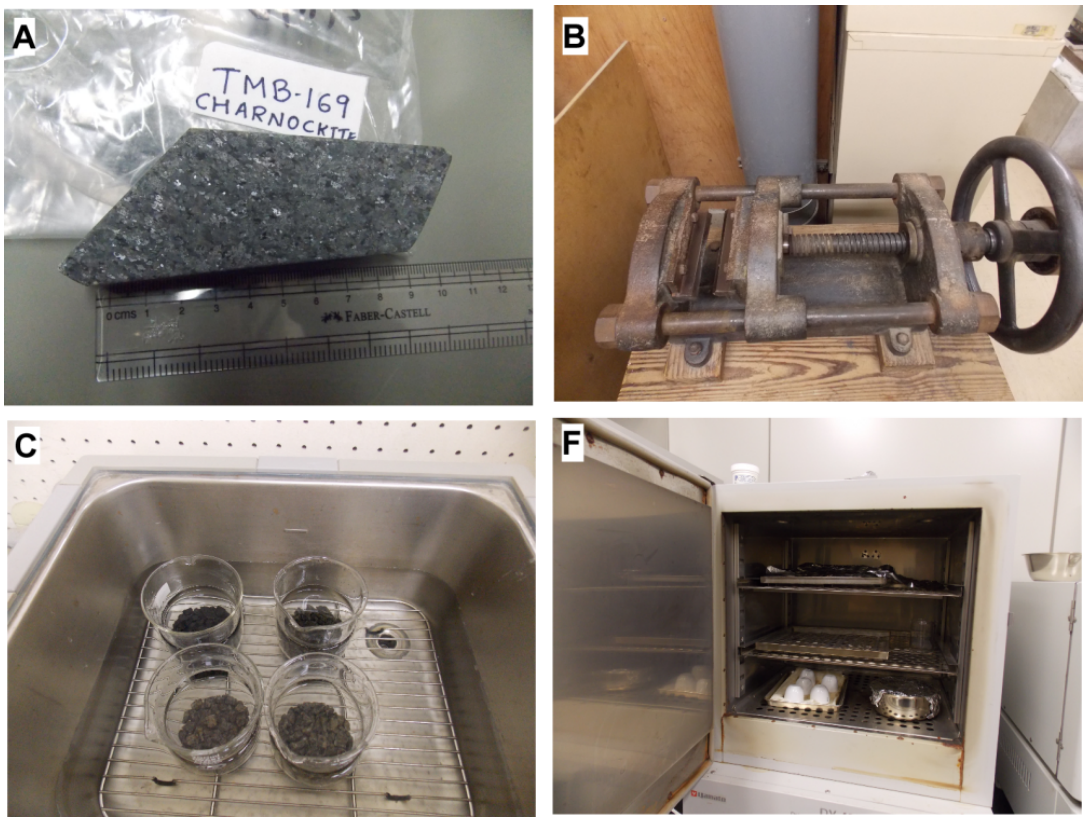

Fig. 3.3: Steps for XRF sample preparation *A) Polished rock sample B) Crushing Machine C) Crushed samples in Ultrasonic bath D) Heating the samples hot air oven.*

Procedure for bead making

Sample beads are used for XRF analysis. Fusion bead method is used for bead preparation. Fusion beads are preferred as it reduces analytical errors caused by heterogeneous grain size and mineralogy. Take 2.3000 gm dry powdered sample in a crucible and heat at 900°C for 6 hours using muffle furnace. After 6 hours, decrease the temperature to 200°C and wait for 4 hours. Once properly cooled (wait for 4

hours) weigh out 1.8000 ± 0.0003gm samples into agate mortar(Fig.3.4B) with the help of butter paper and spatula, followed by weighing 2.8800 ± 0.0003gm of Lithium tetraborate ($Li_2B_4O_7$) and 0.7200 ± 0.003gm of Lithium metaborate ($LiBO_2$) (these are acidic and basic flux agents - Fig. 3.4A). Mix well and transfer these weighed samples into platinum crucible. keep the mixture in a bead making machine. Switch on the machine and heat up to 1000°C (Fig. 3.4C) and after 15 minutes beads will be ready (Fig. 3.4D). These beads have flat bottom, which are homogeneous representation of the rock sample without any mineral structure.

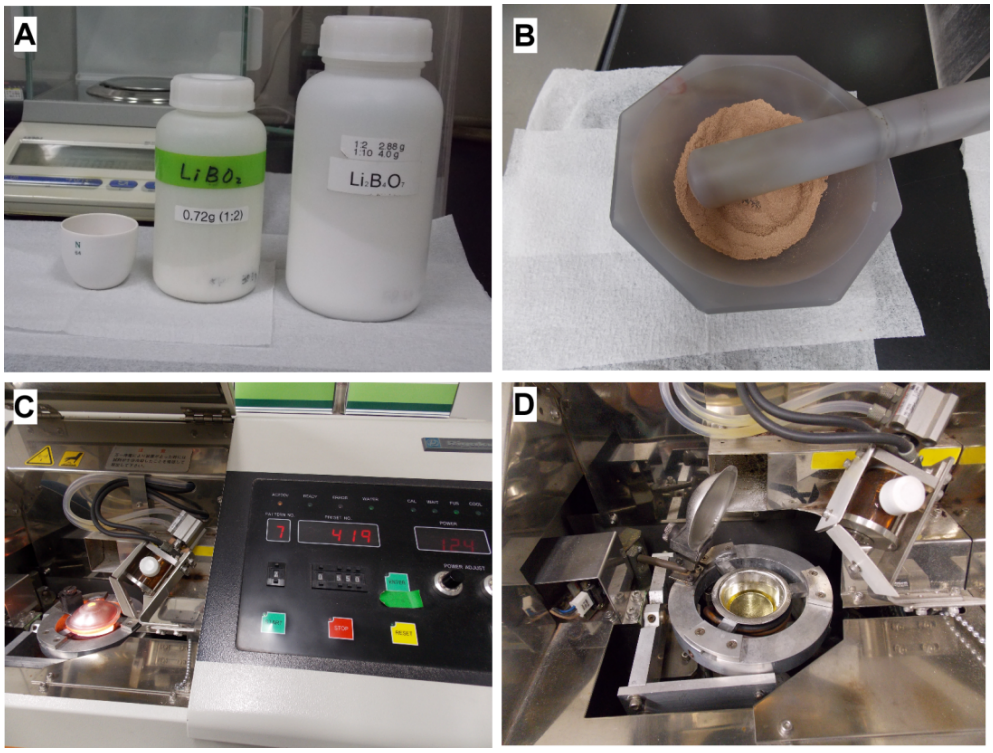

Fig. 3.4: Steps for XRF sample preparation *A) Flux agents B) Weighed samples C) Heating the weighed sample D) glass bead*

The prepared beads are mounted on the sample stage and inserted (around 26 samples at a single time into the XRF channel (Fig.3.5A,B). Major elements are be detected by Proportional counter (Pc) and trace elements by Scintillation counter (Sc). Basalt sample (JB-1b) is used as the standard. Major element measurement takes 15minutes and trace elements up to 30 minutes on each sample

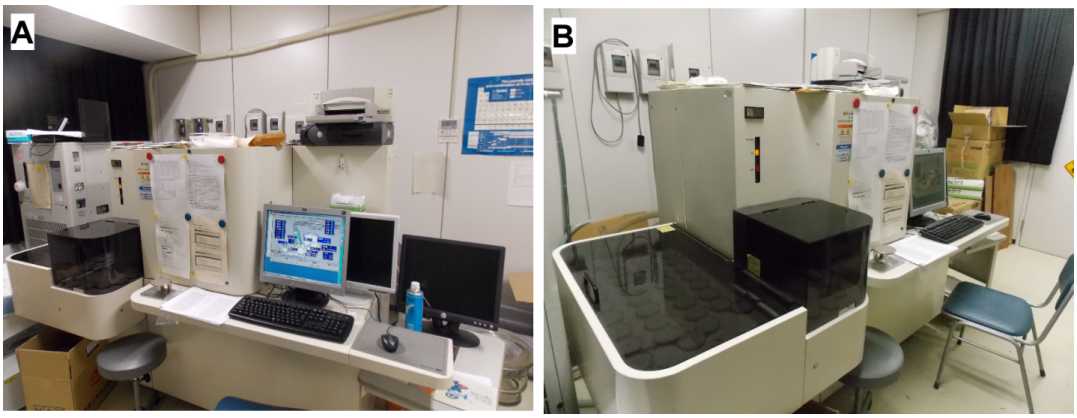

Fig. 3.5: A) XRF machine at Niigata University, Japan B) Sample channel of XRF machine

MAP MAKING

All the thematic maps were prepared in GIS platform using Arc GIS software.

Lithological map

The primary data referred for the preparation of lithological map are District Resource Maps of Palghat, Coimbatore, Malappuram and Trichur districts published by Geological survey of India. The District Resource Maps were scanned and georeferenced and the rock-types are manually digitized as polygons. Linked geological database is created in the attribute table in GIS platform.

Digital Elevation Model (DEM)

The Digital Elevation Model is prepared by two methods. One by using the ASTER DEM (DEM1) (Fig. 3.6) and other by using the altitude data obtained from GPS in the field.

The ASTER (Advanced Space borne Thermal Emission Reflection Radiometer) Digital Elevation Model is used in the present study which is compared with the Survey of India Topographic maps of the study region and found consistent with

them. The elevation in the study region ranges from 1m to 2062m above Mean Sea Level (MSL). The Digital Elevation Model shows that the north-eastern part of the study region is highly elevated. The easternmost part also slightly elevated region. The central part of the study area consist several isolated hillocks.

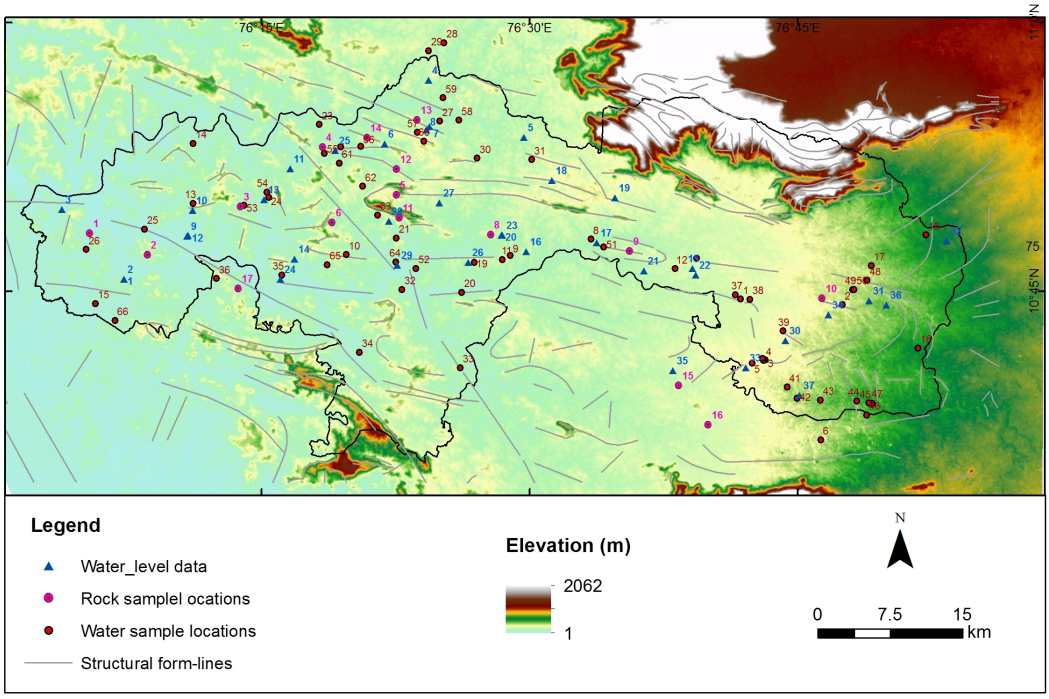

Fig. 3.6: ASTER DEM overlapped with the digitized structural lineaments of the study area

Structural lineament map

The structural lineament map is developed by manually digitizing the structural lineaments from Landsat satellite imagery and ASTER (Advanced SpaceborneThermal Emission Reflection Radiometer) Digital Elevation Model. The ground-truth verification has been carried out during field work and the field data were compared with the map and also incorporated to the map. The foliation strike and dip data obtained from the field and from the published mas were also plotted on the map (Fig. 3.6). The map shows that the rocks in the study area mostly having high dip angles which ranges between 50-80°.

Drainage map

The rivers and water bodies are manually digitized from the Survey of India Topographic maps of the study area (Fig. 3.7). The drainage network is also automatically extracted from the Digital elevation model (DEM) in Arc GIS by using the 3-dimensional analyst (Fig. 3.7). The drainage map shows that the drainage density is high in the north-eastern part of the study region, which is the highly elevated part of the study region. The comparison of both drainage maps suggests that the automatically extracted drainage map is consistent with the manually digitized drainage map.

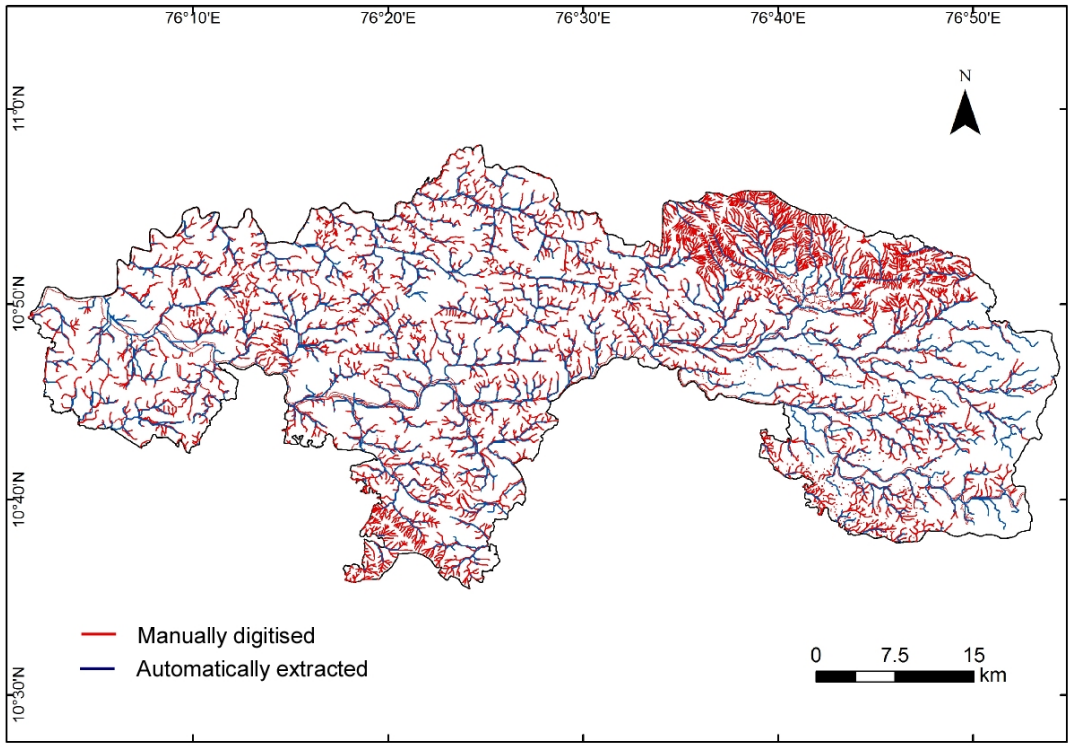

Fig. 3.7: Drainage map of the study area. *See text for description*

Rock sample location map

Detailed fieldwork has been carried out in the study area and 17 rock samples were collected. Field, structural and lithological information were collected. The 17 rock

sample locations were plotted on the geological and structural map. The foliation strike and dip data were also plotted on the map.

WATER SAMPLE COLLECTION

Water samples are collected in three different ways for three different analyses. Totally 66 water samples were collected for major cation anion analysis, 32 water samples for isotopic analysis were collected during pre–monsoon, monsoon and post monsoon seasons separately and 17 samples were collected for Rare Earth Element analysis. For chemical analysis 66 water samples were collected in high-density polyethylene bottles.



Fig. 3.8: Water sample collection in the field

Approximately 30 ml water samples were collected mainly from the open wells, located using GPS. Field parameters like temperature, EC and pH were measured in the field itself by potable meters. The bottles were first rinsed and samples were filtered and stored. For isotopic analysis 40 ml samples were collected and the samples were filled up to the brim and were immediately sealed to avoid exposure to air and were labelled accordingly. 32 samples were collected for pre-monsoon, monsoon and post monsoon seasons separately. 20ml samples were collected and

acidified in the field itself for REE analysis. The chemical analyses were done for calcium, sodium potassium, magnesium, sulphate, phosphate, nitrate, chloride, fluoride and silica.

pH measurement

Principle of operation. Potentiometric pH meters measure the voltage between two electrodes and display the result converted into the corresponding pH value. The glass electrode for measuring the pH has a glass bulb specifically designed to be selective to hydrogen-ion concentration.

Major Ion Measurement

Ion: an atom or a group of atoms that has either an excess or a deficiency of electrons major ions in water, positive charge (*cations*), negative charge (*anions*):

H^+, Na^+, K^+, Ca^{2+}, Mg^{2+}, OH^-, Cl^-, SO_4^{2-}, NO_3^-, HCO_3^-, PO_4^{3-}

Mole: unit of amount of substance.

By definition, the mole is the amount of substance of a system that contains as many elementary entities as there are atoms in 0.012 kilogram (12g) of carbon-12. The elementary entities, which must be specified, may be atoms, molecules, ions, electrons, other particles, or even specified groups of such particles.

1 mole = $6.022*10^{23}$ molecules or atoms (or other units)

conversion from mg/L to mmol/L

Working and Principle

- A sample of the mixture to be analyzed (*analyte*) is injected into a carrier fluid (the *eluent)*
- the combination is passed through a column containing a stationary fixed material (*adsorbent*)

- Compounds contained in the analyte are then partitioned between the stationary adsorbent and the moving eluent/analyte mixture
- Different dissolved materials adhere to the adsorbent with different forces
- The ones that adhere strongly are moved through the adsorbent more slowly as the eluent flows over them
- As the eluent flows through the column the components of the analyte will move down the column at different speeds and therefore separate from one another
- A *detector* is used to analyze the output at the end of the column. There are various detectors; our IC has an *electrical conductivity* detector.
- Each time analyte molecules/ions emerge from the chromatography column the detector generates a measurable signal which is usually printed out as a peak on the chromatogram.
- A *suppressor* is being used to reduce the background conductance of the Eluent and at the same time enhance the conductance of the sample ions
- implementation of the chromatographic method

Detection of ions

The *chromatogram* is a record of detector output (electrical conductivity) versus time as the analyte passes through the chromatography system. It usually consists of a series of several peaks corresponding to the different times in which components of the analyte mixture emerge from the column. The number of peaks corresponds to the minimum number of different substances (compounds or ions) contained in the analyte.

Siemens: unit of the conductance, the reciprocal of the resistance in ohms (S = amperes/volts), or in SI units: one second cubed- ampere squared- per kilogram- per meter squared ($1s^3\ A^2 \cdot kg^{-1} \cdot m^{-2}$), 1 uS is 1 micro Siemens or 10^{-6}S

Eluent

Eluent is the mobile phase that transports the sample ions through the ion chromatograph plumbing, including the columns. For anion analysis we are using a mixture of Sodium Carbonate (Na_2CO_3) Sodium Bicarbonate ($NaHCO_3$) dissolved in water

The pH, ion concentration, and ion types in the eluent determine the partitioning of the analyzed ions between the stationary phase (ion exchange resin in the columns) and the eluent.

Calibration

Standards are needed to calibrate the IC (to identify peaks and to determine the concentrations of our samples)

We are making standards by diluting a commercial solution, named *Dionex Seven Anion Standard*. This solution is designed for routine anion determinations. It contains fluoride (20 mg/L); chloride (30 mg/L); nitrite (100 mg/L); bromide (100 mg/L); nitrate (100 mg/L); phosphate (150 mg/L); sulphate (150 mg/L)

The peak area is plotted versus anion concentration and a trend line is fitted through the data. The equation of the trend line is then used to convert peak areas from measured samples into concentrations.

OXYGEN ISOTOPE ANALYSIS

Oxygen isotope analyses of aliquots of water samples were carried out at the Stable Isotope Laboratory of the Indian Institute of Science, Bangalore, India. The stable isotope ratios of the water were measured using a Thermo Scientific GasBench II interface connected to a Thermo Scientific MAT 253 isotope ratio mass spectro-meter (Thermo Scientific, Bremen, Germany). All the isotopic ratios reported in this study are presented in the standard δ notation: δ is defined as the relative difference, in parts per thousand (%), between the isotope ratio of the sample ($\delta^{18}O_{sample}$ and δD) and the water reference (VSMOW) as in the following equation:

$\delta_{sample} = (R_{sample}/R_{VSMOW}-1) \times 10^3‰$ (1)

where R = $^{18}O/^{16}O$ or $^{2}H/^{1}H$. Routine analyses of water samples involved loading 200 mL of the sample water into a exetainer glass vial (Exetainer, High Wycombe, UK) followed by equilibration with a gaseous mixture of CO_2 and He (0.25% of CO_2in He) at a constant bath temperature of 30 – C for oxygen isotope ratio determination. A mixture of $H_2$and He (2.0% of H_2in He) was used for hydrogen isotope equilibration experiments. Oxygen isotopic analyses of water samples along with standards were carried out in batches, with each batch consisting of 32 samples. The run time for an individual sample was 12 min with the acquisition of four working gas peaks and five sample gas peaks. Of the 32 samples in a batch, in addition to the water samples, an internal laboratory standard, WWW_OASIS, an international laboratory standard and a few blanks were also analysed. Each sample with equilibrated $CO_2$was analysed for $\delta^{18}O$ after a minimum of 18 h equilibration time. The separation was carried out using a PORAPLOT Q column (Agilent Technologies, Haryana, India), which was baked prior to the analyses of individual batches. Repeat analyses of internal laboratory standards yielded a standard deviation of 0.08% after correcting them for any observed drift. The internal laboratory standard (WWW_OASIS) was calibrated using international standards (VSMOW, GISP) and other inter-laboratory standards procured from MPI, Jena, Germany (BGP_J1, RWB_J1 and WWW_J1) and the NARM standard from PRL, Ahmedabad, India.

Chapter 4

Geological Setting

This chapter discuss about the geology of southern India with emphasis on Southern Granulite Terrane. Geology of the study area is discussed separately with field relations and descriptions.

Chapter 4
Geological Setting

The Indian peninsula is a shield or a stable landmass dissected by several deep crustal shear zones. It comprises of the Archaean Dharwar craton that has numerous schist belts, Proterozoic sedimentary basin such as Cuddapah, Tertiary sediments along the eastern and western coast and the Southern Granulite Terrain. Fermor line divides the Dharwar craton and SGT on the basis of degree of metamorphism (Fermor, 1936). The Southern Granulite Terrain (SGT), lies to the south of the Dharwar Craton and is distinguished by the change in metamorphic conditions from upper amphibolite grade rocks in the Dharwar to granulite grade rocks in the SGT. The grade of metamorphism evidently increases from north to south in peninsular India. The northern part of SGT comprises of Neoarchaean to Neoproterozoic meta-igneous rocks, granulites and eclogites, exposed in the regions of Nilgiri Block, Namakkal Block, Biligirirangan hills and Madras Block. To the south of the Palghat Cauvery Shear Zone (PCSZ), the terrain has undergone metamorphism during the *ca*. 550 Ma Pan-African Orogeny and is a vital fragment of the Gondwana supercontinent assembly. The south of PCSZ comprises of Madurai Block, Trivandrum Block and Nagercoil Block characterized by the presence of charanockites, meta-pelites, calc-silicates, felsic ortho and para gneisses and migmatites.

SOUTHERN GRANULITE TERRANE

Structures

Southern Granulite Terrain (SGT) is composed of several proterozoic granulite blocks dissected by various prominent shear zones (Drury and Holt, 1980; Ghosh et al., 2004; Ishwar-Kumar et al., 2013). The major shear zones are Moyar shear zone, Bhavani shear zone, Mettur shear zone, Palghat-Cauvery shear zone, Attur shear zone, Achankoil shear zone, Karur -Oddanchatram shear zone, Dharmapram shear

zone, West-coast shear zone (Drury and Holt, 1980; Ghosh et al., 2004; Ishwar-Kumar et al., 2013) (Fig. 4.1).

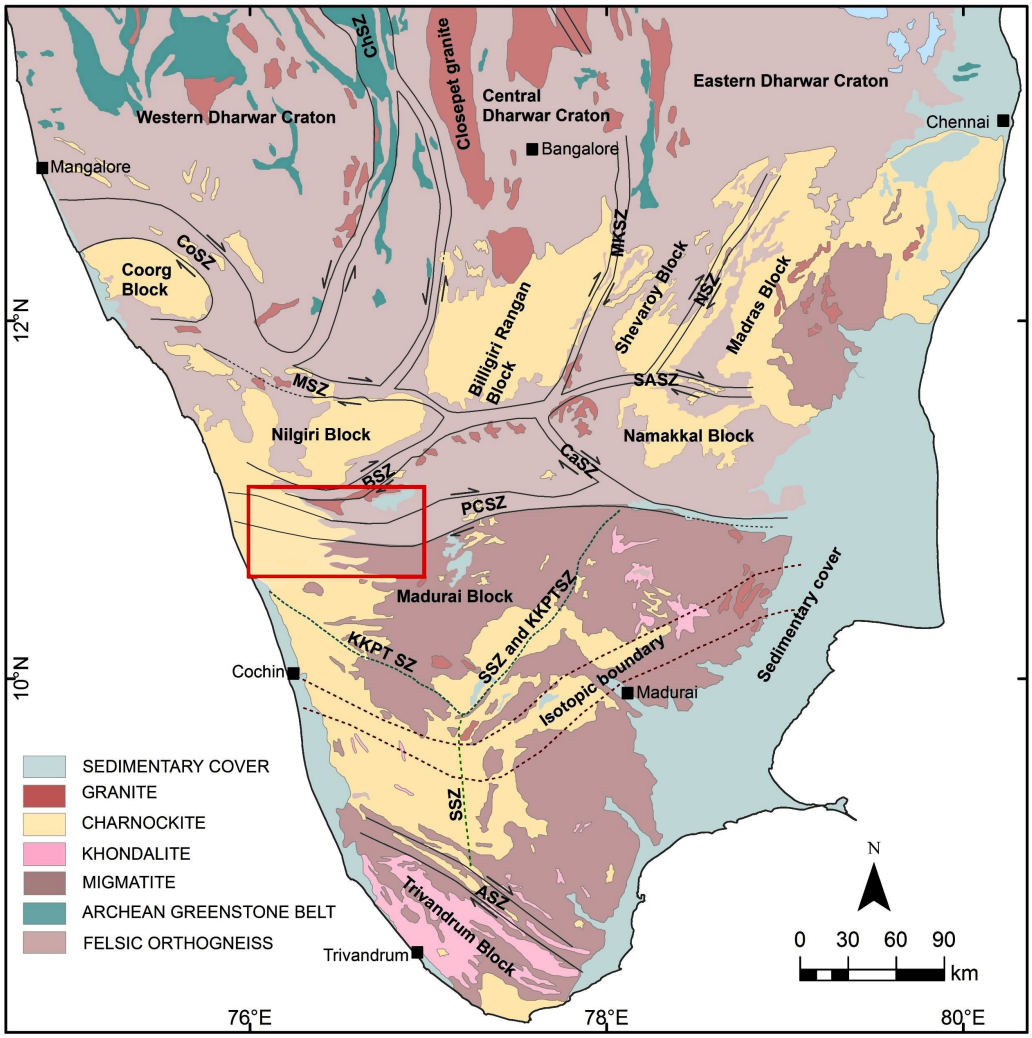

Fig. 4.1: Tectonic framework of southern India with major shear zones *(after Drury and Holt, 1980; Ghosh et al., 2004; Ishwar-Kumar et al., 2013)**. The red rectangular box represents study area. Abbreviations: MSZ: Moyar shear zone, BSZ: Bhavani shear zone, MSZ: Mettur shear zone, PCSZ: Palghat-Cauvery shear zone, Attur shear zone, Achankoil shear zone, Karur -Oddanchatram shear zone, Dharmapram shear zone, West-coast shear zone*

Geology

Major Archean domains in SGT are Coorg Block, Nilgiri Block, Shevroy Block, Biligirirangan Block and Proterozoic domains are Madurai, Achankoil, Ponmudi and

Nagarcoil units. SGT is mainly covered by charnockites, quartzo-feldspathic gneiss, khondalites, calc-silicates, amphibolites, quartzites, ultramafics, Iron stones and metasediments (Fig. 4.1).

Geochronology

The ages of blocks and units of SGT is heterogeneous and ranges between 2500-500Ma (both magmatic and metamorphic age).

Palghat-Cauvery shear zone

Palghat-Cauvery lineament is one of the most significant lineaments in southern India, as it is a continental shear zone that separates two contrasting geological domains. The major structural trends in the Palghat-Cauvery shear zone are NWW-SEE in western part, EW in the centre and again NWW-SEE in eastern part of the shear zone. Several interconnected shear zones such as Moyar shear zone, Bhavani shear zone, Salem-Attur shear zone, Dharmapuram shear zone, Karur-Oddanchatram shear zone combined together are called as Palghat-Cauvery shear zone system (Fig. 4.1).

Palghat-Cauvery shear zone is proposed as a high pressure granulite belt which separates two crustal domains (Collins et al., 2007). By thermo-barometric studies pressure-temperature conditions at Palghat-Cauvery shear zone (PCSZ) are estimated at 7.3-9.3 kbar and 700-800°C (Harris et al., 1982; Raith et al., 1988). Seismic reflectance studies and Tomographic studies indicated that this shear zone is dipping south (Rai et al., 1993). From the field and petrographic studies of rocks from surroundings of Palghat-Cauvery shear zone it is found to have had undergone high pressure-temperature metamorphism and indicated a palaeo-suture (Sajeev et al., 2009; Santosh et al., 2009). Protolith age of rocks in Palghat-Cauvery shear zone varies between 2900-2500Ma (Plavsa et al., 2012). There is a major controversy regarding the age of metamorphism along the Palghat-Cauvery shear zone. Most of the previous studies on PCSZ are mainly concentrated along the western part of the shear zone. Therefore the extension of the PCSZ towards the western part is least

studied and very trivial. Any further studies on the western part would provide an insight into the geological setting and evolution of PCSZ.

GEOLOGY OF THE STUDY AREA

Lithology

The regions of interest for this study are the areas in the western end of PCSZ constituting the Palakkad and Thrissur districts of Kerala. This region lies within the well-known Palghat Gap of the Western Ghats bounded to the north by the Nilgiri Block and to the south by the Madurai Block. The major rock types in the area are charnockite, clinopyroxene gneiss, felsic gneiss, hornblende-biotite gneiss, migmatite, biotite gneiss with sporadic occurrences of two-pyroxenite, amphibolite, garnet-bearing biotite gneiss and calc-silicate rocks to the north-eastern part of the field area (Fig. 4.2).

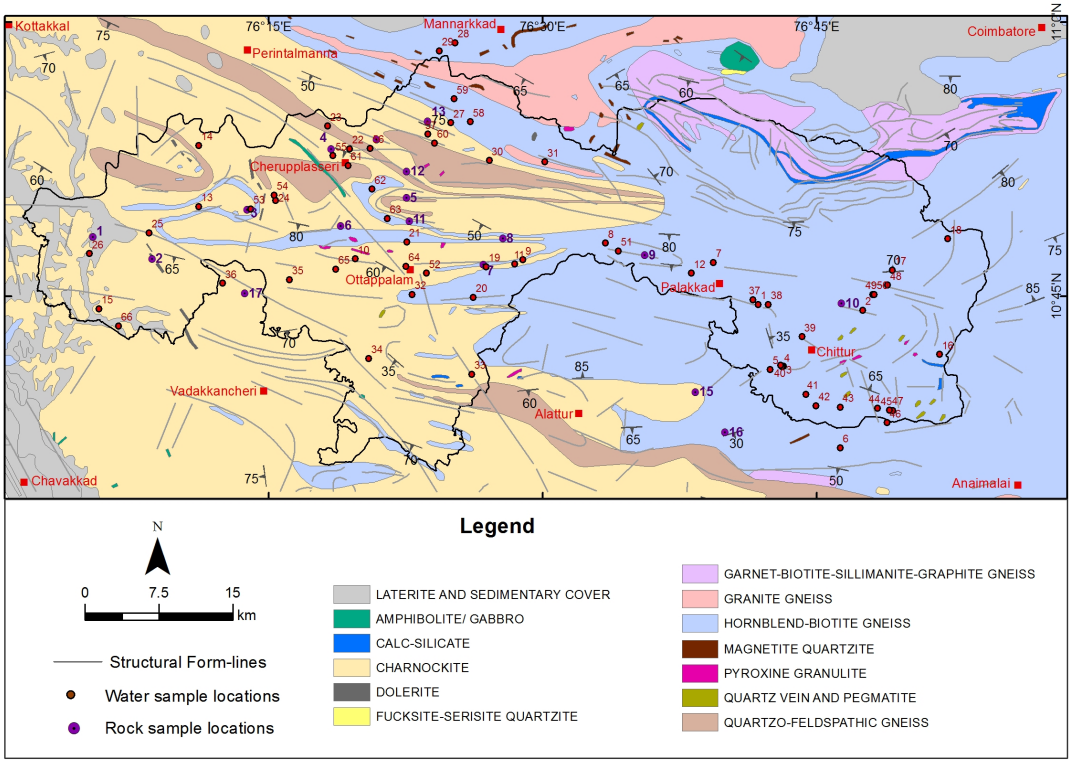

Fig. 4.2: Geological map of the study area with water and rock sample locations.
Geological map is after GSI District Resource Maps and structural lineaments traced from DEM and Landsat data

A total of 17 rock samples were collected from different parts of the field among them 8 were Charnockite, 5 Hornblende Biotite gneiss, 1 Biotite gneiss and 2 Clinopyroxene gneiss. Charnockite samples were collected mainly from western parts of the field, where as the hornblende-biotite samples were seen in the eastern parts. Biotite gneiss is collected from the eastern most part of the study area. Details of the samples collected are summarized in Table 4.1.

Table 4.1 Rock sampling location and rock types

Sample No.	Latitude	Longitude	Area name	Rock type
1	N10' 48 224'	E 76' 05.398'	Aloor	Charnockite
2	N10' 47.032'	E 76' 08.626'	Mudavannur	Charnockite
3	N10' 49.726	E 76' 13.824'	Churakkod	Charnockite
4	N10' 53 043'	E 76' 18.426'	Cherpullassery	Charnockite
5	N10' 50.368	E 76' 22.555'	Kizhoor	Charnockite
6	N 10' 48 .840'	E 76' 18.965'	Kottakulam	Charnockite
7	N 10' 46.711'	E 76' 26.767'	Lakkidi	Charnockite
8	N 10' 48.141'	E 76' 27.832'	Pathiripala	Charnockite
9	N 10' 47.233	E 76' 35.604'	Edathara	9.Hb Gneiss, 9.A Mesosome 9.B Melonosome
10	N 10' 44 .591'	E 76'46.366'	Thenari	Hb Biotite Gneiss
11	N 10' 49.102'	E 76' 22.726'	Varode	11.A.Charnockite 11.B Gneiss(contact zone)
12	N 10' 51.815'	E 76' 22 .570	Adakkaputhur	12.A Charnockite 12.B .Gneiss
13	N 10' 54.546'	E 76' 23.723'	Thirunarayanapuram	13.A.dark Coloured Charnockite
14	N 10' 53.553	E 76' 20 905	Mangode	13.B Light coloured Charnockite
15	N 10' 39.745'	E 76' 38.355'	Kakkayur	Gneiss
16	N 10 ' 37.537	E 76' 39.990'	Pallassena	16.A .Charnockite 16.B.Gneiss
17	N 10 ' 45.143'	E 76' 13.697	Desamangalam	Charnockite

Field details and sample collection

Rock samples were collected from quarries and roadside exposures. The western part of the field is dominated by pyroxenite and charnockite while the eastern part is characterised by the presence of hornblende-biotite gneiss and biotite gneiss. Charnockites are well foliated and presences of dyke intrusions are noted in the locations at Mudavannur (sample no. 2), Cherpullassery (sample no. 4), Varode

(sample no. 11) and Thirunarayanapuram (sample no. 13). The intruded dykes are observed parallel to the general foliation which is usually E-W to N80°E-S80°W. Charnockites are not always foliated, in many locations massive charnockite occurrences are seen in the areas of Aloor (sample no. 1), Adakkaputhur (sample no. 12), Desamangalam(sample no. 17), Thenari-Vellinezhi (sample no. 10) and Kakkayur (sample no. 15). These charnockite occurrences have pegmatite intrusions in them and in some locations it is seen associated with granitic gneisses. These charnockites have disrupted bands of quartzo-feldspathic gneiss seen as enclaves or blocks within them. Beach sediments cover the westernmost part near to the coastal region. Several NW-SE trending dolerite dykes are also present within charnockites.

Hornblende-biotite gneiss and biotite gneiss are found in Edathara and Pallassena areas (sample no. 9). These are well-foliated dark coloured rocks (Fig. 4.3C, D, and F). Highly migmatized hornblende biotite gneisses are found in some of these areas. The leucosomes and melanosomes formed during migmatization are well segregated. Melt pockets are seen in these rocks. Evidences for shearing and isoclinal folding are also observed (Fig. 4.3D).

Granitic gneiss, amphibolite, garnet-biotite-sillimanite-graphite gneiss, calc-silicate and laterite are present in the north-eastern part of the study area. Thin bands of calc silicates are present as enclaves within the garnet-biotite-sillimanite-graphite gneiss. Several thin patches of magnetite quartzite are exposed within the hornblende-biotite gneiss, which are mainly present in the north-central part of the study region. The south-eastern part contains several thin patches of quartz-vein and pegmatite, which are mostly trending in northeast direction (Fig. 4.2).

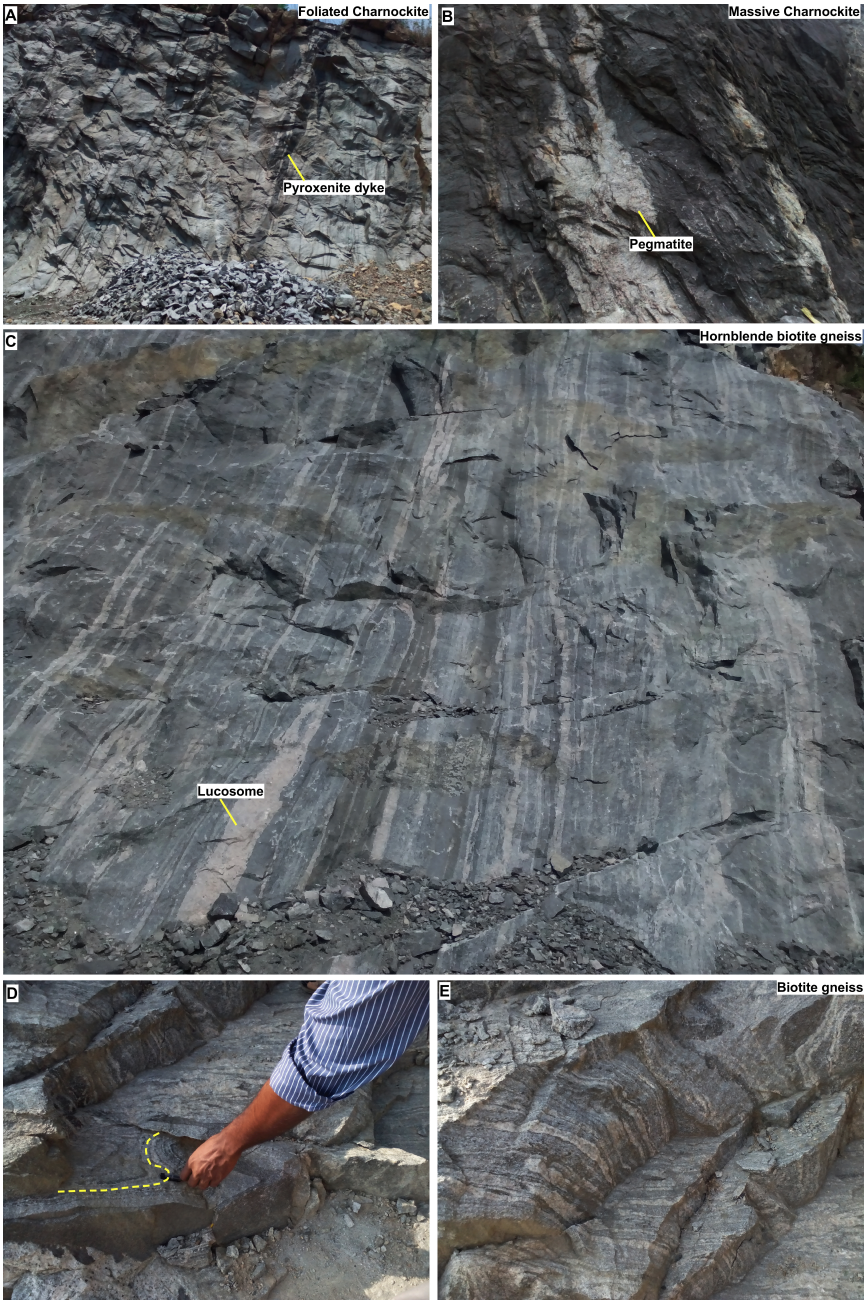

Fig. 4.3: Field exposures for foliated and massive charnockite and hornblende-biotite gneiss and biotite gneiss from the study area. *A) Foliated charnockite with pyroxenite dyke intruded parallel to the foliation. B) Massive charnockite exposure intruded by pegmatite. C) Highly foliated hornblende-biotite gneiss with pockets of disrupted lucosome entrapped within the foliation plane. D) Isoclinaly folded and sheared hornblende-biotite gneiss exposure. E) Well-foliated biotite-gneiss exposure from the study area.*

Structures

The study region is located in the western part of Palghat-Cauvery Shear Zone (PCSZ) and is dominated by east-west trending structures (Fig. 4.1, 2). The western part of the study area is intruded by NW-SE trending dolerite dykes. The north-eastern part of the study region has high-density of structural lineaments (Fig. 4.4).

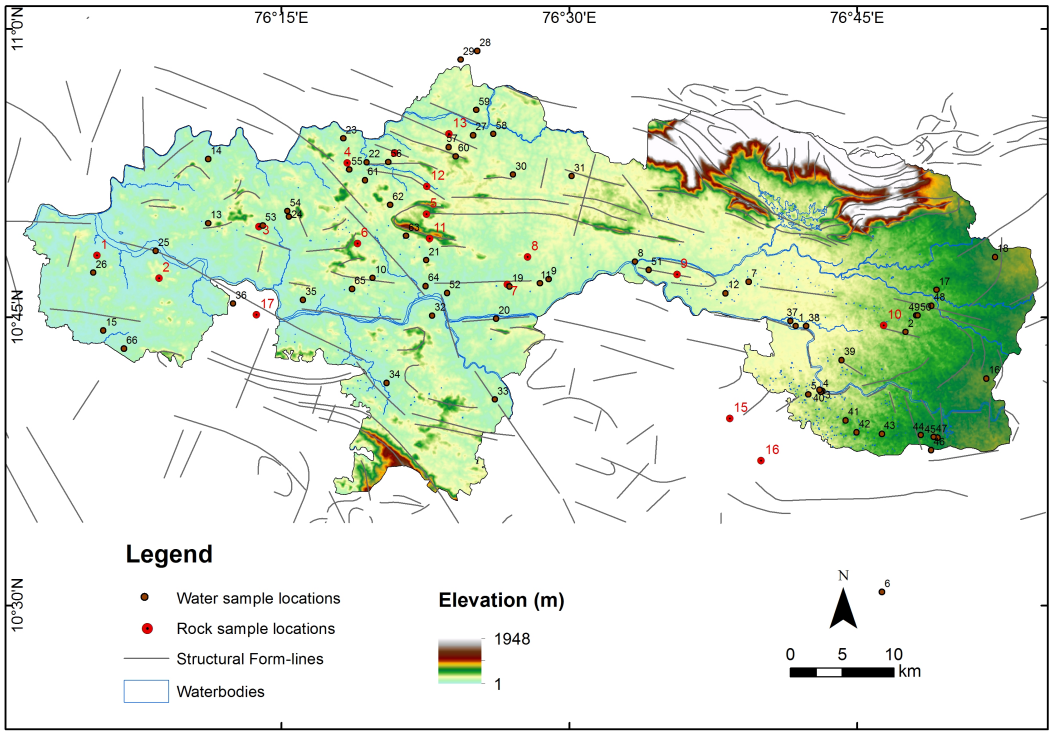

Fig. 4.4: Structural lineament map of study area overlapped with ASTER DEM with sample locations.

The regional structural lineaments are trending NNW-SSE with a varying 70° to 80° dip. In the north-eastern part of the study area is highly deformed and mainly dipping towards south. However most of the rock types in the south-eastern part of the study area are dipping towards north. There are two NW-SE trending shear/fault zone passing between Vadakkancheri and Ottappalam (Fig. 4.2 and 4.4), situated towards the southeast of the study area. The lineaments on both sides of the shear zone indicate a right lateral movement.

Geological cross-section

A geological cross-section (Fig. 4.5) is prepared for a section along AB from the study region. The 2-dimentional cross-section is prepared along line AB which is about 50km length and the altitude along this section ranges from 100m to 2000m. The elevation data for along the cross-section has been taken from ASTER Digital Elevation Model. The major rock-types in the northern part are granitic gneiss; hornblende-biotitegneiss, garnet-biotite-sillimanite-graphite gneiss and calc-silicate which are in strike mostly E-W and dipping towards south. In the southern part of the region along AB line, major rock-types are hornblende-biotite gneiss, garnet-biotite-sillimanite-graphite gneiss and quartzo-feldspathic gneiss, which are mostly dipping towards north. The lithological and structural relations when plotted in a two-dimensional geological cross-section suggest the presence of syncline in the central part of the region with cross-section along the AB line.

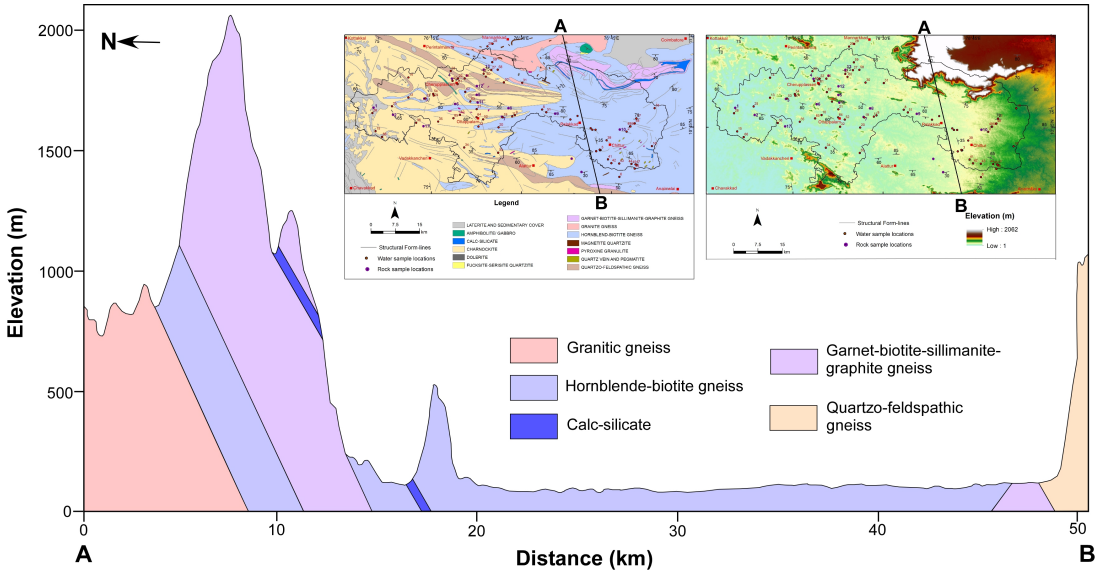

Fig. 4.5: Geological cross-section drawn across A-B along the eastern side of the study area.

Chapter 5

Petrology and Geochemistry

The chapter summarised the Petrographic description of all the studied samples and textural analysis. The rock chemistry for all the samples and its interpretation is also discussed. Mineral chemistry of all the major minerals are also analysed and discussed.

Chapter 5
Petrology and Geochemistry

PETROGRAPHY

Thin-sections were made out of all the samples from 21 locations for their petrographic studies and mineral chemical analysis. The major rock types of the study area are charnockite, felsic gneiss and hornblende-biotite gneiss. Charnockite is dominant in the western part while hornblende-biotite gneiss is present towards the eastern side of the study area. Samples AJ-1 to 8, AJ-11 to 14 and AJ-17 are charnockite and samples AJ-9 and 10 are hornblende-biotite gneiss (Fig. 5.1). These rocks preserve simple mineral assemblages and textures. This chapter discusses the two major rock types of the area and its geochemistry.

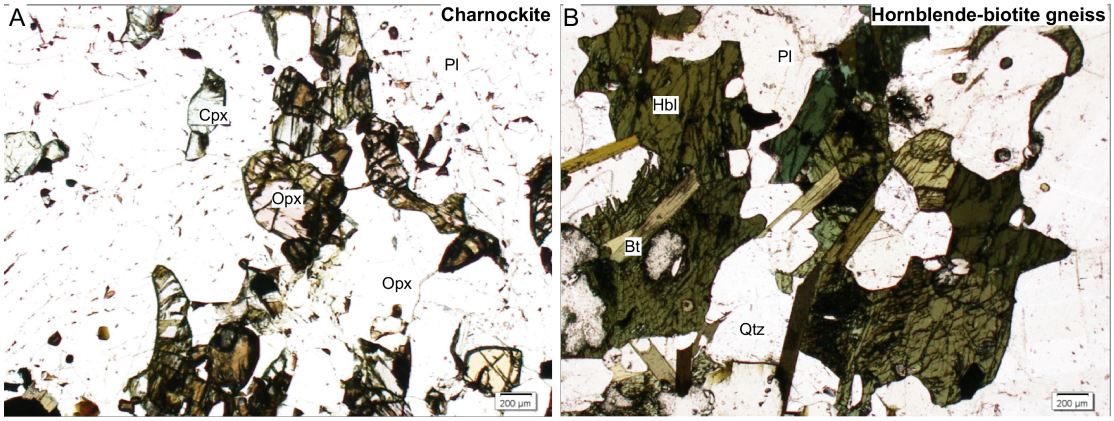

Fig. 5.1: *Photomicrograph of charnockite (A) and hornblende-biotite gneiss (B) from the study area*

Charnockite

Charnockite is mostly found in the western part of the study area. The rock mainly consists of felsic minerals like alkali feldspar, plagioclase, quartz and mafic minerals like orthopyroxene, biotite and minor amounts of hornblende (Fig. 5.1A). Orthopyroxene grains are around 0.5 to 1 cm in dimension. Biotite formed during

later stage is found asscociated with orthopyroxene. Plagioclase is found in very little amount compared to alkali feldspar in these charnockites.

Hornblende-biotite gneiss

This rock type occurs to the eastern side of Palakkad. The major mineralogy is hornblende, biotite, plagioclase feldspar and quartz. The rock is well foliated and the foliations can be easily observed. Hornblende and biotite are seen associated with each other. Plagioclase and quartz are found in moderate amounts. Alkali feldspar is absent in this rock.

Detailed mineralogical textural descriptions of the observed samples are summarized in Table 5.1 and discussed bellow:

Table 5.1 Petrological summary of all the samples from the study area

Sample no.	Orthopyroxene	Clinopyroxene	Hornblende	Alk.Feldspar	Plg.Feldspar	Spinel	Biotite	Rock type
AJ/1	□	—	△	○	□	—	□	Charnockite
AJ/3	○	○	△	○	□	—	□	Charnockite
AJ/4	—	△	△	○	□	★	□	Clinopyroxene gneiss
AJ/5	□	△	□	△	□	—	□	Charnockite
AJ/9A	—	—	□	△	△	—	□	Hornblende-biotite gneiss
AJ/9B	—	—	△	□	□	—	△	Hornblende-biotite gneiss
AJ/10	—	—	△	□	□	—	△	Hornblende-biotite gneiss
AJ/11A	—	—	△	□	□	—	□	Hornblende-biotite gneiss
AJ/11B	△	—	□	□	○	—	□	Charnockite
AJ/12A	□	□	○	□	□	—	★	Charnockite
AJ/12B	□	—	□	□	□	—	○	Charnockite
AJ/13A	—	—	△	□	□	—	△	Hornblende-biotite gneiss
AJ/13B	○	□	○	△	△	—	★	Charnockite
AJ/14	○	—	○	□	□	—	○	Charnockite
AJ/16A	—	—	—	□	□	—	△	Biotite gneiss
AJ/16B	—	—	△	□	□	—	△	Hornblende-biotite gneiss
	□	Abundant	△	Moderate	○	Less	★	Rare
	—	Absent						

Sample: AJ-1

This charnockite sample has fine-grained orthopyroxene with grain size varying between 0.5-0.4mm. Orthopyroxene grains are partly resorbed and rimed partly by abundant hornblende and minor biotite coronas (Fig. 5.2A). Hornblende coronas are also observed around the grain boundaries of quartzo-feldspathic minerals in the matrix (Fig. 5.2B). Minerals like apatite (~100 mm) are observed along with hornblende, plagioclase and quartz within the matrix assemblage (Fig. 5.2C).

Sample: AJ-3

This sample is equigranular and rich in hornblende with minor amounts of clinopyroxene and orthopyroxene (Fig. 5.2D). Most of the mineral grains are subherdral to euhedral with grain size varying between 1.5-2.0 mm. Biotite is found along the grain boundaries of orthopyroxene probably indicating late stage hydration during orthopyroxene breakdown. Matrix is rich in plagioclase with minor quartz and k-feldspar. Minor apatite and zircons are observed as inclusions within plagioclase in the matrix.

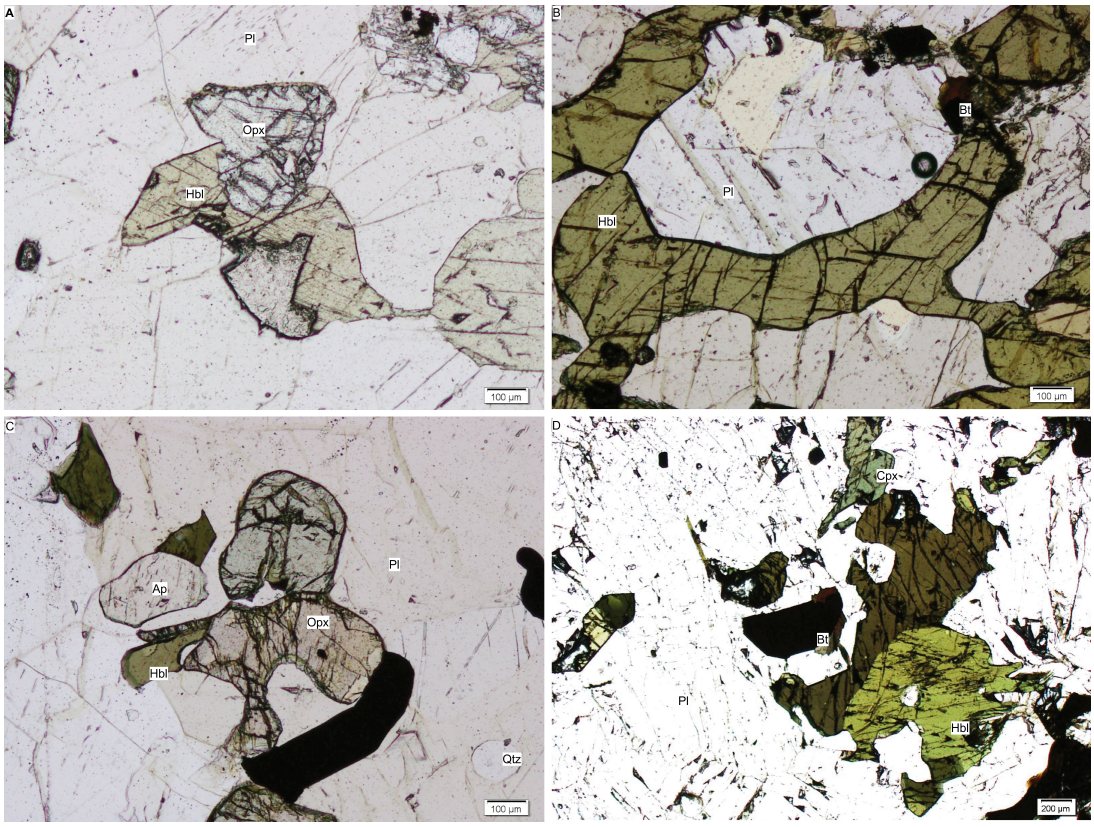

Fig. 5.2: Representative photomicrographs of samples AJ-1 and 3*. A) Orthopyroxene grains are partly resorbed and rimed by partly coronas of abundant hornblende. B) Hornblende coronas observed around the grain boundaries of quartzofeldspathic matrix. C) Minor occurrence of apatite (~100 mm) associated with orthopyroxene, hornblende, plagioclase and quartz. D) Enhedral hornblende with minor amounts of clinopyroxene and biotite.*

Sample: AJ-4

This is a clinopyroxene and hornblende rich gneissic sample. In certain domains hornblende-plagioclase symplectite associated with quartzo-feldspathic matrix and late stage biotite are observed (Fig. 5.3A). Orthopyroxene is absent in all the observed sections of this sample. Euhedral plagioclase and apatite is found as inclusion within clinopyroxene. Late stage biotite is formed along the grain boundaries of clinopyroxene and felsic matrix (Fig. 5.3B). Minor fine spinel grains have been also observed along with plagioclase in the matrix of this sample (Fig. 5.3C).

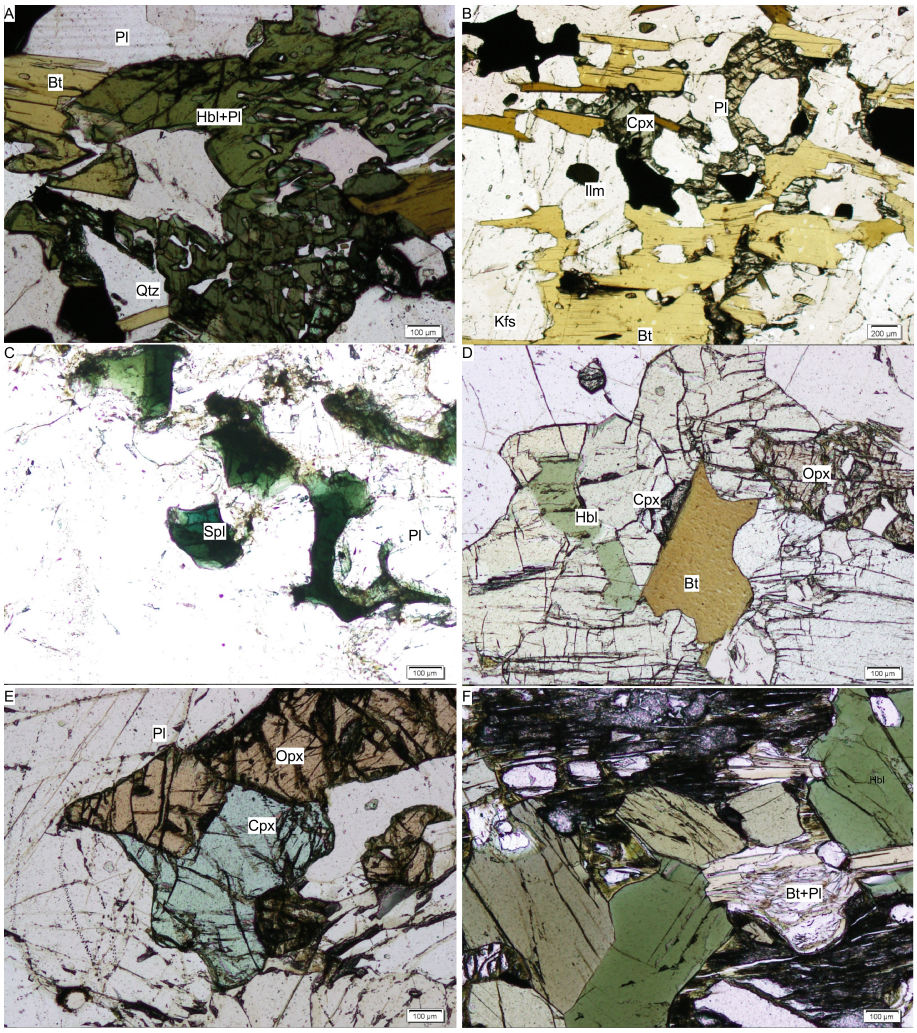

Fig. 5.3: Representative photomicrographs of samples AJ-4 and 5*. A) Hornblende-plagioclase symplectite associated with late stage biotite in quartz and feldspar matrix B) Late biotite formed along the grain boundaries of clinopyroxene C) Fine grained spinel observed along with plagioclase in the matrix. D, E) Clinopyroxene,*

orthopyroxene and hornblende assemblage in AJ-5 sample F) Late stage biotite-plagioclase intergrowth associated with hornblende.

Sample: AJ-5

This sample has moderate amounts of clinopyroxene, orthopyroxene and hornblende (Fig. 5.3D,E). The minerals have varying grain size and are mostly subhedral while biotite grains are deformed and altered (Fig. 5.3F). Clinopyroxene is abundant compared to that of orthopyroxene and is fine grained. Late stage hornblende is observed as partial coronas around resorbed clinopyroxene and later stage biotite replaces hornblende and grows along the grain boundary (Fig. 5.3F). This sample consists of relatively more alkali feldspar compared to that of plagioclase. Quartz is mainly associated with alkali feldspar and plagioclase. Quartz and biotite intergrowth is also observed in the matrix.

Sample: AJ-9A

This rock is rich in quartzo-feldspathic minerals in the lucosome domain (Fig. 5.4A). Biotite is seen along with fine-grained hornblende formed along the foliation.

Sample: AJ-9B

This is a feromagnesium domain rich in hornblende and biotite (Fig. 5.4B). Inclusions of plagioclase and quartz are found within porphyroblastic hornblende. Apatite inclusions are also found inside hornblende. Minor inclusions of hornblende are observed within plagioclase.

Sample: AJ-10

This hornblende-biotite gneiss sample consists of two generations of hornblende represented by green and brown colour (Fig. 5.4C). The green hornblende forms a

partial rim over brown hornblende that would have been formed in a later stage. Biotite is seen cutting across the grain boundary of hornblende and plagioclase indicating a later stage overprinting.

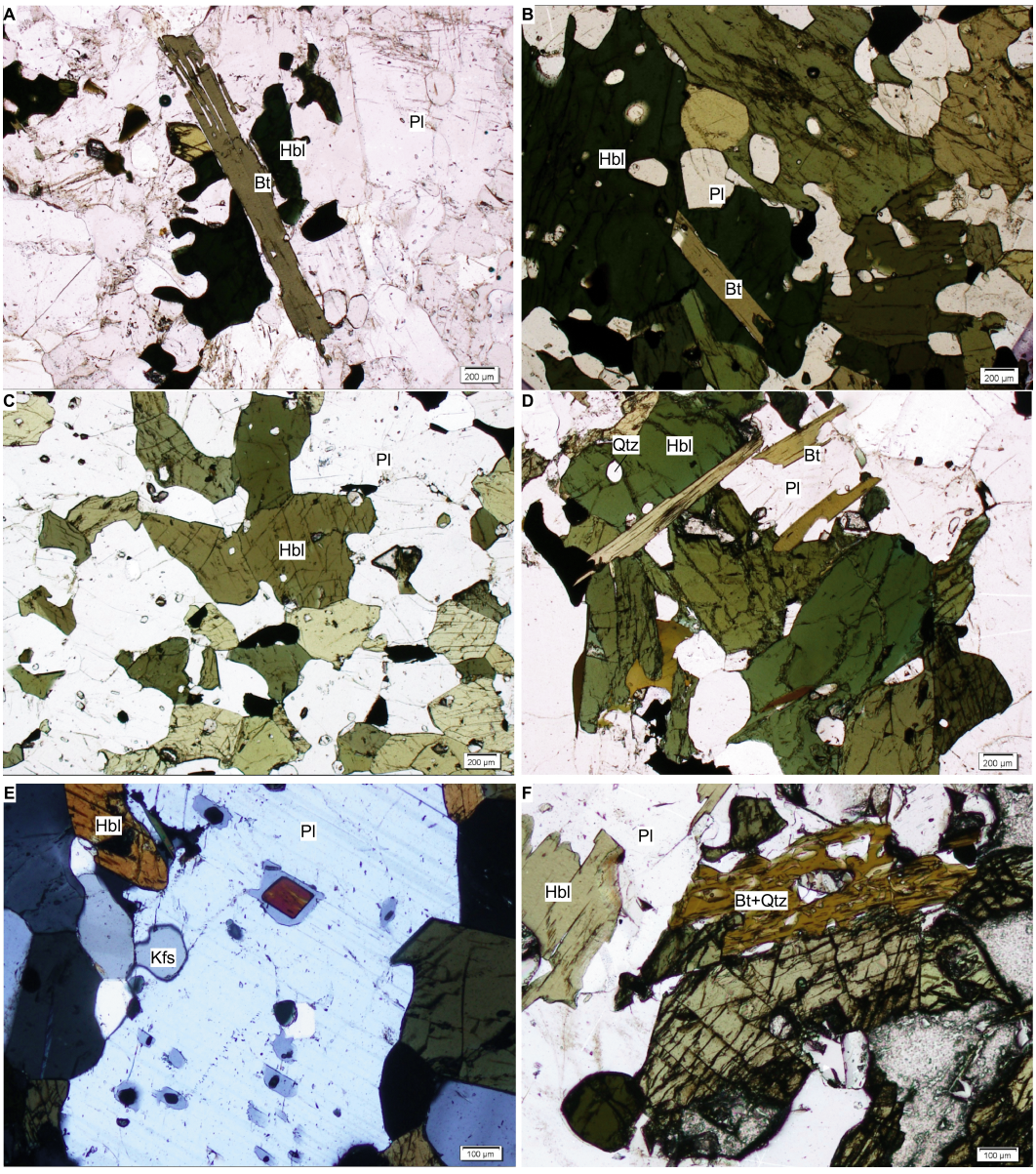

Fig. 5.4: Representative photomicrographs of samples AJ-9A,B, 10 and 11A, B*. A) Quartzo-feldspathic minerals with minor biotite and hornblende B) Inclusions of plagioclase and quartz are found within porphyroblastic hornblende C) This hornblende-biotite gneiss sample consist of two generations of hornblende (green and brown) D) Hornblende porphyroblast and late biotite growing across the grain*

boundaries E) Biotite-quartz intergrowth is observed in association porphyroblstic hornblende F) Inclusions of euhedral K-feldspar and hornblende are found inside subhedral plagioclase.

Sample: AJ-11A

This sample is an equigranular hornblende gneiss (Fig. 5.4D). Feldspar inclusions in hornblende and vice-versa indicate that both these minerals are in equilibrium. Late exsolution of ilmenite in hornblende as laths are observed. Later stage growth of biotite is seen along the cleavage plane. Inclusions of euhedral alkali feldspar and hornblende are found inside subhedral plagioclase (Fig. 5.4E).

Sample: AJ-11B

This section shows abundant fine-grained orthopyroxene with moderate amounts of hornblende and biotite. Alkali feldspar content is more than that of plagioclase. Biotite-quartz intergrowth is observed in association porphyroblstic hornblende (Fig. 5.4F).

Sample: AJ-12A

This is a equigranular clinopyroxene and orthopyroxene rich rock with less hornblende. The grain size varies between 0.1 to 0.2 mm. There is no biotite indicating very less hydration and late stage alteration.

Sample: AJ-12B

Orthopyroxene is found to have been breakdown to hornblende in this sample. Considerable amount of Ti in amphibole indicates that it would have come from the opaque minerals.

`Sample: AJ-13A

This sample is fine-grained equigranular hornblende-biotite gneiss (Fig. 5.5A). Apatite inclusions are seen inside hornblende.

Sample: AJ-13B

This sample has abundant coarse-grained clinopyroxene with minor amount of hornblende growing along the cleavage plane (Fig. 5.5B). Late stage orthopyroxene is found to have grown around opaque minerals and clinopyroxene. Ti exsolution from clinopyroxene grows in the grain boundary. Very late stage biotite growth can be seen though Ti content is very poor, restricted to one or two grains. This rock is mainly quartzo-feldspathic. Textures like myrmekite, perthite and anti-perthite can be observed.

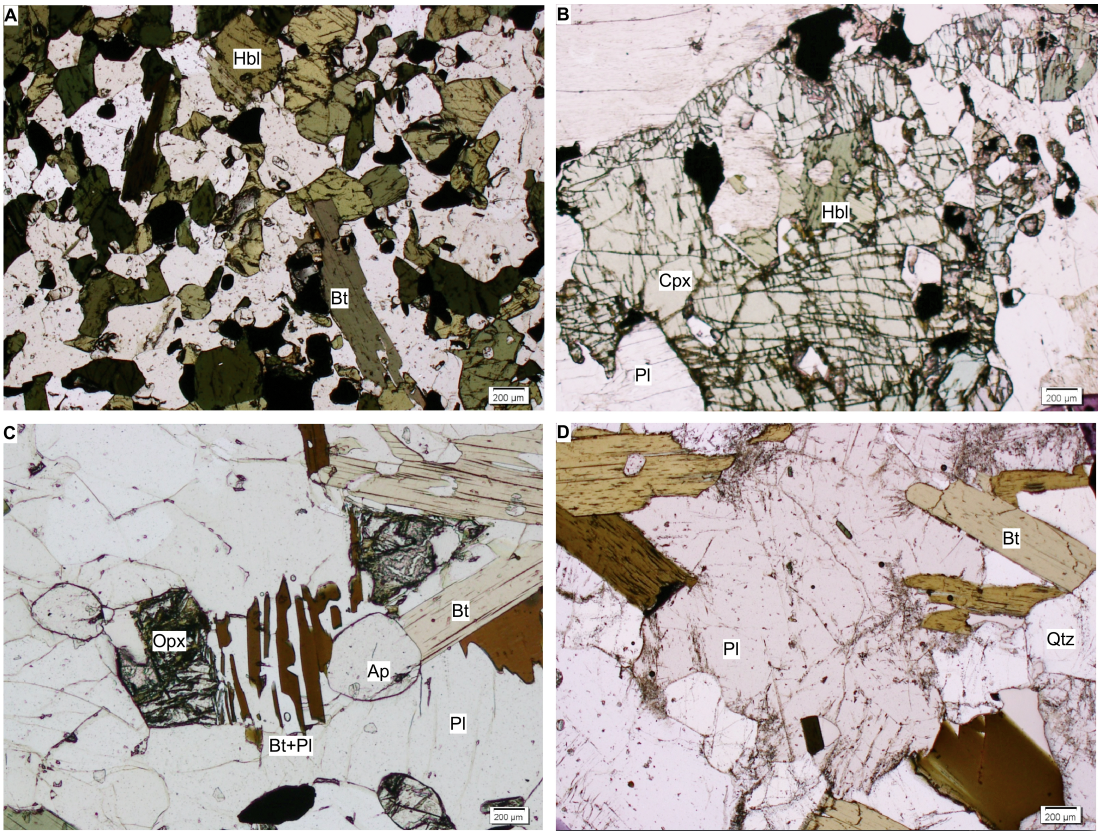

***Fig. 5.5: Representative photomicrographs of samples AJ-13A, B, 14, and 16A**. A)* Fine-grained equigranular hornblende-biotite gneiss *B)* coarse-grained clinopyroxene with minor hornblende growing along the cleavage planes *C)* Fine-grained partly altered orthopyroxene, and overprinted by biotite bearing assembalge *D) Biotite grains in the felsic rich biotite gneiss sample.*

Sample: AJ-14

This sample consists of fine-grained orthopyroxene, which are partly altered (Fig. 5.5B). There are no inclusions in orthopyroxene. Minor amount of hornblende is seen in association with orthopyroxene. Biotite is seen along the foliation layering and has formed after hornblende. Inclusions of quartz and feldspar are seen in hornblende. Myrmekite, anti-perthite and perthite textures are observed. Subhedral plagioclase has quartz inside it exhibiting poikilitic texture.

Sample: AJ-16A

This sample is biotite gneiss (Fig. 5.5C). Biotite is seen to be altering to chlorite.

Sample: AJ-16B

This hornblende-biotite gneiss sample has abundant hornblende and biotite in it. These minerals are found to be mostly equigranular.

GEOCHEMISTRY

Whole rock geochemistry analyses of 17 samples (13 charnockite, 2 hornblende-biotite gneiss and one biotite gneiss) were determined in this study. The results are presented in the Table 5.2. The whole rock chemistry of the charnockite gives: SiO_2: 61.76; TiO_2: 0.85; Al_2O_3: 16.24; FeO: 6.06; MnO: 0.09; MgO: 2.08; CaO: 4.50; Na_2O: 4.11; K_2O: 3.32; P_2O_5: 0.30 (Table 5.2): The Harker variation diagrams, FeO, CaO, TiO_2, and Na_2O shows a negative trend with SiO_2 whereas K_2O and MgO show a positive trend with increasing SiO2 while Al_2O_3 shows only scatter (Fig. 5.6). Charnockites have ~60.94 wt. % SiO_2 (<71 wt. %) (Fig. 5.6). These rocks have high-Al with Al_2O_3 >14.68 wt. % contributed by plagioclase and hornblende (Fig. 5.6). The Fe content (Fe_2O_3) is between 5-8 wt.% while Mg is about 0.3 to 4.8 wt.%. This indicates the presence of ferromagnesian minerals like orthopyroxene and hornblende. The alkaline content of the rock denoted by Ca, Na and K with CaO (2.7-6.7 wt. %)

Na_2O (3.5-5.3 wt. %) and K_2O (1.4-6.4 wt.%) (Fig. 5.6)are of the minerals like alkali feldspar and plagioclase feldspar. The presence of TiO_2 about 0.3 to 3.0 wt.% along with Fe and Mg is from the mineral biotite and amphibolite (Table 5.1).

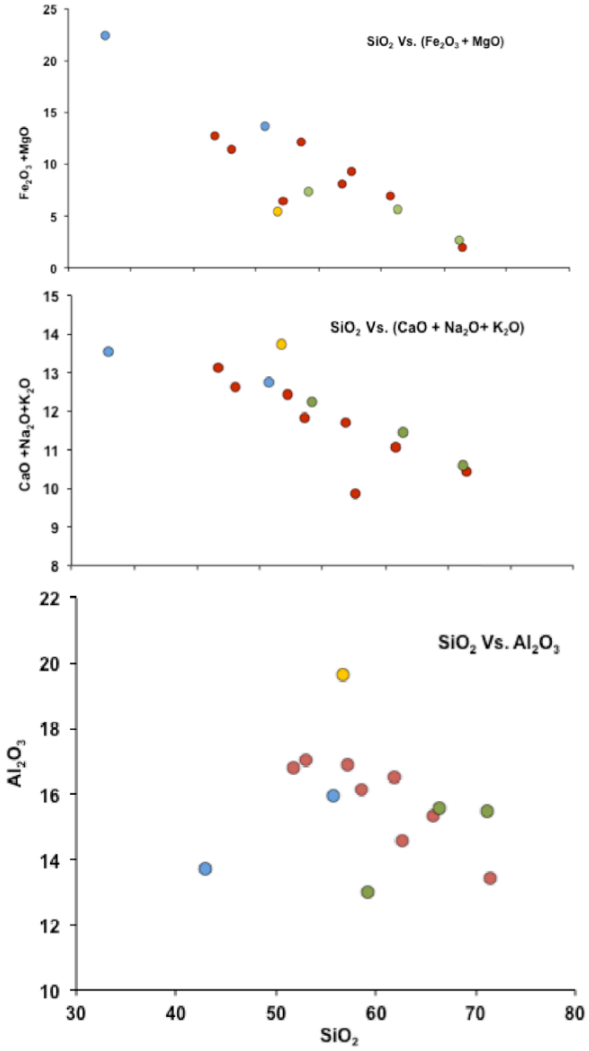

Fig.5.6: Harker variation diagrams for the major elements of charnockite and gneiss samples

The Trace and Rare Earth Element (REE) chemistry analyses shows abundance of Large Ion Lithophile Elements (LILE) like CS, Rb, Sr, Th, U and K when normalized to Upper Continental Crust (UCC) composition (Fig. 5.7), Taylor and McLennan,

1995). This elements are also are known to be mobile in nature due to their large ionic radius and indicates the fluid induced mobility in the crust. High field strength elements measured such Hf, Ti, Nb depleted when compared UCC, except for Zr that shows enriched pattern. Transition elements Ni, Cu, Cr also show abundance in which Co shows high abundance (Fig. 5.7).

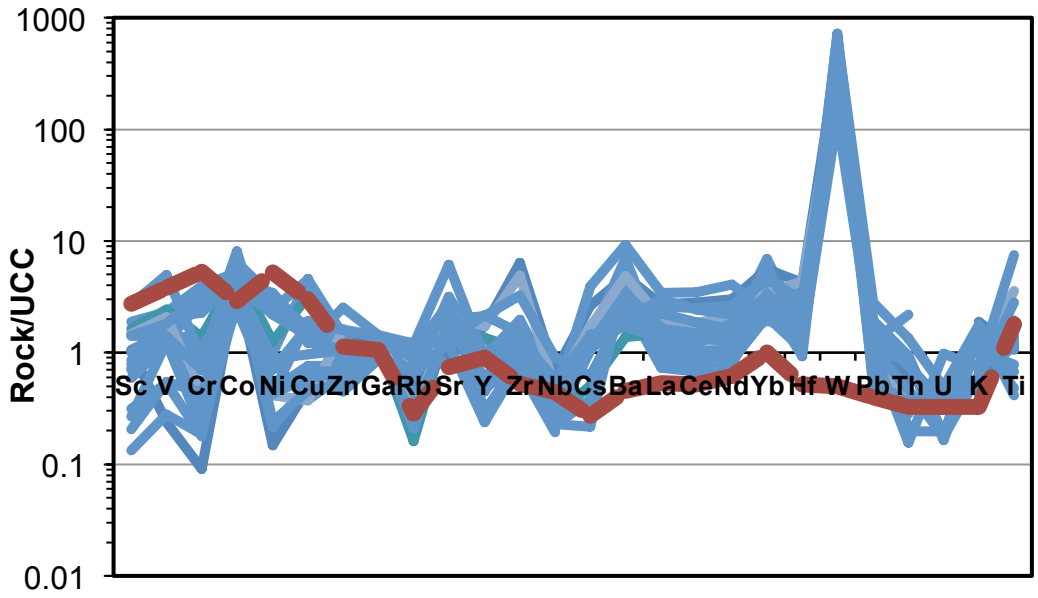

Fig. 5.7: Spider diagram showing Trace and Rare Earth Element (REE) chemistry analyses normalized to Upper Continental Crust values.

AFM plot (Fig.5.8A) indicates charnockites are derived from a magma with theolitic composition, may be anhydrous reduced basaltic source (Frost et al., 2001). Modified Alkali Line Index (MALI) diagram (Fig. 5.8B) shows that the charnockite samples are Calc – Alkaline to Alkali-Calcic. The charnockite samples are very iron rich - ferroan character (Fig.5.8C), which indicates, rock samples are derived by fractional crystallization or partial melting of reduced basaltic source (Frost and Frost 1997). A/CNK plot vs. SiO_2 plot (Fig. 5.8D) indicates that the protolith of both charnockite and the biotite gneiss may of sediment.

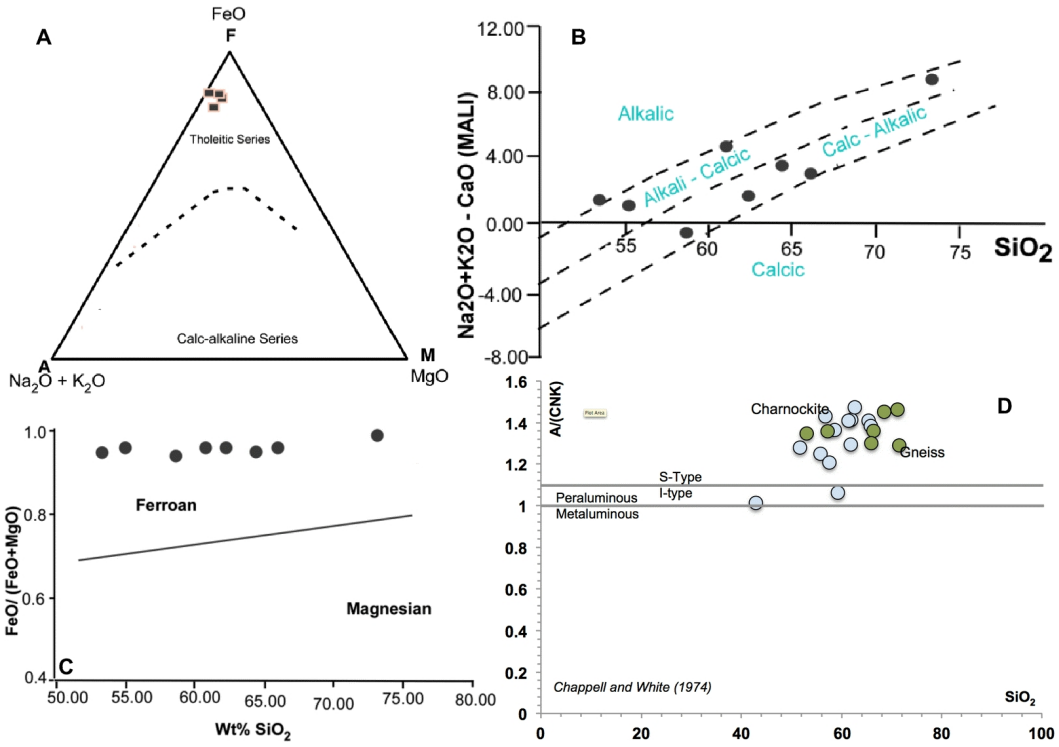

Fig. 5.8: Geochemical plots using the charnocite and gneissic samples from the study area *A) AFM diagram showing the boundary of tholeiitic lava (after Irvine and Baragar, 1971) B: Chemical classification based on Alkali content (boundaries modified after Frost et al. 2001) C) Fe-Mg variation in charnockite rock samples (after Frost and Frost 2008). D) A/(CNK) vs. SiO2 diagram showing aluminous nature of the samples (after Chappel and White, 1974)*

To conclude, the whole geochemical data reveals that the charnockite and biotite gneiss were crystallized products of fractionated theoliitic magma composition. The magma-differentiated was calc-alkaline, ferroan in their composition. A/CNK values also indicate sediment mixing with mamgma, making it peraluminous.

MINERAL CHEMISTRY

Major minerals present in charnockite are orthopyroxene, clinopyroxene hornblende, plagioclase K-feldspar and quartz.

Clinopyroxene

Clinopyroxene is observed only in clinopyroxene gneiss and some charnockite samples which has similar X_{Mg} range of 0.767-0.683 with Al_2O_3 up to 3.22. Most of the clinopyroxenes are augite ($Aug_{87.5-65.9}$) with minor calcium-Tschermak component (Ca-$Ts_{7.9-4.6}$) and calcum-Eskola content (Ca-$Es_{2.2-0.5}$)

Biotite

Biotite is observed all the analysed samples. The X_{Mg} ranges from 0.452-0.466. TiO_2 content is high, with a range of 6.59-6.70 wt%. Biotite in the charnockite occurs as a secondary mineral with slightly higher X_{Mg} (0.477-0.478) and lower TiO_2 content (4.55-4.75 wt%).

Hornblende

Hornblende is observed in only in the two-pyroxene granulite samples. The composition varies from K-Tschermakite to magneshio-hornblende (based on Leake (1978); Leake et al. 1997)) (Fig. 5.9). The TiO_2 content is relatively high ranging from 2.341-1.478 wt%. The X_{Mg} content varying from 0.982-0.523

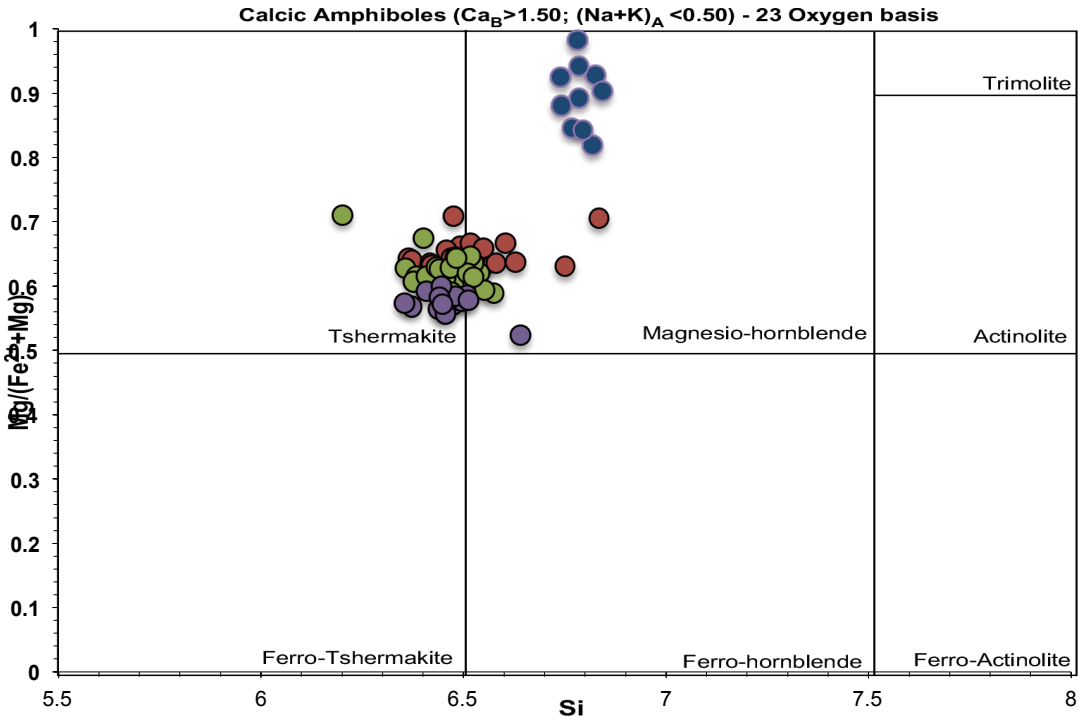

Fig. 5.9: Amphibole chemistry for all the studied thin-sections

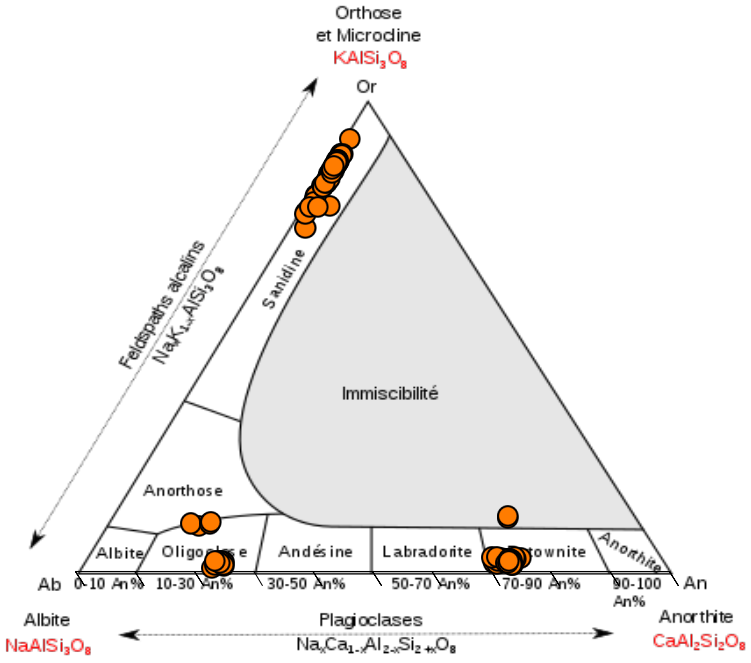

Fig. 5.10: Feldspar chemistry for all the studied thin-sections

Feldspars

In all the analyzed samples (Fig. 5.10), the major feldspar is plagioclase with minor to moderate amount of K-feldspar in charnockite and hornblende-biotite gneiss and has comparable composition. Plagioclases in chanockite ($Or_{1.8\text{-}1.3}Ab_{51.1\text{-}49.3}An_{49.0\text{-}47.6}$) and hornblende-biotite gneiss ($Or_{2.0\text{-}1.8}Ab_{48.8\text{-}48.4}An_{49.7\text{-}49.4}$) have similar composition. The plagioclase in two-pyroxene granulite is anorthite-rich ($Or_{1.5\text{-}0.9}Ab_{31.5\text{-}27.8}An_{71.4\text{-}67.0}$). K-feldspar composition ranges between $Or_{1.5\text{-}0.9}Ab_{31.5\text{-}27.8}An_{71.4\text{-}67.0}$ in charnockties and $Or_{1.5\text{-}0.9}Ab_{31.5\text{-}27.8}An_{71.4\text{-}67.0}$ in hornblende-biotite gneiss.

Table 4.2 Major and trace element data for all the samples collected from the study area

	AJ-1	AJ-2	AJ-3	AJ-4	AJ-5	AJ-6	AJ-8	AJ-9A	AJ-10	AJ-11	AJ-11A	AJ-11B	AJ-12A	AJ-12B	AJ-13A	AJ-13B	AJ-14	AJ-15	AJ-16A	AJ-17
SiO2	61.85	65.32	65.76	55.74	58.59	57.54	61.79	71.16	66.36	65.92	59.20	57.20	51.70	53.04	42.95	71.46	62.62	68.49	56.77	61.40
TiO2	0.777	0.659	0.391	0.584	0.840	0.976	0.542	0.241	0.564	0.511	0.615	0.529	1.79	1.41	3.74	0.206	0.696	0.339	0.913	0.778
Al2O3	16.53	14.68	15.31	15.95	16.12	15.63	17.72	15.48	15.57	15.14	12.99	16.91	16.81	17.03	13.72	13.44	14.55	14.69	19.66	15.77
Fe2O3	5.97	4.99	4.71	8.85	8.89	7.26	5.21	2.02	4.30	3.72	4.32	4.60	10.57	9.62	16.66	1.79	6.45	2.91	4.31	5.90
MnO	0.078	0.070	0.051	0.137	0.121	0.101	0.144	0.023	0.060	0.046	0.060	0.056	0.147	0.131	0.234	0.025	0.059	0.046	0.029	0.081
MgO	2.04	1.77	2.22	4.81	3.25	3.63	0.29	0.62	1.35	2.33	3.05	1.86	2.17	1.82	5.73	0.15	2.80	0.83	1.11	1.75
CaO	5.02	3.88	3.99	6.69	6.25	5.02	2.70	2.61	3.59	3.15	4.39	4.11	5.86	5.79	7.50	0.94	3.21	2.61	3.69	4.64
Na2O	4.27	3.84	3.60	4.04	4.14	3.55	4.58	3.70	3.83	2.99	2.17	4.03	4.44	4.69	3.55	3.53	3.39	3.86	5.27	4.29
K2O	2.41	2.69	3.46	2.04	1.43	4.40	6.40	4.28	4.01	5.50	5.69	4.30	2.84	2.16	2.49	5.95	3.28	3.64	4.78	2.26
P2O5	0.318	0.305	0.130	0.341	0.302	0.531	0.138	0.108	0.244	0.573	0.882	0.231	0.553	0.546	1.06	0.028	0.250	0.110	0.384	0.262
	99.26	98.19	99.62	99.17	99.94	98.63	99.50	100.24	99.88	99.87	93.37	93.81	96.88	96.23	97.64	97.50	97.31	97.53	96.92	97.12
Sc	11.6	7.8	11.6	20.9	17.9	16.1	11.5	3.5	8.7	6.5	7.9	9.4	16.2	15.5	29.9	1.5	15.6	2.3	3.0	11.1
V	92.2	77.9	80.1	138	146	122	14.3	32.2	68.6	72.0	76.0	83.7	124	83.7	297	16.6	110	32.6	74.3	83.5
Cr	34.5	32.4	50.5	138.1	48.1	79.2	3.2	6.2	15.0	118	100	40.1	15.4	9.9	31.4	6.4	116	15.3	7.3	24.1
Co	81.2	51.2	38.3	52.0	51.4	46.8	41.7	50.1	35.6	42.7	37.9	27.2	41.0	60.5	64.3	62.2	39.6	24.3	27.8	39.4
Ni	14.0	19.7	16.7	48.9	25.2	57.7	2.9	4.3	9.3	68.4	56.6	14.5	8.3	8.5	62.2	4.8	43.7	8.7	8.5	17.7
Cu	43.1	115	9.4	114	80.0	42.6	12.1	13.3	19.1	37.9	31.7	39.0	9.3	48.1	30.5	11.4	35.2	14.9	17.0	24.3
Zn	68.3	60.0	45.2	102	92.3	97.2	80.6	31.7	54.2	59.0	62.0	59.2	115	113	180	37.8	72.4	46.0	47.5	74.6
Ga	20.0	15.9	16.9	21.2	20.8	20.8	24.5	14.8	18.3	19.2	15.8	19.1	24.2	23.3	24.4	21.1	19.1	15.4	24.4	20.4
Rb	45.8	35.7	65.6	24.5	18.0	69.6	61.8	79.3	68.9	116	131	74.9	29.2	23.4	135	136	117	74.6	96.9	27.9
Sr	569	805	610	929	684	1115	319	943	674	970	2132	871	748	687	472	263	491	418	859	653
Y	22.2	12.3	10.9	29.3	29.7	20.3	38.0	6.6	10.6	9.9	19.9	18.5	37.7	47.2	47.4	18.2	21.5	5.2	10.5	13.0
Zr	269	234	134	161	202	376	1216	160	191	280	322	240	934	621	283	272	246	154	164	259
Nb	10.3	5.0	4.8	6.3	7.0	12.6	16.8	5.3	5.4	8.0	9.7	5.7	12.0	22.7	9.7	13.7	14.4	5.9	11.9	5.5
Cs	5.2	0.0	0.0	0.0	1.9	4.7	9.7	0.0	4.4	5.1	14.4	0.8	6.3	2.3	5.4	4.2	5.2	3.9	1.2	1.4
Ba	1183	1911	1507	899	762	2565	2650	3170	1808	3842	5047	2577	2654	1346	941	971	1101	1247	1869	1744
La	42.6	26.8	21.9	39.5	44.1	48.3	81.0	33.1	33.1	32.2	103	36.2	60.1	78.4	40.1	67.5	89.7	50.6	49.5	26.2
Ce	95.2	54.0	43.3	87.6	91.0	107	180	59.9	66.8	59.4	223	79.6	118	159	86.7	120	156	70.4	85.1	52.1
Nd	41.5	26.1	20.4	41.6	41.9	49.0	77.9	23.2	27.4	26.8	105	39.0	55.2	68.2	47.0	42.0	56.6	22.1	33.2	25.4
Yb	15.1	9.6	6.7	9.0	10.3	9.8	12.3	12.3	7.3	6.9	5.3	5.3	7.5	10.1	7.1	13.2	6.2	4.6	4.3	7.4
Hf	9.7	9.6	5.4	7.8	7.3	13.4	24.7	9.9	7.2	12.6	22.9	11.6	25.2	17.2	7.1	7.8	7.8	6.2	8.7	9.4
W	1445	1030	792	729	881	871	926	1365	775	725	614	432	510	672	256	1346	475	570	461	708
Pb	9.8	13.2	23.0	14.5	21.1	23.9	38.2	34.2	23.9	33.0	38.9	33.5	21.3	21.5	20.5	56.4	25.3	21.5	30.2	11.3
Th	3.7	3.0	3.5	2.4	2.0	5.6	5.8	8.9	2.3	2.1	10.1	2.0	3.5	5.0	1.7	14.3	23.5	8.9	8.3	3.8
U	0.0	0.0	0.0	0.0	0.0	0.0	0.0	0.5	0.0	0.6	0.5	0.0	0.0	0.5	2.7	1.4	0.0	0.0	1.0	0.0

Chapter 6

Hydrogeochemistry

Hydrogeochemistry of samples including major cations and anions, rare-earth elements and oxygen isotope results were discussed. The results are contoured and demonstrated on the map to assess the variations

Chapter 6
Hydrogeochemistry

Groundwater is a fundamental natural resource for the national economic growth and secures provision of drinking water, which plays a fundamental role in human resource development. Ground water is extensively used for domestic, industrial and irrigation purposes. The quality of ground water provides an insight into the geological history of rocks and indicates the processes involved in ground water recharge, discharge and storage (Walton, 1970). Variations in ground water quality, in an area are a function of physical and chemical parameters that are greatly influenced by geological formations and anthropogenic activities (Subramani et al., 2005; Magesh and Chandrasekhar, 2011). The chemistry of ground water is not only related to the lithology of the area and the residence time but it also reflects on the characteristic inputs from the atmosphere, soil, weathering processes, and also pollutant sources. This study was carried out to understand the chemistry of ground water and to delineate the role of rocks in the evolution of water chemistry (Table 6.1). The physical parameters like E_c, and pH measured in the field are discussed below.

Thematic maps and Interpretation

pH map: The pH map is generated using the data from chemical analyses results of water samples collected from 66 locations. The 3-dimensional pH map is made using the crated pH contour maps. The map suggests that pH varies from 5.16 to 7.73 in the study region and the eastern part of study area has high PH compared to the west (Table 6.1).

Salinity map: The 3-dimensional map for salinity across the study area is made using the crated contour-maps. The map suggests that Salinity varies from 0.03 to 0.5 in the study region and the eastern part of study area has high Salinity compared to the west (Table 6.1).

Table 6.1 Chemical analysis for the collected water sample

lab num	sample id	LAT-LONG	pH	Temp °C	Conductivity µS/cm	Salinity PSU	TDS µmol/L	DOC ppm	Si µmol/L	Alkalinity µmol/L	F µmol/L	Cl µmol/L	NO3 µmol/L	PO4 µmol/L	SO4 µmol/L	Na µmol/L	K µmol/L	Ca µmol/L	Mg µmol/L	HCO3 µmol/L	SSP µmol/L
10600	A16-1	N 10°44'33.5" E 76°41'47.6	6.670	26.800	723.000	0.341	484.410	3.599	894.000	4340.000	12.000	2365.000	321.000	-	398.000	2825.000	450.000	1580.000	644.000	5292.319	59.556
10601	A16-2	N 10°44'14.7" E 76°47'30.2	6.780	28.300	2.240	0.103	1.501	4.419	421.000	5924.000	22.000	10900.000	5287.000	-	813.000	3885.000	103.000	3395.000	3720.000	7222.917	30.329
10602	A16-3	N 10°41'10.5" E 76°43'10.5	7.560	31.600	435.000	0.185	291.450	1.633	340.000	4061.000	37.000	590.000	12.000	-	123.000	1075.000	23.000	1191.000	706.000	4936.454	36.661
10603	A16-4	N 10°41'08.3" E 76°43'04.9	6.640	27.600	736.000	0.341	493.120	1.679	695.000	5618.000	25.000	2078.000	104.000	-	335.000	2663.000	29.000	1252.000	1606.000	6850.962	48.505
10605	A16-5	N 10°40'59.7" E 76°42'26.1	7.140	28.200	699.000	0.319	468.330	2.065	692.000	4469.000	27.000	1596.000	719.000	-	383.000	2364.000	935.000	1392.000	649.000	5444.646	61.779
10606	A16-6	N 10°36'42.6" E 76°46'16.6	7.030	28.300	425.000	0.192	284.750	1.796	666.000	3310.000	41.000	786.000	128.000	-	199.000	1280.000	101.000	935.000	723.000	4033.867	45.443
10607	A16-7	N 10°46'51.1" E 76°39'20.1	6.900	26.900	682.000	0.320	456.940	1.562	991.000	3889.000	28.000	1784.000	712.000	-	520.000	2570.000	401.000	1244.000	969.000	4740.805	57.311
10608	A16-8	N 10°47'54.2" E 76°33'25.4	7.340	27.100	627.000	0.292	420.090	1.562	556.000	4274.000	32.000	1796.000	286.000	-	323.000	2065.000	77.000	1345.000	1022.000	5202.870	47.505
10609	A16-9	N 10°48'39.3" E 76°28'54.4	6.210	27.600	250.000	0.115	167.500	1.085	479.000	736.000	0.000	1392.000	196.000	-	15.000	1153.000	89.000	380.000	185.000	897.774	68.733
10610	A16-10	N 10°47'02.3" E 76°19'45.0	5.900	28.600	538.000	0.243	360.460	1.396	367.000	1308.000	18.000	3210.000	0.000	-	228.000	3588.000	297.000	387.000	286.000	1595.633	85.235
10611	A16-11	N 10°46'46.3" E 76°28'27.6	6.280	28.500	287.000	0.130	192.290	0.997	557.000	887.000	6.000	1611.000	60.000	-	59.000	1780.000	174.000	221.000	193.000	1081.933	82.517
10665	A16-12	N 10°46'15.7" E 76°38'07.6	6.840	28.300	549.000	0.249	367.830	2.615	527.000	2847.000	9.000	1945.000	274.000	-	385.000	163.000	4114.000	96.000	146.000	3470.933	94.645
10666	A16-13	N 10°49'54.4" E 76°11'10.5	5.900	28.100	144.000	0.068	96.480	1.157	435.000	1019.000	0.000	283.000	6.000	-	42.000	177.000	6222.000	386.000	795.000	1243.081	84.420
10667	A16-14	N 10°53'14.9" E 76°11'10.5	5.630	27.500	154.000	0.073	103.180	1.438	232.000	610.000	0.000	677.000	340.000	-	69.000	209.000	5856.000	364.000	683.000	744.168	85.278
10668	A16-15	N 10°44'19.0" E 76°05.43.2	5.550	27.800	143.000	0.068	95.810	2.285	123.000	236.000	0.000	363.000	62.000	-	31.000	443.000	63.000	64.000	61.000	287.910	80.190
10669	A16-16	N 10°41'49.5" E 76°51.42.9	7.390	29.100	1000.000	0.454	670.000	2.281	877.000	4200.000	23.000	2225.000	932.000	-	47.000	2496.000	107.000	2515.000	1800.000	5111.423	37.626
10670	A16-17	N 10°46'25.7" E 76°49.07.1	6.980	30.100	871.000	0.386	583.570	3.055	852.000	4708.000	21.000	3388.000	41.000	-	826.000	2965.000	79.000	1611.000	1636.000	5738.267	48.387
10671	A16-18	N 10°48'08.8" E 76°52.10.1	7.730	30.800	906.000	0.396	607.020	3.179	580.000	731.000	34.000	2084.000	0.000	-	778.000	3158.000	250.000	1573.000	2010.000	887.045	48.748
10672	A16-19	N 10°46'36.9" E 76°26.53.3	5.620	28.900	235.000	0.106	157.450	1.329	339.000	451.000	0.000	1125.000	557.000	-	22.000	1146.000	103.000	233.000	267.000	350.197	71.412
10673	A16-20	N 10°44'56.6" E 76°26.11.1	6.080	27.700	182.000	0.085	121.940	1.429	315.000	684.000	0.000	766.000	61.000	-	64.000	820.000	101.000	214.000	167.000	834.379	70.737
10674	A16-21	N 10°47'58.5" E 76°22.32.9	6.640	30.700	404.000	0.175	270.680	2.999	769.000	2873.000	9.000	981.000	21.000	-	225.000	1287.000	39.000	578.000	911.000	3503.527	47.105
10675	A16-22	N 10°53'04.5" E 76°19.25.8	7.200	27.800	140.000	0.067	93.800	1.207	227.000	690.000	0.000	381.000	73.000	-	50.000	429.000	40.000	248.000	186.000	840.465	51.938
10676	A16-23	N 10°53'78.8" E 76°17.73.0	7.200	28.400	523.000	0.237	350.410	1.135	1340.000	3334.000	18.000	241.000	0.000	-	1202.000	585.000	72.000	1563.000	966.000	4061.028	20.621
10677	A16-24	N 10°50'14.6" E 76°14.83.4	6.040	27.100	156.000	0.075	104.520	1.876	227.000	180.000	0.000	611.000	523.000	-	13.000	790.000	84.000	156.000	121.000	219.576	75.934
10678	A16-25	N 10°48'27.9" E 76°08.27.2	7.140	27.400	307.000	0.142	205.690	1.288	473.000	1926.000	12.000	668.000	93.000	-	193.000	838.000	50.000	747.000	341.000	2346.473	44.939
10679	A16-26	N 10°47'19.7" E 76°05.11.6	5.700	27.700	551.000	0.253	369.170	1.683	237.000	463.000	0.000	253.000	2.000	-	44.000	283.000	50.000	169.000	97.000	364.832	55.593
10680	A16-27	N 10°47'29.2" E 76°24.58.6	6.370	27.200	126.000	0.061	84.420	1.335	160.000	348.000	0.000	501.000	151.000	-	39.000	579.000	87.000	140.000	95.000	424.460	73.918
10681	A16-28	N 10°58'52.3" E 76°25.11.7	5.670	27.900	121.000	0.059	81.070	1.289	280.000	598.000	0.000	212.000	141.000	-	5.000	278.000	30.000	185.000	110.000	729.526	51.078
10682	A16-29	N 10°58'25.1" E 76°24.20.3	5.480	28.000	91.000	0.046	60.970	1.630	332.000	301.000	0.000	257.000	102.000	-	20.000	299.000	43.000	95.000	84.000	367.209	65.643
10683	A16-30	N 10°52'25.9" E 76°27.04.1	6.580	28.000	295.000	0.135	197.650	1.176	1496.000	2936.000	8.000	184.000	0.000	-	64.000	424.000	124.000	793.000	519.000	3580.555	29.462
10684	A16-31	N 10°52'21.3" E 76°30.06.9	5.530	28.400	144.000	0.068	96.480	2.307	136.000	290.000	0.000	1000.000	74.000	-	22.000	745.000	114.000	151.000	100.000	353.788	77.387
10685	A16-32	N 10°45'05.6" E 76°22.50.9	5.910	28.300	193.000	0.089	129.310	0.994	245.000	481.000	0.000	884.000	272.000	-	90.000	773.000	353.000	152.000	114.000	386.772	80.891
10686	A16-33	N 10°40'44.0" E 76°26.06.9	6.270	29.700	734.000	0.326	491.780	1.486	866.000	3197.000	19.000	3590.000	81.000	-	498.000	5111.000	52.000	687.000	578.000	3899.612	80.320
10687	A16-34	N 10°40'96.0" E 76°20.28.6	5.540	28.800	253.000	0.114	169.510	1.349	460.000	738.000	11.000	1053.000	20.000	-	210.000	1232.000	110.000	272.000	197.000	900.329	74.103
10688	A16-35	N 10°45'54.5" E 76°16.07.6	6.820	29.200	301.000	0.134	201.670	0.873	27.000	914.000	7.000	1041.000	376.000	-	150.000	1155.000	217.000	400.000	259.000	1114.342	67.553
10689	A16-36	N 10°45'42.8" E 76°11.89.0	5.160	27.700	89.000	0.045	59.630	1.145	347.000	133.000	0.000	416.000	84.000	-	3.000	441.000	44.000	60.000	43.000	162.258	82.483
11045	A16-37	N10°44'49.0" E076°41'30.4'	6.190	27.000	1040.000	0.493	696.800	4.781	959.000	3993.000	36.000	6377.000	250.000	23.000	726.000	4339.000	216.000	1442.000	1209.000	4870.704	63.211
11046	A16-38	N10°44'32.8" E076°42'19.6'	6.600	29.100	623.000	0.279	417.410	5.560	1091.000	5149.000	44.000	1103.000	63.000	26.000	370.000	2138.000	207.000	756.000	1367.000	6279.274	52.484
11047	A16-39	N10°42'47.2" E076°44'10.7'	6.810	27.000	611.000	0.238	409.370	9.065	932.000	5059.000	82.000	950.000	2.000	24.000	282.000	2512.000	51.000	868.000	1111.000	6167.988	56.429
11048	A16-40	N10°41'14.3" E076°43'01.4'	7.070	27.700	703.000	0.324	471.010	5.748	889.000	4812.000	69.000	2088.000	327.000	23.000	423.000	2468.000	43.000	1053.000	1329.000	5863.734	51.318
11049	A16-41	N10°39'38.7" E076°44'23.7'	7.070	25.100	651.000	0.316	436.170	4.518	562.000	4228.000	28.000	2227.000	48.000	18.000	440.000	2141.000	64.000	1210.000	1010.000	5152.092	49.831
11050	A16-42	N10°39'01.01" E076°44'57.7'	6.920	25.200	278.000	0.134	186.260	3.899	440.000	2095.000	28.000	350.000	0.000	17.000	92.000	716.000	26.000	623.000	428.000	2553.771	41.383
11051	A16-43	N10°38'56.2" E076°46'16.1'	7.030	38.000	466.000	0.178	312.220	5.980	763.000	2815.000	31.000	1555.000	0.000	17.000	434.000	1323.000	201.000	951.000	660.000	3430.615	48.612
11052	A16-44	N10°38'52.6" E076°48'18.7'	7.170	26.700	304.000	0.142	203.680	4.862	531.000	2438.000	30.000	687.000	0.000	16.000	153.000	1104.000	59.000	646.000	449.000	2969.957	51.506
11053	A16-45	N10°38'44.8" E076°49'10.0'	7.400	25.600	1029.000	0.502	689.430	4.256	1288.000	5745.000	54.000	2303.000	866.000	18.000	616.000	4522.000	69.000	2504.000	679.000	9425.169	59.056
11054	A16-46	N10°38'05.5" E076°48'50.8'	7.290	28.900	508.000	0.228	340.360	6.309	971.000	4872.000	53.000	514.000	37.000	20.000	226.000	762.000	201.000	1544.000	771.000	5932.246	29.378
11055	A16-47	N10°38'46.7" E076°48'58.8'	6.830	27.600	774.000	0.359	518.580	6.198	906.000	4126.000	28.000	2545.000	755.000	18.000	370.000	1852.000	95.000	1879.000	974.000	5030.311	40.563
11056	A16-48	N10°45'36.8" E076°48'52.0'	7.060	27.300	984.000	0.462	659.280	7.104	1017.000	9853.000	118.000	8156.000	135.000	24.000	1622.000	13072.000	112.000	1832.000	1846.000	12006.842	78.188
11057	A16-49	N10°45'06.0" E076°48'04.1'	6.620	26.600	513.000	0.240	343.710	3.646	2315.000	2805.000	0.000	1747.000	263.000	119.000	214.000	868.000	426.000	1268.000	698.000	3420.671	39.693
11058	A16-50	N10°45'06.0" E076°48'08.7'	6.710	27.400	811.000	0.378	543.370	4.240	1372.000	3716.000	46.000	4417.000	213.000	23.000	280.000	3196.000	77.000	1259.000	1010.000	4531.191	59.058
11059	A16-51	N10°47'28.5" E076°34.07.7'	5.960	27.800	293.000	0.134	196.310	4.144	591.000	505.000	7.000	1976.000	604.000	11.000	39.000	1439.000	235.000	345.000	247.000	616.044	73.875
11060	A16-52	N10°46'16.1" E076°23'37.5'	6.580	26.000	260.000	0.123	174.200	3.160	274.000	1252.000	9.000	978.000	0.000	11.000	201.000	720.000	50.000	419.000	360.000	1526.858	49.709
11061	A16-53	N10°49'47.0" E076°14.1'7"	6.550	24.100	159.000	0.080	106.530	7.241	441.000	533.000	7.000	934.000	0.000	10.000	6.000	673.000	69.000	241.000	166.000	650.029	64.578
11062	A16-54	N10°50'31.7" E076°15'18.2'	6.230	25.000	730.000	0.356	489.100	4.975	657.000	648.000	11.000	4315.000	285.000	20.000	258.000	3158.000	215.000	881.000	886.000	790.425	65.623
11063	A16-55	N10°52'41.3" E076°18'31.2'	6.080	25.900	279.000	0.133	186.930	2.623	517.000	707.000	7.000	1021.000	622.000	11.000	262.000	1135.000	67.000	344.000	293.000	862.436	65.362
11064	A16-56	N10°53'05.3" E076°20'33.7'	5.560	25.700	267.000	0.127	178.890	5.136	404.000	693.000	0.000	1775.000	465.000	10.000	25.000	1412.000	86.000	223.000	159.000	845.429	79.681
11065	A16-57	N10°53'52.1" E076°23'43.1'	5.470	24.800	119.000	0.060	79.730	6.073	381.000	429.000	7.000	667.000	96.000	9.000	15.000	561.000	0.000	162.000	109.000	523.330	67.428
11066	A16-58	N10°54'32.9" E076°25'62.7'	5.470	27.500	57.000	0.032	38.190	5.145	279.000	407.000	4.000	302.000	49.000	9.000	1.000	281.000	67.000	50.000	35.000	496.525	80.370
11067	A16-59	N10°55.48.0" E076°25.08.5'	5.670	27.300	98.000	0.049	65.560	5.455	401.000	575.000	0.000	331.000	254.000	10.000	4.000	428.000	100.000	109.000	67.000	701.467	75.000
10668	A16-60	N10°53'22.9" E076°24.04.6'	6.310	25.500	143.000	0.071	95.810	4.051	533.000	1119.000	8.000	276.000	0.000	12.000	21.000	510.000	58.000	225.000	136.000	1364.901	61.141
10669	A16-61	N10°52'08.8" E076°19'21.2'	6.740	30.000	265.000	0.117	177.550	6.708	1028.000	1406.000	12.000	799.000	0.000	15.000	146.000	766.000	73.000	331.000	457.000	1714.376	51.567
10670	A16-62	N10°50'51.6" E076°20'39.1'	6.630	25.800	193.000	0.093	129.310	5.460	408.000	1157.000	49.000	714.000	5.000	12.000	109.000	590.000	78.000	298.000	309.000	1410.937	52.392
10671	A16-63	N10°49'14.8" E076°21'29.5'	5.880	27.400	55.000	0.031	36.850	3.047	251.000	363.000	12.000	95.000	54.000	3.000	11.000	193.000	17.000	54.000	83.000	442.826	54.264
10672	A16-64	N10°46'38.3" E076°22'30.7'	6.450	26.200	208.000	0.099	139.360	2.061	321.000	455.000	4.000	954.000	400.000	4.000	62.000	904.000	74.000	222.000	190.000	554.943	70.360
10673	A16-65	N10°46'28.8" E076°18'40.8'	6.630	28.600	345.000	0.155	231.150	5.728	474.000	1335.000	9.000	1687.000	207.000	8.000	172.000	1048.000	937.000	316.000	247.000	1628.004	77.904
11074	A16-66	N10°43'22.4" E076°05'47.6'	5.540	28.300	137.000	0.065	91.790	4.094	382.000	350.000	10.000	915.000	18.000	3.000	11.000	818.000	115.000	90.000	75.000	426.985	84.973

Alkalinity map

The alkalinity map is generated using the data from the chemical analyses results of water samples collected from 66 locations. The 3-dimensional alkalinity map is made using the crated contour maps of Alkalinity. The map suggests that Alkalinity varies from 133 to 9828 in the study region and the eastern part of study area has high Alkalinity compared to the west (Table 6.1).

pH

pH is the measure of hydrogen ion concentration and thus determines the acidic or alkaline nature of the water sample. The pH of natural water is slightly acidic (5.0-7.5) as a result of dissolved carbon-di-oxide and organic acids (fulvic and humic acids) derived from the decay and subsequent leaching of plant materials (Langmuir, 1997). In this study pH values of the samples ranges from 5.14 to 7.73.pH value 5.14 measured at western part where as 7.73 shown at the eastern side.

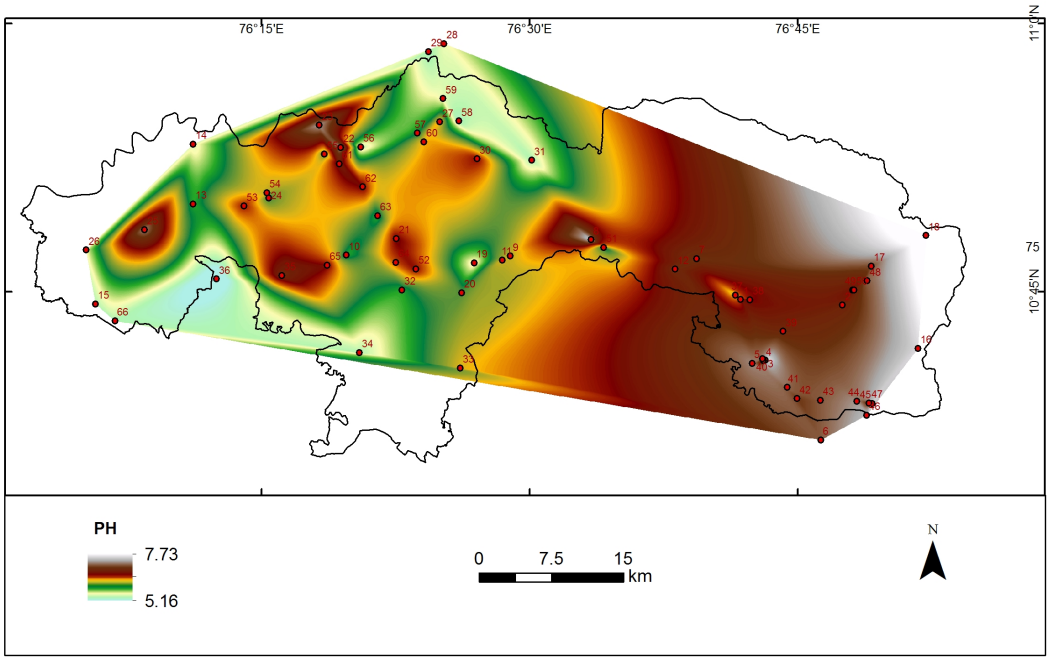

Fig. 6.1: pH variation map for the study area. *See text for description*

Electrical conductivity (EC)

Electrical conductivity is the measure of concentration of electrolytes in water in the form of ions (Kranth, 1987). It is measured in terms of microsiemens/cm. Most of the

inorganic salts, acids and bases when dissolved in water, make it a good conductor, while organics do not. The E_c values of water in the study area shows a hike in the eastern side and lowest values are recorded from the western side, which indicates the quality variations of ground water in two different litho units. The values of Ec ranges from 2.24µS/cm to 1040µS/cm. The highest values shown at the eastern side ie 1040µS/cm

Hydrogeochemical analyses were carried out to understand the chemical evolution of ground water in the study area. Major cations (Ca^{+},Mg^{2+},K^{+},Na^{+}) and major anions (Cl, F, SO_4, PO_4,NO_3) were analysed for 66 samples. The concentrations of these ions in the samples are given in the Table 6.1. The analyses were carried out in the Indo–French cell at IISc, Bengaluru, following all the standard analytical protocol. The evaluation of data was done by using common standard techniques of hydrochemistry, which includes graphical representations like Hill-Piper diagrams, Pie diagrams, Durovdigrams and schoeller diagrams.

Calcium

Calcium is a major constituent of rocks and soils. The principal source of calcium in groundwater is silicate minerals like feldspars, pyroxenes, amphiboles and carbonates like calcite and dolomite. Calcium concentration in the present study area varies from 50 to 5395µmol/L.

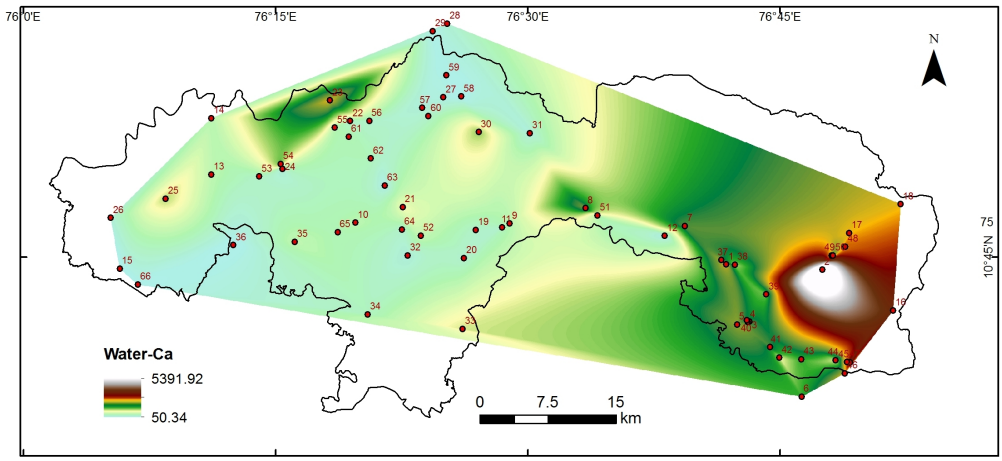

Fig. 6.2: Calcium variation map for the study area.

Magnesium

Magnesium is an important component of igneous, metamorphic and sedimentary rocks. Minerals like chlorite, serpentine, biotite, hornblende and olivine are the main sources of magnesium. Magnesium determines the hardness of water along with calcium. The concentration of magnesium varies from 35µmol/L to 3720µmol/L from the east to west of Palakkad area.

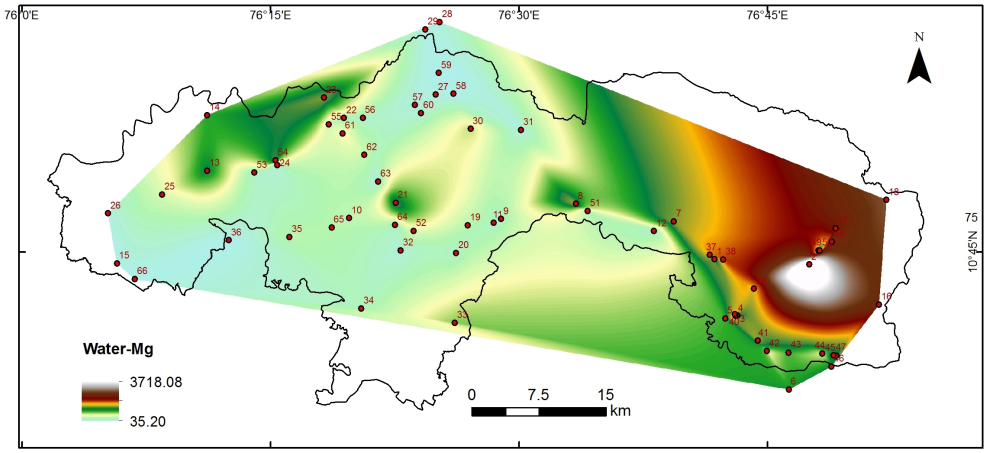

Fig. 6.3: Magnesium variation map for the study area

Sodium

Sodium salts are highly soluble in water and once leached from rocks and soils they remain in solution. The main sources of sodium in groundwater are plagioclase feldspar, feldspathoids and clay minerals. Sodium values ranges from 163µmol/L to13072µmol/L in the present study Fig 6.4

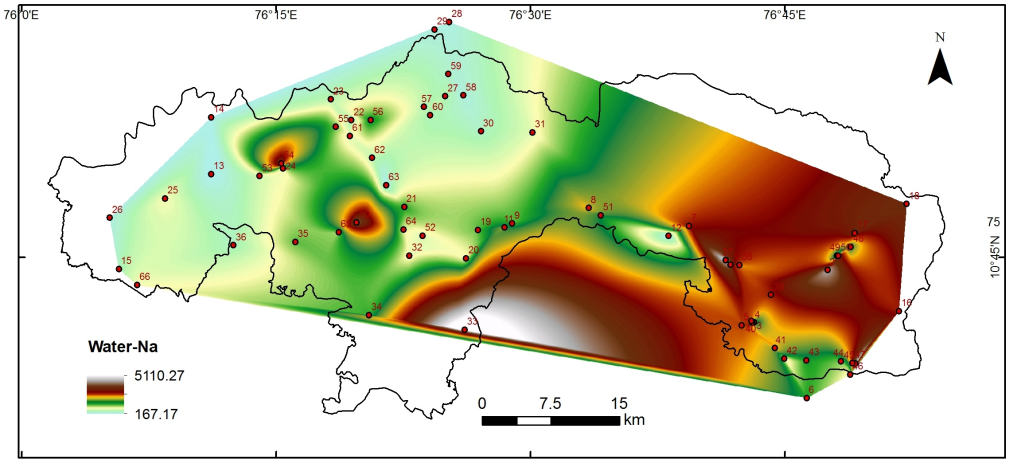

Fig. 6.4: Sodium variation map for the study area

Potassium

Potassium is abundant in igneous and metamorphic rocks. The concentration of potassium in ground water is a function of the rate of weathering of silicate minerals such as orthoclase, microcline and biotite. The concentration of potassium in most natural waters is very low due to the resistance of potassium minerals to decomposition by weathering and fixation of potassium in clay minerals (Golditch, 1938). Potassium value in the present samples varies from 0 to 6222µmol/L

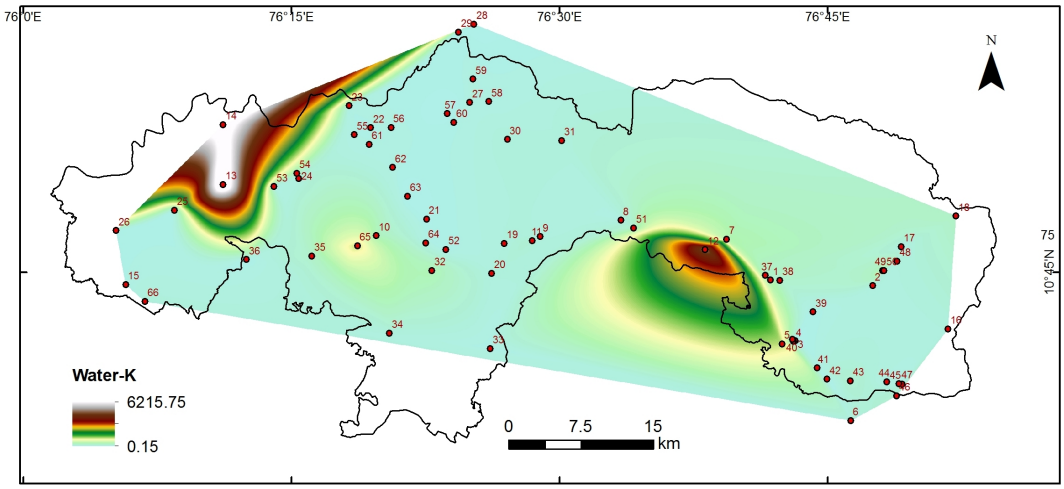

Fig. 6.5: Potassium variation map for the study area

Silica

Silica in ground water is a good indicator of weathering and percolating conditions. Silica released as a result of chemical weathering of silicate minerals, so the silica in ground water is mainly from water rock interaction. Silica value in the present study ranges from 27µmol/L to 2315µmol/L.The highest silica values shown at the eastern part compared to western side of the study area Fig. 6.6.

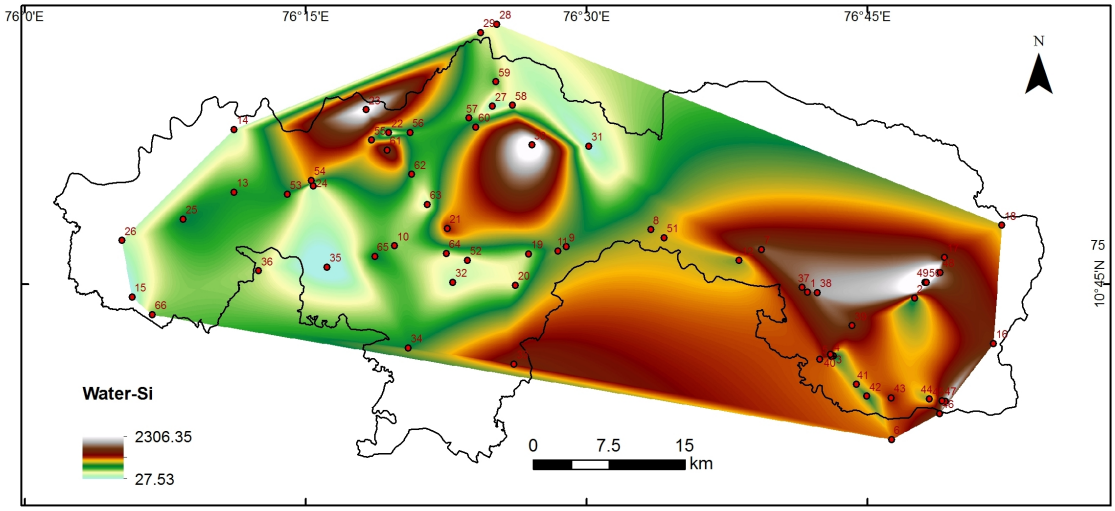

Fig. 6.6: Silica variation map for the study area

Chloride

The main sources of chloride are sodalite, apatite, mica and hornblende. In ground water they are present as sodium chloride. The chloride concentration of East to west of Palakkad region varies from 95µmol/L to 109000µmol/L

Nitrate

In groundwater, very small quantities of nitrates are present which are obtained through earth's hydrosphere and biosphere. The main source of nitrate in ground water is from the decomposition of organic matters. Presence of nitrates in the samples varies from 0 to 5287µmol/L

Sulphate

The sources of sulphates are sulphur minerals and sulphides of heavy metals, which are commonly found in the igneous and metamorphic rocks. The sulphur values in the present study varies from 1 to 1622µmol/L

Fluoride

Fluoride occurs in water as fluoride ions. The main sources of fluoride in ground water are fluorite and other hydroxyl minerals. In the present analysis fluoride values varies from 0 to 118µmol/L

Carbonates and bicarbonates

The primary sources of CO_3 and HCO_3 in ground water is dissolved CO_2. The solubility of CO_2 in water decreases with increase in temperature and pressure. Water charged with CO_2 dissolves carbonate minerals as it passes through soils and rocks, giving rise to bicarbonates. Carbonates and bicarbonates along with hydroxides are responsible for the alkalinity of water. In this study carbonate values were high along the eastern side and low from the western side.

Alkalinity

Alkalinity of surface and ground water is mainly derived from the dissolution of carbonate minerals and from CO_2 present in the atmosphere and from the soil above water table. Three carbonate species (HCO_3, H_2CO_3 and CO_3^{2-}) contribute to the total alkalinity, and their relative proportions being dependent on pH, and temperature. High alkalinity values are shows in the Eastern side of the study area than that of western part. 133µmol/Lto 9853µmol/L fig 6.7

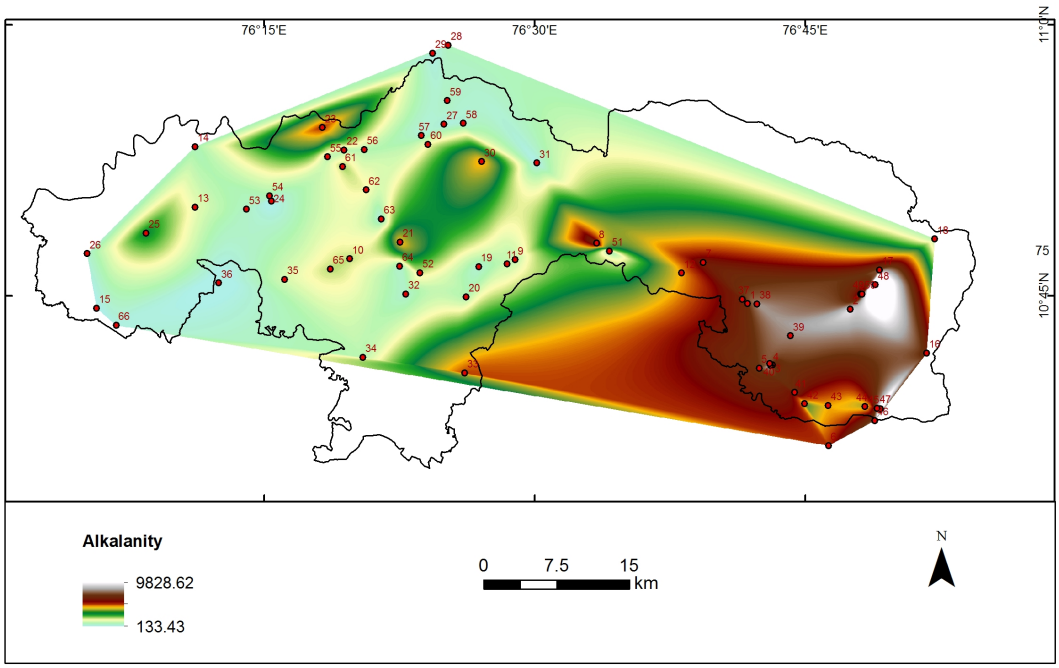

Fig. 6.7:* Alkalinity *variation map for the study area

Salinity

Salinity is the total concentration of all dissolved salts in water. It is a strong contributor to conductivity. Salinity is not measured directly, derived from the conductivity measurements. Calcium, Magnesium, sodium, Carbonates and chlorides are making up the salinity values in the ground water. Salinity in the present analysis varies from 0.03 to 0.5 PSU in the study region eastern part of the area has high salinity compared to the west. Fig 6.8. It is strange the western part is near to costal region .So it may be attributed to the rock types.

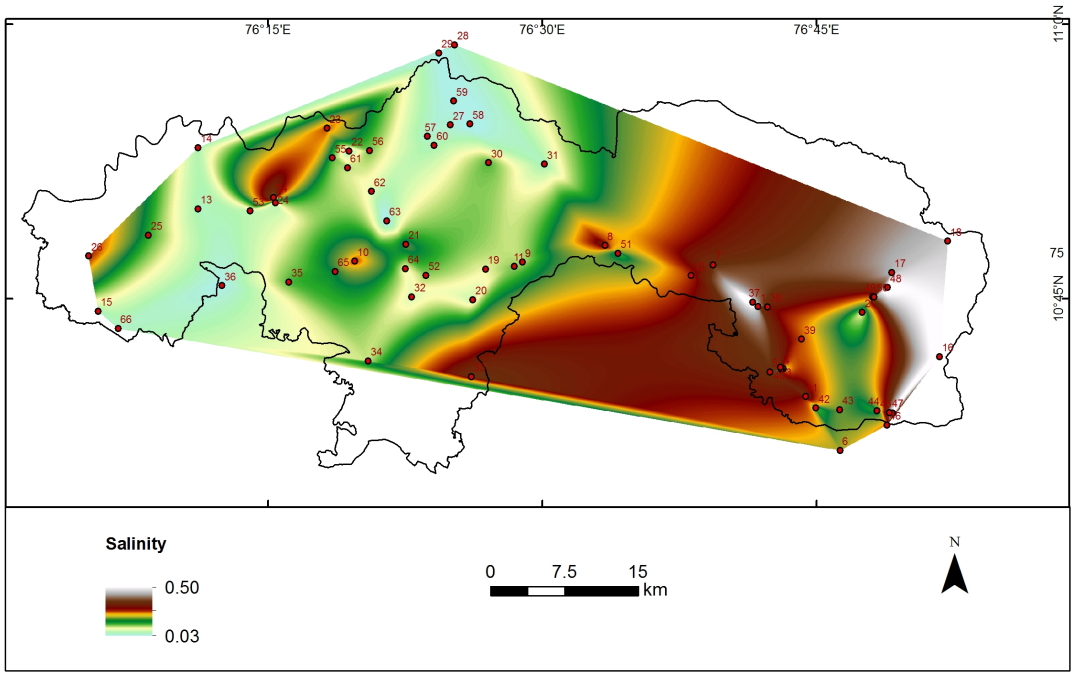

Fig. 6.8:* Salinity *variation map for the study area

Total dissolved solids (TDS)

Total dissolved solids (TDS), is defined as the concentration of all the dissolved minerals in the water. TDS is a direct measurement of the interaction between ground water and sub-surface minerals. TDS indicates the general nature of water and its quality. Hence high values of total dissolved solids in ground water indicates long time contact and interaction of ground water with the rocks and low values show that

they are attributed from some other sources. In the present study the total dissolved solids infers a water rock interaction scenario.TDS values in the present study ranges from 1.5008 µmol/Lto 696.8µmol/L

Piper-Hill Diagram

Graphical representation of chemical analyses enables us to understand the complex groundwater system better. The Piper-Hill diagram (Piper, 1953) is used to infer hydrogeochemical facies. These plots include two triangles, left triangle for plotting cations as a single point and the right triangle for plotting anions. The cation and anion fields are combined to show a single point in a diamond–shaped field, from which inference is drawn on the basis of hydrogeochemical facies concept (Back and Hanshaw,1965).The tri-linear diagram reveals the similarities and differences in chemistry of ground water samples as those with similar properties tend to plot together forming groups(Todd,1980).

Piper plot shows that most of the 66 groundwater samples from the study area fall in the region of $CaHCO_3$ type and NaCl type and in the tie line between them. The HCO_3 waters are very young and a common type of water in almost all the fresh water sources including groundwater. The NaCl waters are very common near the seashore due to salt water intrusion from the oceans and seas. In the present study the water samples near to the seashore are $CaHCO_3$ type, less alkaline and tend to have a lower pH because of their acidic nature. In contrast the eastern region which is away from the cost are NaCl type and are more alkaline with stable pH~7, the reasons for high NaCl in water are intense evaporation, salt water intrusion near beach environments and old water that have not participated in the hydrological cycle usually found in association with the oil fields known as Brines. In this study the possibility of brines and sea water intrusion are eliminated because the locations are 300 km away from the coast. Another possibility for salinity is the reaction of water with the saline minerals of rock and intense evaporation. Fig 6.9

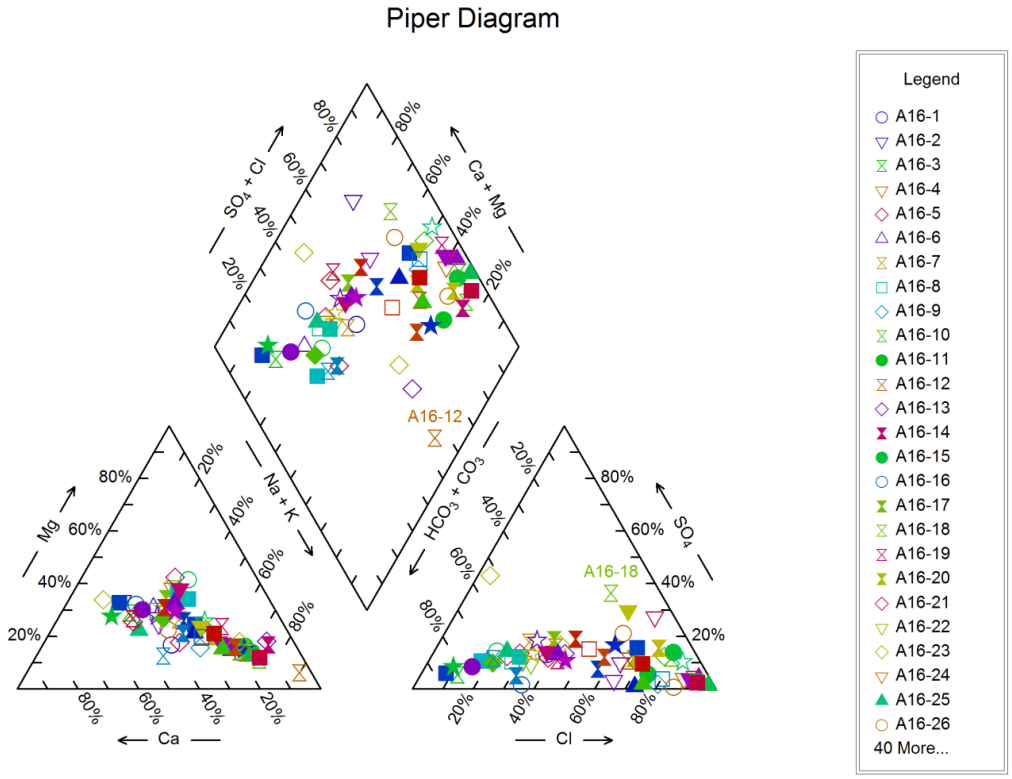

Fig. 6.9: Piper plot for 66 groundwater samples from the study area

Pie charts

Pie charts represent the total concentrations of major cations and anions of water samples by means of a circle. The segments of the circle are indicative of the percentage composition, in degrees. The diagrams of this type are most useful for indicating the composition of water on a geologic section or column. It provides a quick visual comparison of individual chemical analysis.

Pie charts are prepared for 66 samples. These charts indicate the percentile distribution of Si, Na, Mg, Ca, So_4, Cl,HCO_3, NO_2 and K. As per the pie charts it can be inferred that Si percentage is high in 18 samples that were collected from the eastern part of the area where charnockite is the major rock type. Few samples showing high Mg percentage were collected from the region where biotite gneiss is prominent. Other important inference from the pie charts is the hike in HCO_3 in 9

samples that were collected from the eastern region where the gneissic rocks are dominant. Mg and HCO_3 determines the alkaline nature of water hence the eastern part shows high alkaline nature. Fig 6.10

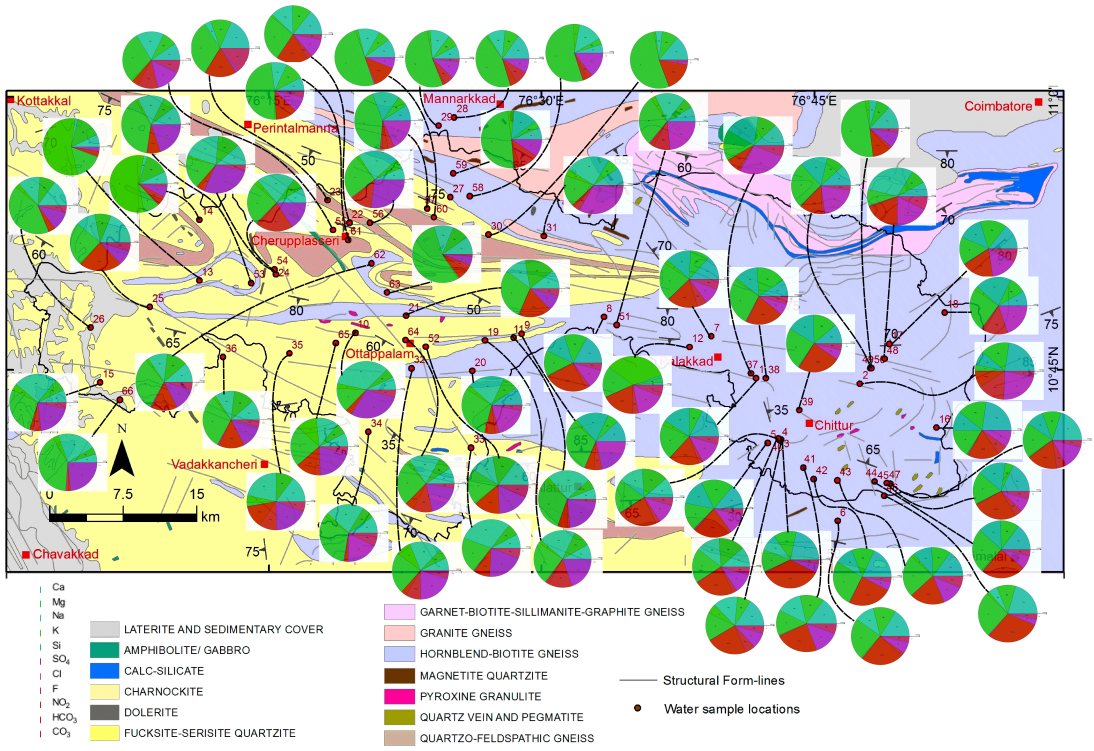

Fig. 6.10: Cation and anion composition plotted on geological map of the study area. *See Annexure 2 for detailed pie diagrams and enlarged print*

Water quality of the area

This study also attempts to determine the water quality index (WQI) of ground water collected from different locations in the study area. The chemical and physical analyses data obtained for 66 samples were observed in detail to develop a water quality index (WQI). 59 of the total samples collected are from open wells and 9 from bore wells. The study area extends from Alur in the west and to Chittur in the East. This region is bounded by the Western Ghats in the northern and southern side. This is one of the most populated regions of Kerala having a population density of 627 according to the district census handbook, Palakkad, Kerala, Census of India, 2011.

The major factors contributing to the pollution of groundwater is increase in anthropogenic wastes in the cities, runoff from rural regions, dumping areas, open defecations. Natural factors that change the chemistry of groundwater is rock-water interaction by contribution from the rocks and minerals through which water resides for a long time and interacts during its traverse.

A freshwater is the backbone of a healthy ecosystem. For a highly populated country like India water scarcity can cause instability in political, economic and social grounds. In humans about 80% of the diseases are caused by drinking water. However fresh water does not exist everywhere due to which in some parts of the world people are suffering from scarcity and contaminated water related problems. WQI is a well-known indicator of water quality proposed by Horton (1965). With time WQI of rivers as well as groundwater from several parts of the world has been reported. The WQI is based on the strong logic that some of the exclusively selected parameters can give a good indication of an overall water quality. (Prerna et. al., 2014, Cade, 2011) and it also allows us to infer the bulk quality of water (Zhenghui et al., 2012).

WQI determination

There are many different methods to calculate the Water Quality Index. The method adopted to calculate the WQI in the present study is from Sharma et. al. (2014), and Hameed et al. (2010). Among the physico-chemical parameters a total of 12 parameters were considered to calculate the WQI and each parameter was a given a definite weightage ($\mathbf{W_{ai}}$) ranging from 1 to 5 depending on its importance on the overall quality of water. The weightage values are of each parameter is taken from Sharma et. al. (2014). The weightage 5 is given to the parameter affecting the water quality most and 1 is assigned to the parameter affecting the least. The assigned weight of each parameter is shown in Appendix 3.

Relative weights (W_r) calculation: The relative weight of each parameter is the ratio of weightage of that parameter to the sum of weightage of all parameters (equation 1). The relative weight of each parameter is shown in Appendix 3

$$W_r = \frac{W_{ai}}{\sum_{i=1}^{n} W_{ai}} \quad (1)$$

Quality rating scale (Q_i) calculation: The next step involves the calculation of Quality rating scale **(Q_i)** for each parameter, measured as percentage, which is the ratio of the concentration of a parameter **(C_i)** in the water sample to its standard value **(S_i)** as mentioned in the WHO and BIS guidelines.

$$Q_i = \frac{C_i}{S_i} * 100 \quad (2)$$

For calculating the Q_i values for pH, another method is used which is on the basis of it's ideal value (Vi).The ideal value (V_i)for pH is 7 (Sharma et. al., 2014 and Abdul Hameed et. al. 2010). The calculation of $Q_{pH,}$is mentioned below.

$$Q_{i(pH)} = \frac{c_i - v_i}{s_i - v_i} * 100 \quad (3)$$

Sub Indices (SI) calculation: The Q_i values is used to construct the **Sub Indices**(SI) for each parameter, which is the product of relative weight **(W_r)** and Quality rating scale **(Q_i)**. Once the SI for each parameter has been calculated the sum of SI for each parameter constitutes the Water Quality Index **(WQI).**

$$SI = W_r * Q_i \quad (4)$$

$$WQI = \sum SI_i \quad (5)$$

The physiochemical parameters measured during the study were used to calculate the Water Quality Index (WQI), which is a powerful tool for determining the quality of water bodies. A total of 66 groundwater samples were analyzed all along the stretch of Palakkad district from east to the extreme west. The analytical results of different physical and chemical parameters show variations and some anomalies in different parts of the field. The study suggests that ground water in western Palakkad is more

acidic than ground water in the central and eastern side and does not qualify the WHO and BIS quality rating scale based on pH. Ground water in the western side of Palakkad is more susceptible to change in pH.

TDS values are higher in the Eastern side and are minimum towards the west of Palakkad, which can be related to the population density which is more in the eastern side. Most of the borehole wells show a trend of higher TDS values and open wells show lower TDS values.

Water with high E_c values indicates higher pollution level. (Pradeep, 1998; World Health Organization 2011; Mona and Shuchi, 2012).E_c values have a very similar trend as TDS. In general groundwater in the eastern side has more electrical conductivity than that in the west. Household wastes, detergents and organic wastes contribute majorly towards increase in E_c.

Alkalinity of water is the ability to neutralize the acidity produced through pollution. The collected samples show a range in alkalinity from 10 to 361 ppm. In general alkalinity also shows a similar trend, the ground waters of the western side of Palakkad district are less alkaline as compared to the eastern region. The high alkalinity is related to the excess bicarbonates, carbonates and organic acids such as hummic acids or it may be related to the overuse of artificial fertilizers.

Major cations and anions were analysed and results are discussed in the previous division. All the water samples in the central and western part does not show any anomalies in major cations. Most of them fall under the desirable limit prescribed by BIS and WHO. Some hike and anomalies are seen in the eastern side. Major anions show similar characteristics throughout the entire field.

Water Quality Index of water samples

The computed WQI of the 66 groundwater samples is shown in Appendix 3 which shows a wide range in quality indices ranging from 2.10 to an upper limit of 140.28 (Fig. 6.11). According to the scale suggested by Yadav et. al,. 2010, out of 66 groundwater samples, 9 samples are having either poor, very poor or unsuitable water

quality type and all of these lie in the eastern part of the study area, 9 water samples are have good water quality and 48 are of excellent quality type. According to the scale of Radhakrishnan et. al., 2010, most waters are of excellent or good quality and only one sample in the eastern side, A16-2 is unsuitable or poor quality. Fig 6.11

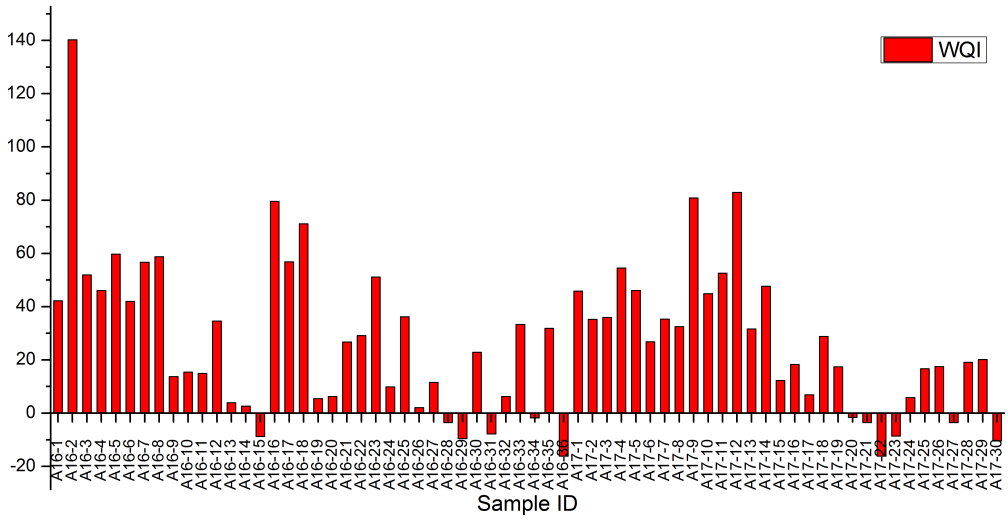

Fig. 6.11: WQI diagram for all the water samples

Reactions between groundwater and aquifer minerals determine the quality of groundwater. Groundwater chemistry of an area is controlled by different processes like evaporation and precipitation. Hence Gibbs plot is applicable in this study to differentiate the influences of rock water interaction. Gibbs recommended a simple plot of TDS versus the weight ratio of $Na^+/(Na^+ + Ca^{2+})$ and Cl^- / Cl^- + HCO_3 to delineate the rock water interaction, evaporation and precipitation on water chemistry Fig (6.12A,B). The data points in the figure illustrates that most of the samples of Palakkad region fall in the water–rock interaction field, which suggests that water-rock interaction controls the maximum levels of quality parameters of water in the present study.

Sodium is an important ion used for the classification of water on the basis of its suitability for drinking as 'suitable for drinking purpose', 'doubtful' or 'unsuitable' for drinking. Percentage of sodium is widely used for assessing the suitability of water

for irrigation purposes (Wilcox 1995). Na^+ is expressed as percentage sodium or soluble–sodium percentage (% Na). The Na^+ % is calculated using formula

$$Na^+\% = [Na^+ + K^+/Ca\ 2^+ + Mg\ ^{2+} + K^+ + Na^{2+}] \times 100$$

In sodium percentage Wilcox plot, Fig (6.12C) illustrates that out of 66 samples, the maximum samples falls in 'very good' to 'good limit'. Only 4 samples fall in the doubtful area and no representation shows unsuitable limit. Na^+% show a good result for drinking quality of ground water for the entire area.

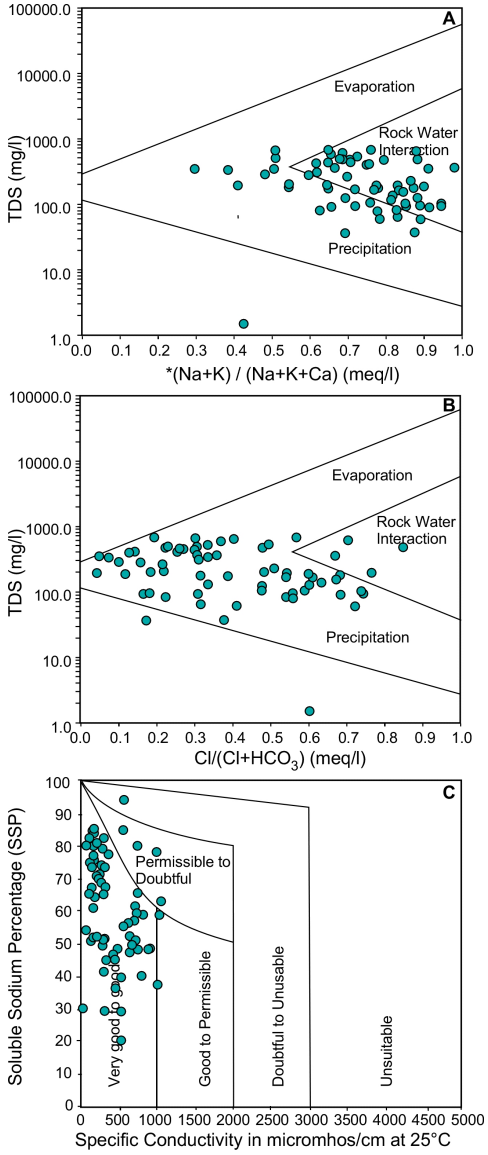

Fig. 6.12: Gibbs (A,B) and Wilcox (C) plot for the water samples studied.

Oxygen Isotopic Analysis

Isotopic techniques are effective tools for fulfilling hydro geochemical needs. Commonly stable isotopes are used for these analyses: however the most commonly used are those of hydrogen and oxygen. In the present study we have analysed the water samples for ^{18}O. Variations in stable isotope ratios of natural compounds are controlled by chemical reactions. The stable isotopes are usually measured using an isotope ratio mass spectrometer.

Oxygen Isotope chemistry of 32 water samples across 3 seasons of pre-monsoon (PR), monsoon (MO) and post-monsoon (PO) were determined using the Ion Ratio Mass Spectrometer (IRMS) facility at Centre for Earth Sciences (CEaS), IISc Bangalore (analytical conditions are described in Chapter 3). Seasonal variations have been found in all seasons in 3 seasons.

$\delta^{18}O$ values for the pre-monsoon seasons varies from -5.09 to -0.97 ‰, while for the monsoon season it ranges from -1.33 to 8.54 ‰ and post-monsoon it varies between -2.95 to -1.35 ‰,when compared with the standard SMOW. On the other hand, the local marble (Walayar) shows highly depleted $\delta^{18}O$ values of nearly 20‰indicating that it might have deposited in shallow crustal level non-marine environment (Kasting et al., 2006) (Fig. 6.13). Such marked differences in the oxygen isotopes points to effect of precipitation and climate (temperature)on the ground water (phreatic water). As understood, the high temperature causes rapid evaporation and leading to the concentration of the heavy ^{18}O isotope in the ground water.

While the oxygen isotope is related to the climatic conditions the water chemistry is much governed by the host rocks. The host rock composition contributes to the quality of the groundwater, as shown by the alkalinity and pH conditions of the water (see Fig. 6.14). As discussed before, in this Chapter, country rocks in the study area i.e., charnockite and biotite gneiss, are peralumnious in nature and are rich in alkalis. The high content of major elements such as silica in the samples shows the influence of host rock in the ground water quality.

However, Rare Earth Element (REE) concentration in all the samples is found to depleted, regardless of the seasons (Fig. 6.14), although there are a few anomalies present. This indicates to the fact that very few REE has been mobilized to the groundwater from the rocks that accommodated in all season. The mobilization of REE in rocks is caused during high temperature metamorphism and by brine fluids having (highly alkaline) passing through the rocks. But, the alkaline index of the water is not high that it is portable for drinking and can be used for agricultural uses. Hence the two possible mechanisms by which the REE could be released to the ground water are by weathering /erosion of soils and by the anthropogenitic activity. It is important to determine the geochemistry of the weathered rock profiles nearby the sampling sources and to compare its chemistry to that of the ground water. The study area- Palakkad District- is known for cultivation. Therefore, the contribution of the agricultural activity in the quality of the ground water should also be examined, which will be helpful to check the groundwater getting contaminated through the usage of agro-chemicals.

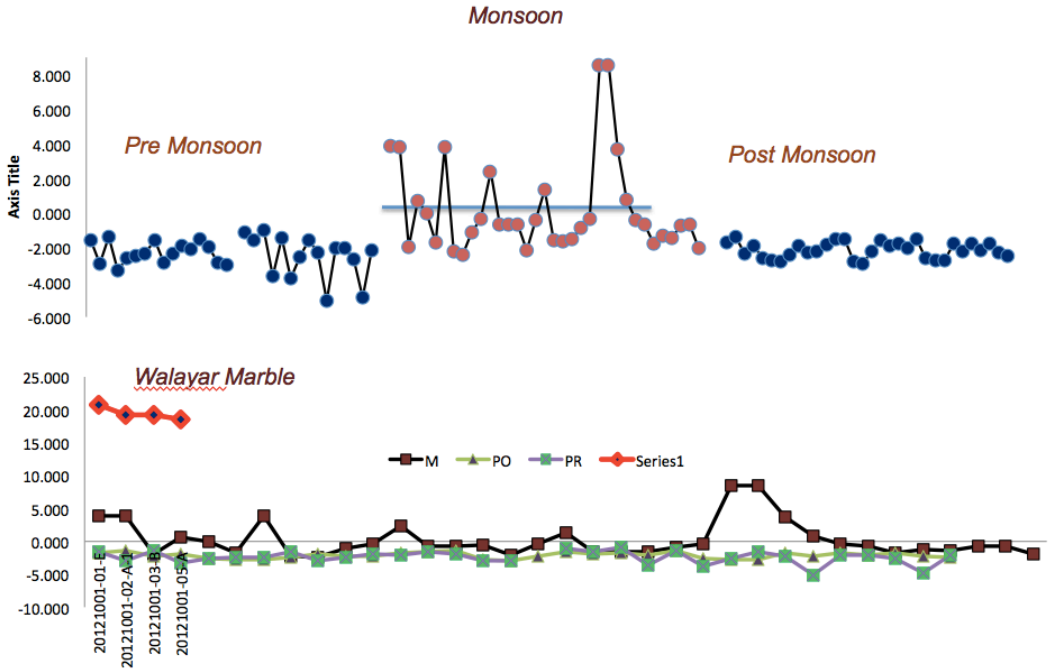

Fig. 6.13: Oxygen isotope data for the seasonal water samples

Table 6.2 Oxygen isotope data for seasonal water samples

LAT	LONG	pH			Conductivity (µS/cm)			Salinity (PSU)			18O		
		PR	M	PO	PR	M	PO	PR	M	PO	PR	M	PO
N10.45.908	E076.16.113	5.4	5.4	5.2	292.4		292.6	0.1529		0.153	-1.578	3.869	-1.355
N10.46 .954	E076.19.742	6	5.2	5.8	556		0.2756	0.2934		523	-2.903	3.846	-2.325
N10.47.967	E076.22.551	6.2	6	6.1	398	393	381	0.2086	0.206	0.1996	-1.400	-1.971	-1.697
N10.53.073	E076.19.434	7.1	6.4	7.4	310	171.7	171.4	0.1621	0.0906	0.0905	-3.295	0.698	-1.900
N10.58.405	E076.24.335	5.6	5.1	5.4	156.5	122.9	130.3	0.0829	0.066	0.0697	-2.592	0.003	-2.625
N10.58.877	E076.25.207	5	5.1	5	104.7	113.2	70.6	0.057	0.0612	0.0404	-2.482	-1.677	-2.755
N10.52.213	E076.30.069	5.2	4.4	4.5	136	143.7	146.5	0.0726	0.0765	0.0779	-2.364	3.799	-2.806
N10.53.788	E076.17.730	6.7	6.9	6.7	493	519	430	0.2594	0.2734	0.2257	-1.591	-2.194	-2.436
N10.50.146	E076.14.834	5.9	4.5	5.9	216.8		282.6	0.1137		0.1478	-2.874	-2.380	-1.917
N10.49.936	E076.11.247	6.9	5.1	6.8	117.9	100.7	52.7	0.0636	0.0551	0.0316	-2.364	-1.140	-2.271
N10.45.428	E076.11.890	4.9	4.5	4.4	75.4	88.2	84.3	0.0427	0.0489	0.047	-1.885	-0.303	-2.236
N10.44.522	E076.41.732	6.4	6.2	6.4	735	963	669	0.3911	0.5174	0.3549	-2.057	2.398	-1.814
N10.44.237	E076.47.503	6.8	6.3	7.1	571	1231	63.1	0.3015	0.6682	0.0368	-1.499	-0.661	-1.520
N10.40.978	E076.42.449	6.9	6.7	6.8	793	748	652	0.423	0.3982	0.3456	-1.974	-0.655	-1.470
N10.38.702	E076.46.278	6.7	6.5	6.6	351	510	401	0.1837	0.2686	0.2102	-2.876	-0.637	-2.810
N10.37.991	E076.52.175	7.4	6.9	7.6	1002	1063	190.2	0.5392	0.5734	0.1	-3.014	-2.145	-2.955
N10.41.814	E076.51.715	6.8	6.9	6.9	580	1399	73.4	0.3064	0.7637	0.0418		-0.404	-2.185
N10.46.715	E076.49.388	6.5	6.7	6.7	631	597	645	0.3342	0.3157	0.3418	-1.110	1.337	-1.576
N10.47.644	E076.53.028	6.8	6.5	6.9	555	622	503	0.2929	0.3293	0.2648	-1.575	-1.591	-1.909
N10.46.333	E076.40.484	6.7	6.5	6.4	437	515	397	0.2294	0.2713	0.2081	-0.979	-1.632	
N10.46.254	E076.38.124	6.2	5.8	6.1	490	404	439	0.2578	0.2118	0.2305	-3.622	-1.511	-1.769
N10.47.065	E076.36.404	5.6	5.3	5.2	288.8		256.8	0.151		0.1343	-1.426	-0.831	-2.028
N10.47.895	E076.33.436	6.5	6.4	6.4	530	52.1	614	0.2794	0.0316	0.3249	-3.792	-0.354	-1.482
N10.46.986	E076.28.906	5.3	4.8	5.3	201.7	96.8	183.1	0.106	0.0531	0.0964	-2.533	8.528	-2.587
N10.44.307	E076.05.719	5.4	4.4	5.1	89.5	298.3	90.5	0.0496	0.156	0.0501	-1.596	3.695	-2.746
N10.47.567	E076.05.743	5.2	5	5.3	170.6	116.7	144.2	0.09	0.063	0.0767	-2.264	0.798	-2.747
N10.53.260	E076.11.394	5.4	4.6	5.1	200	124.9	187.6	0.105	0.067	0.0987	-5.09400939	-0.408	-1.784
N10.46.635	E076.26.785	6.4	6.5	6.5	287.6	219.6	337	0.1504	0.1151	0.1763	-2.021	-0.644	-2.243
N10.44.936	E076.26.182	6.5	5.3	6.3	206.9	212	155.6	0.1086	0.1112	0.0824	-2.024	-1.785	-1.791
N10.40.725	E076.26.114	6.5	5.8	6.3	776	50.1	705	0.0307	0.0307	0.3746	-2.678	-1.283	-2.131
N10.45.025	E076.22.977	5.4	5	5.3	232.3	294.2	229.1	0.1217	0.1538	0.12	-4.882	-1.431	-1.756
N10.40.960	E076.20.286	5.6	5	5.7	251.8	228.9	52.7	0.1318	0.1199	0.0396	-2.136	-0.702	-2.261

Rare Earth Elements (REE) in ground water analyses

Rare earth elements (REE) occur mainly in naturally occurring minerals. These REE get released into groundwater by the process of weathering of rocks and minerals that will enhance the concentration of REE in groundwater. So the concentration of REE in groundwater is controlled mostly by the REE concentration of rocks, which interacts or resides for a long time. In the present study 17 water samples were collected and analysed for REE analysis Table 6.3. ΣREE values have positive relation with pH of water samples (Fig. 6.13). Few of the water samples showing anomalously high values are comparable with REE values of local rock sample REE values.

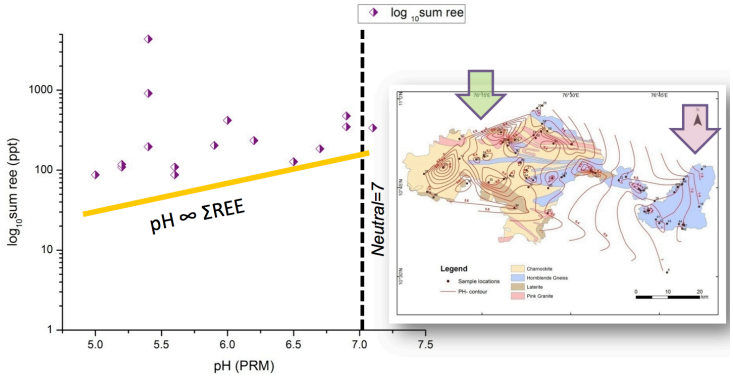

Fig. 6.14: Relation between ΣREE and pH of analysed water samples



Table 6.3: REE chemistry data for water samples

Sample No	Li 7Li ppt	Rb 85Rb ppt	Sr 86Sr ppt	Ba 135Ba ppt	La 139La ppt	Ce 140Ce ppt	Pr 141Pr ppt	Nd 146Nd ppt	Eu 151Eu ppt	Sm 152Sm ppt	Gd 158Gd ppt	Tb 159Tb ppt	Dy 163Dy ppt	Ho 165Ho ppt	Er 166Er ppt	Tm 169Tm ppt	Yb 172Yb ppt	Lu 175Lu ppt	Pb 208Pb ppt	Th 232Th ppt	U 238U ppt
1	432.2	6217	668800	254900		22.69	6.696	15.05	31.21	97.84	5.88	6.736	6.515	5.455	6.368	5.053	7.441	5.543	31.59	5.804	38.25
2	1538	3415	2443000	611700	58.23	11.49	7.469	31.05	66.67	226.4	3.834	0.542	3.312	1.02	3.152	0.504	4.35	1.081	27.37		250
3	469.7	1174	476200	305300	21.87	35.18	4.009	18.25	31.33	108.3	3.973	0.379	4.144	0.887	2.987	0.341	2.706	0.328	13.14		226.9
4	2261	1479	601500	490000	32.57	5.698	4.644	22.72	51.36	171.9	5.364	0.522	6.692	1.919	9.297	1.575	18.3	4.646	10.59		58.18
5	160.9	19080	688100	175200	6.869	7.759	0.819	4.016	18.15	61.53	0.43	-0.237	0.84	0.059	2.046	0.331	5.317	1.404	80.81		75.81
6	853.4	525.7	381800	239700		1.29	0.391	3.165	23.96	83.57	0.206	-0.338	0.307	-0.162	0.209	-0.247	0.342	-0.1	6.408		20.2
7	1419	10050	400500	240000		4.458	0.689	3.915	24.1	83.67	0.708	-0.166	0.958	0.292	2.553	0.591	8.729	2.323	27.13	0.166	33.13
8	590.6	964.1	501500	315300	20.32	1.65	2.619	12.34	32.48	108.9	1.697	-0.039	1.516	0.241	1.275	0.019	1.571	0.248	10.73		159.1
9	692.7	4089	220700	413100	9.108	2.576	0.842	6.698	41.53	140.1	1.029	-0.142	0.753	0.024	0.712	-0.096	0.648	-0.04	23.27		0.685
10	238.7	3765	252700	361800	37.64	32.92	12.3	65.01	39.03	132.7	10.59	0.875	6.615	1.475	4.432	0.459	4.338	0.601	30.83		0.197
14	196.9	3712	245800	417700	47.23	96.66	13.51	66.99	43.54	151.3	16.37	1.995	13.21	3.099	9.374	1.417	10.04	1.821	88.91	0.001	1.486
18	15450	17010	890600	155200	10.89	10.12	2.194	8.502	17.25	57.22	2.209	0.429	3.452	1.042	4.339	0.824	7.349	1.544	95.82	0.02	3270
22	119.3	4144	114700	69620	20.57	14.06	3.079	12.3	7.583	25.49	1.741	0.088	1.093	0.141	0.673	-0.032	0.499	0.012	75.27		4.298
26	136.6	2506	50500	74900	17.1	24.2	4.373	20.52	8.7	29.65	3.814	0.351	2.779	0.692	2.361	0.331	2.785	0.41	57.19	0.34	1.418
27	308.1	5170	30010	56730	203.5	131	64.21	286.1	16.09	68.43	44.39	5.838	34.11	8.074	23.59	3.245	20	3.282	46.07	0.718	0.332
31	415.4	3047	66140	100300	1319	1800	202.4	656.7	29.82	127.5	98.36	10.19	50	9.916	26.86	3.614	23.3	3.312	124	0.211	3.813
33	655.5	968.9	315900	183900	22.22	21.8	3.885	16.97	19.49	67.11	3.432	0.431	2.805	0.737	2.277	0.41	3.704	0.863	218.3	0.108	5.581

Chapter 7

Discussion and conclusion

Interpretations and evaluation of results are discussed in this chapter. Relation between rock and water chemistry is demonstrated. Contribution of rock towards water chemistry is also discussed

Chapter 7
Discussion and Conclusion

This study has attempted to understand and evaluate the influence of rocks and minerals to the variation in composition of groundwater. The contribution of rocks to the chemistry of groundwater depends on the residence time of water and the processes like weathering, involved in the release of constituents from rock into water. Petrology, rock chemistry and hydrogeochemistry have been done to study the rock-water interaction in detail and to characterize water.

From the petrographic studies, it is seen that the eastern part is dominated by hornblende-biotite gneiss and the western part by charnockite. The chemistry of minerals in charnockite indicates relatively high Fe composition with mainly pyroxene, biotite and amphibole as ferromagnesian minerals. Amphiboles are mainly magnesio-hornblende and plagioclase is Al rich. The SiO_2 content in the collected rock samples from the study area ranges from 52.39 to 71.16 wt.%. The spatial distribution of SiO_2 content in the study area is comparable with the distribution of K_2O content (1.43 to 6.39 wt. %). The MgO distribution (ranges from 0.29 to 4.89 wt.%) in the study region is found comparable with theCaO distribution (2.61 to 6.68wt.%) from the rock chemistry with low MgO and CaO contents in the eastern part. The Na_2O content in the collected rock samples varies from 3.06 to 5.27 wt.% and low-Na_2O contents are noticed in the north-eastern and north-western part of the study area.

The water chemistry analyses results show that the study region has pH ranging from 5.16 to 7.73, salinity varying from 0.03 to 0.50 PSU and alkalinity from 133.43 to 9828.62 μmol/L (Fig. 6.1). The eastern part of the study area has high in pH, salinity and alkalinity compared to western region. Variation in the spatial distribution of salinity and alkalinity are almost comparable in the study area. The low salinity in the western part of the study region compared to the eastern part is strange as the western part is closer to the coastal region. All pH, salinity and alkalinity spatial distribution

pattern especially the salinity and alkalinity can be found comparable with distribution of rock-types in the study region. The charnockite region is low in pH, salinity and alkalinity and hornblende-biotite gneiss region has high pH, salinity and alkalinity. The high pH and alkalinity of water samples from the eastern part of the study area can be attributed to the rock-types which include the presence of calc-silicate granulite and garnet-biotite-sillimanite-graphite gneiss in the north-eastern part of the study area which is highly elevated region (Fig. 7.1).

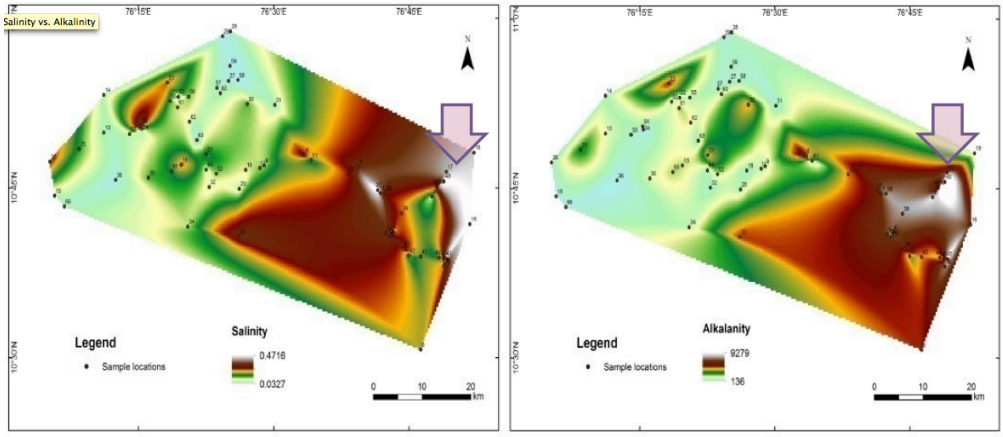

Fig. 7.1: Comparison of salinity and alkalinity of water samples from the study area

Variation in the spatial distribution of Mg (varies from 35.20 to 3718.08 µmol/L) was found comparable with Ca (50.34 to 5391.92 µmol/L) distribution in water chemistry, with high Mg and Ca content from the water samples collected from the easternmost part of the study area (Fig. 7.2). Similarly Si (ranges from 27.53 to 2306.35 µmol/L) distribution was comparable with Na (167 to 5110 µmol/L), having high Si and Na content samples from eastern part of the study region. The K content in the collected water samples from the study area varies from 0.15 to 6215.75 µmol/L.

The spatial distribution of Si found to be comparable from both rock chemistry (SiO_2) and water chemistry (Si) with high Si content in the eastern part of the study region (Fig. 7.2). The variation in the spatial distribution of Mg and Ca contents (MgO, CaO in rock chemistry; Mg, Ca in water chemistry) found different between rock and water chemistry. Rock chemistry shows high MgO and Cao in the western part and water chemistry suggests high Mg and Ca in eastern part of the study region. No clear

matching was found between K_2O and Na_2O distribution of rock chemistry from the study region with the K and Na distribution of water chemistry respectively (Fig.7.2). A comparison with the rock and water chemistry in the study area is given in Fig. 7.2. The figure shows that the silica concentration is high in water as well as the local rock around the eastern part of the study area. Calcium-high in the rock (western part) is not matching well with the calcium-high region (eastern part) in the water samples. This can be justified by the structural setting of the region. The eastern part of the study area consist of southward dipping rocks in the north and northward dipping rocks in the south, representing a analytical structure.

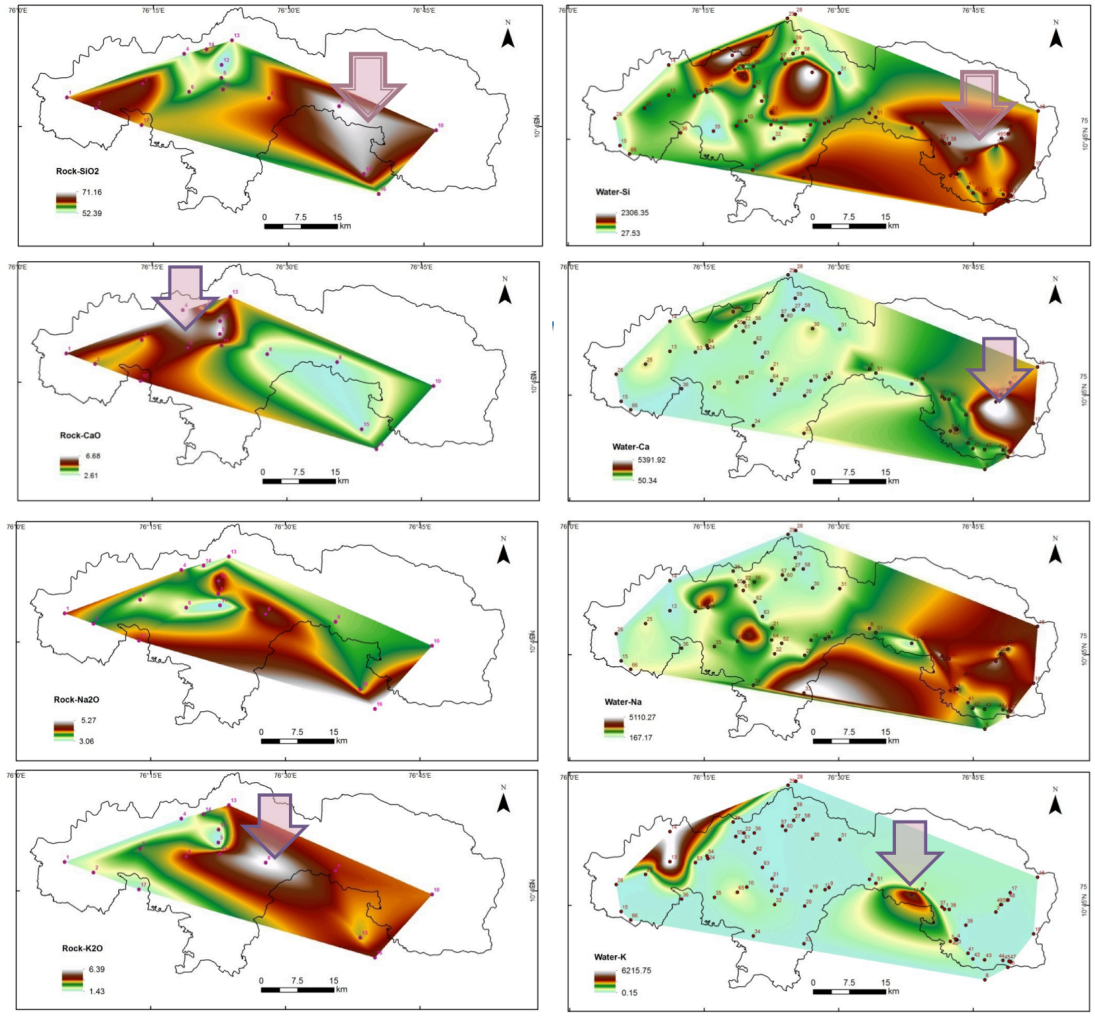

Fig. 7.2: Comparison for silica and alkali content in local rock and the water samples. *See text for description*

Calc-silicate and marble rocks are exposed well in the northern part while minor occurrences observed in the south. Thus there may be a layer of calc-silicate along the synclinal structure for the eastern part of the study area. High-calcium content and high salinity in water from eastern side can thus be justified with this presence of calc-silicate and/or marble in contact with water table. Oxygen isotope data also in good agreement with the cation composition of the water samples collected from the study area. The seasonal water samples show constant high in $\delta^{18}O$ values for the monsoon water samples compared to that of pre-monsoon and post-monsoon samples. The $\delta^{18}O$ values for that of marble samples from northern part of the study area (Walayar region) (unpublished data from Prof. M. Satish Kumar; personal communications) also shows depleted values (Fig. 7.3).

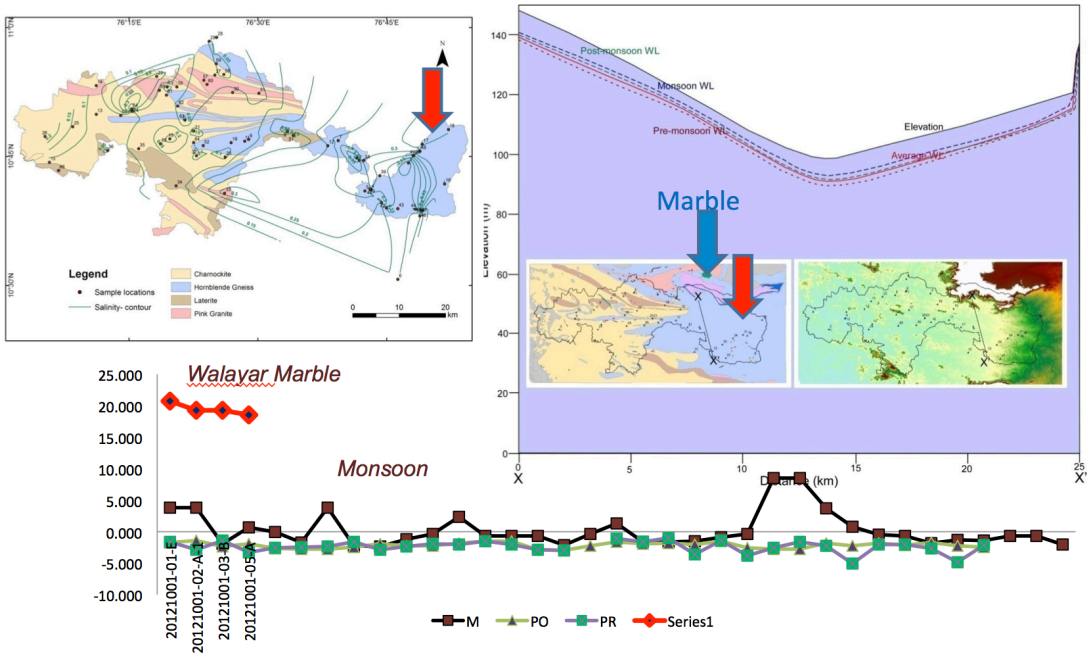

Fig. 7.3: Cross section of the study area with comparison to salinity and oxygen isotope results. *See text for discussion.*

When REE chemistry of water is normalized with local rock, most of it falls below 1 indicating the contribution of REE by rocks in to water (Fig. 7.4). Few high anomalies suggests external or anthropogenic source for REE in water. It is observed that the oxygen isotope of water varies extensively during different seasons. From all the

results and observations made from this study Water Quality Index for the study area is drawn and it is seen that most of the samples are suitable for drinking except one sample. The detailed structural maps of the region demonstrate a syncline thus explaining the range of alkalinity in the eastern and western part of the study area.

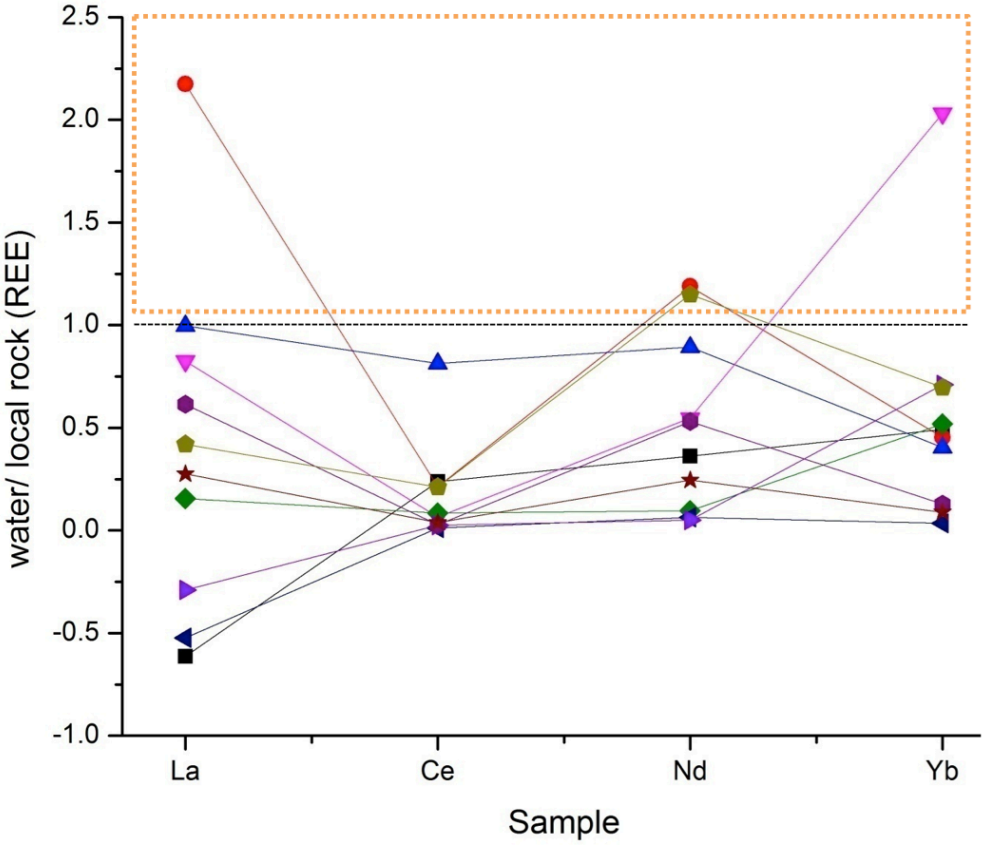

Fig. 7.4: A comparison of water REE normalized to local rock REE

Hydrogeochemical facies and Geochemical equilibria

The present study develops a hydrogeochemical facies in the western part of Palghat – Cauvery Shear Zone. The stability fields of crystalline minerals adequately serve as reference points to predict what minerals will react with groundwater and the direction and extent of the reactions. The Piper plot shows that most of the groundwater falls in the region of $CaHCO_3$ type and NaCl type and the tie line in between them (Fig. 6.9). The data points in Gibbs plot illustrates that most of the samples of Palakkad region fall in the water–rock interaction field. Due to the reaction between minerals in the rocks, Gibbs plot shows geochemical equlibria and

mechanism through the rock-water interaction controlling groundwater chemistry (Fig. 6.12). The derived hydrogeochemical facies of groundwater type is plotted in Fig. 7.5, shows an Si-Cl type mainly in the western part and Si-HCO3 or Ca-HCO3 type towards eastern part of the study area. There are also few locations showing Mg-Cl, Na-HCO3 and K-HCO3 type in the eastern region while K-Cl and Si-NO2 type in the west. This varion is also matching with the geology of the study area with charnockite dominant western region and hornblende-biotite gneiss dominant eastern region.

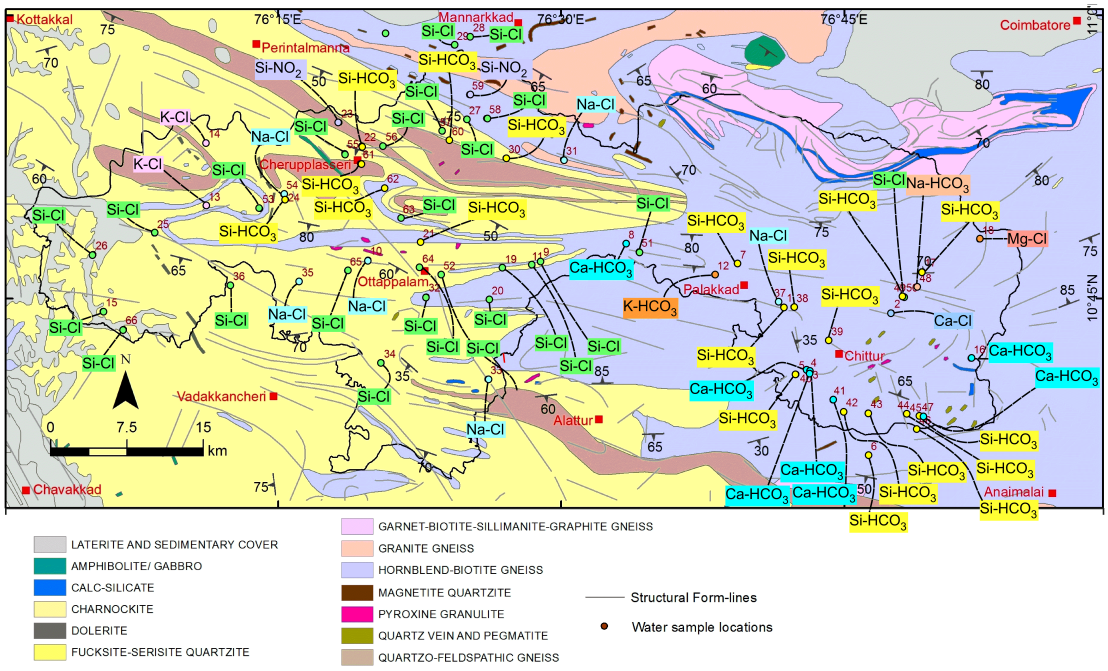

Fig. 7.5: Distribution of different water type in the study area. *See Annexure 2 for enlarged print*

Conclusions

The contour maps for salinity, alkalinity and pH establish the variation of these parameters in groundwater across the region. This will provide the preliminary indications for the contribution of rock types depending on the lithology. The comparison of major and trace element geochemistry of both water and rock samples indicates dissolution of ions from rock into water suggesting a strong influence rock on water chemistry. From the regional structural map of the study area clearly

establish a syncline structure in the region, explains the cause of alkalinity variation due to the layer of calc-silicates beneath the groundwater table. Based on the present results a hydrogeochemical facies for the western part of Palghat–Cauvery Shear Zone, around Palakkad district, a highly agriculture based region with high stress on groundwater consumption is developed for the first time. The current results also recommend future directions such as developing similar information on high-stress groundwater regions in the country especially in the agricultural affected regions of Kerala. Numerical modelling and future projections is also a potential area for research by using the present results of this study.

References

Apodaca, L.E., Jeffrey, B.B., Michelle, C.S., 2002.Water quality in shallow alluvial aquifers, Upper Colorado River Basin, Colorodo.Journal of theAmerican Water Resources Association. 38, 133–143.

Balakrishnan, P., Abdul Saleem and N.D., Mallikarjun., 2011. Groundwater Quality Mapping using Geographic Information System (GIS): A Case Study of Gulbarga City, Karnataka, India. African Journal of Environmental Science and Technology. 5, 1069-1084.

Balasubramanian, A., Sastri, J.C.V., 1994. Ground water resources of Tamarabarani River basin, Tamil Nadu, India, Inland Water Resources.484–501

Bhattacharya, S.K., Gupta, S.K., Krishnamurthy, R.V., 1985. Oxygen and hydrogen isotopic ratios in ground waters and river waters from India.Proceedings of Indian Academy Science.(Earth Planetary Science Section) 94: 283-295.

BinduKumari.,Saumitra., Mukherjee., Neha Singh., 2015. Groundwater Quality Assessment in hard rock terrain of part of Ranchi district, Jharkhand, India: An integrated approach. Volume 5, No 4, 2015ISSN 0976 – 4402.

Brijraj, K., Kaur, P. 2007. Geochemistry of surface and sub-surface waters of Rawalyar lakes, Mandi district, Himachal Pradesh: Constraints on weathering and erosion. Journal of the Geological Society of India. 69, 1020–1030,

Cederstorm, D.J., 1946. Genesis of groundwater in the coastal plain of Virginia. environmental Geology. 41,218–245.

CGWB., 1999, Groundwater Exploration in Kerala as on 31-3-1999, CGWB, Kerala Region, Trivandrum (Unpublished report).

Chan-Ho Jeong., 2001. Mineral-water interaction and hydrogeochemistry in the Samkwang mine area,Korea,Geochemical journal volume 35. 1-12.

Chidambaram S., Ramanathan AL., Srinivasamoorthy, K., 2003. Lithological influences on the groundwater chemistry—Periyar district a case study. In: Conference on coastal and freshwater issue. 173. 12, 625–636.

Chidambaram, S.,Bala Krishna Prasad, M., Manivannan.,R.Prasanna., M.V.Manikandan, S., 2013. Environmental hydrogeochemistry and genesis of fluoride in groundwaters of Dindigul district, Tamilnadu (India) Environmental Earth Science. 1866-6280, V68: 333–342.

Collins, A.S. Clark, C., Sajeev, K., Santosh, M., Kelsey., D.E., and Hand M., 2007. Passage through India: The Mozambique Ocean suture, high-pressure

granulitesand the Palghat-Cauvery shear zone system, Terra Nova. 19(2), 141–147.

Collins, A.S., Santosh, M. Braun, I., and Clark, C., 2007. Age and sedimentary provenance of the southern granulites, South India: U-Th-Pb SHRIMP secondary ion mass spectrometry, Precambrian Research, 155, 125–138.

Comly, H.H., 1945. Cyanosis in infants caused by nitratesin well water.Journal of the American Medical Association, 129, 12–114.

Das, B.K., Kaur, P. 2001 Major ion chemistry of Renukalake and weathering processes, Sirmaur district, Himachal Pradesh, India.Journal of Environmental Geology. 40, 908–917.

Datta, P.S., Tyagi, S.K., 1996. Major ion chemistry of groundwater in Delhi area: Chemical weathering processes and groundwater regime. Journal of the Geological Society of India, 47, 179–188.

Devadas, D. J., Rao, N. S., Rao, B. T., Rao, K.V.S., Subrahmanyam, A., 2007. hydrogeochemistry of the Sarada river basin, Visakhapatnam district, Andhra Pradesh, India. Environmental Geology. 52, 1331–1342.

Drury, S.A., Holt R. W.1980. The tectonic framework of the South Indian craton: A reconnaissance involving LANDSAT imagery, Tectonophysics. 65, T1–T15.

Dwivedi, S. L. and Pathak, V. 2007. A preliminaryassignment of water quality index to Mandakini river, Chitrakoot. Indian Journal of Environmental Protection, 27, 1036-1038

Elango L, Kannan R, Senthil Kumar M., 2003, Major ion chemistry and identification of hydrogeochemical processes of ground water in a part of Kanchipuram District, Tamil Nadu, India. Environmental Geosciences,10, 157- 166.

Elango, L., Kannan, R., Senthil Kumar, M., 2003. Major ion chemistry and identification of hydrogeochemical processes of groundwater in a part of Kancheepuram district, Tamil Nadu. Environmental Geosciences, 1, 157–166.

Elango, L., Kannan, R., SenthilKumar,M. 2003, .Major ion chemistry and identification of hydrogeochemical processes of groundwater in a part of Kancheepuramdistrict, TamilNadu, India. Journal of Environmental Geoscience. 10, 157–166.

Fermor, L.L., 1936. An attempt at the correlation of the ancient schistose formations of peninsular India. Memoir Geological Survey of India, 70,1-324.

Fisher, S. R., Mullican, W. F. 1997. Hydrogeochemical evolution of sodium-sulphate and sodium-chloridegroundwater beneath the northern Chihuahua desert, Trans-Pecos, Texas, U.S.A. Hydrogeology Journal. 5, 4–16.

Garrels, R. M., Mackenzie, F.T., 1971. Evolution of sedimentary rocks. New York: WW Norton.

Ghosh, J.G., M.J.D. Wit, R.E. Zartman., 2004. Age and tectonic evolution of Neoproterozoic ductile shear zones in the Southern Granulite Terrain of India, with implications for Gondwana studies, Tectonics. 23, 1–38,.

Gibbs, R.J., 1970. Mechanisms controlling world water chemistry. Science Journal, 170, 795–840.

Gilly, G., Corrao, G., &Favilli, S. 1984. Concentrationsof nitrates in drinking water and incidence of gastriccarcinomas. First descriptive study of the PiemonateRegion, Italy.The Science of the Total Environment.34, 35–37.

Gowd S., 2005. Assessment of groundwater quality for drinking and irrigation purposes: a case study of Peddavanka watershed, Anantapur District, Andhra Pradesh, Indian Journal of Environmental Geology. 48, 702-712.

Harris and Jayaram.,N.B.W., 1982. Metamorphism of cordierite gneisses from the Bangalore region of the Indian ArchaeanLithos.15, 89-98.

Hem, J.D.,1985.Study and interpretation of the chemical characteristics of natural water (3rd ed.).U.S. GeologicalSurvey Water-Supply Paper, 2254, 263.

Ishwar-Kumar, C., Windley, B.F., Horie, K., Kato, T., Hokada, T., Itaya, T., Yagi, K., Gouzu, C., Sajeev, K., 2013. A Rodinian suture in western India: New insights on India-Madagascar correlations. Precambrian Research 236, 227-251.

Jankowski.J. Acworth, R.I., 1997. Impact of debris flow deposits on hydrogeochemical process and thedevelopment of dry land salinity in the YassRivercatchment, New South Wales, Australia.Hydrogeology Journal. 5, 71–88.

Jayananda, M., Janardhan, A.S., Sivasubramaniam, P., Pencay, J.J. 1995.Geochronologic and istopicconstraintson granulite formation in the Kodaikanalarea,Southern India. Journal of the Geological Society ofIndia. 34, 373–390.

Jeong, C.H. 2001. Effect of land use and urbanization on hydrochemistry and contamination of groundwater from Taejon area, Korea. *Journal of Hydrology*. 253, 194–210

Karanth, K.R., 1987. Groundwater assessment, development and management: Tata McGraw-Hill publishing Company Limited, New Delhi. 720p.

Katz, B.G., Gopalan, T.B., Bullen, T.D., Davis, J.H., 1998. Use of chemical and isotopic tracers to characterisethe interaction between groundwater and surface water in mantled karst. Groundwater Journal. 35, 1014–1028.

Kumar, S., S. Wesnousky, T. Rockwell, W. Briggs, V. Thakur, R. Jayangondaperuma 2005 Paleoseismic evidence of great surface rupture earthquakes along the Indian Himalayan Journal of Geophysical Research. 111 p. B03304, 10.1029/2004JB003309.

Lamb R, Crossley A, Waller S. 2009. A fast two-dimensional floodplain inundation model.Proc ICE Water Manag, 162: 363–370.

Laluraji, C. M., &Gopinath, G. 2000 Assessment onseasonal variation of groundwater quality of phreaticaquifers—a river basin system. Environmental Monitoring and Assessment, 117, 45–57.

Mahesa ,A. Balasubramanian.,2008.Hydrogeochemical studies of Dalvoy lake ecosystem of Mysore city India. Proceedings of Tal 2007: The 12th world lake conference. 337-341.

Mamatha, P.S.M. Rao 2010.Geochemistry of fluoride rich groundwater in Kolar and Tumkur districts of Karnataka Environmental Earth Sciences. 61, 131–142

Mathess, G., 1982.The properties of groundwater, John Wiley, New York.406.

Matthess, G., 1982.The properties of groundwater. Wiley, New York. p 498,

Mayo, A.L., Loucks, M. D. 1995. Solute and isotopicgeochemistry and groundwater flow in theCentralWasatch Range, Utah. Journal of Hydrology (Amsterdam). 172, 31–59.

Mohan, R., Singh, A. K., Tripathi, J. K., Chowdhary,G. C. 2000. Hydrochemistry and quality assessment of groundwater in Naini industrial area, Allahabad.

Nair NGK., et. al., 2000 Alkali granite-syenite-carbonatite association inMunnar Kerala, India;implications for rifting, alkaline magmatism and liquid immiscibility. Journal of Earth Systam Sciences, 99,149–158.

Narayanaswamy, S. 1976. Structure and tectonics of the Achaean crystalline rocks of Kerala. Proceedings of the Seminar on Geology and Geomorphology of Kerala. Geological Survey of India, 68-70.

Nishimiya Y., Tsunogae T., Santosh M. 2008. Petrology and fluid inclusions of garnet-clinopyroxene rocks from Paramati in the Palghat Cauvery shear zone system, Southern India. Journal of Mineralogical and Petrological Sciences 103, 354-360.

Pacheco, F.A.L., Van der Weijden, C.H., 1998. Contributions of water-rock interactions to the composition of groundwater in areas with sizeable anthropogenic input. A case study of the waters of the Fundão area, central Portugal. Water Resources, 32, 3553–3570.

Pandian, K., Shankar., 2007. Hydrochemistry and groundwater quality in the Vaipar river basin, Tamil Nadu.Journal of Geological Society of India, 69.970-982.

Piper, A.M., 1944. A graphic procedure in the geochemical interpretation of water analysis. Transactions of American Geophysical Union, 5, 914-928.

Plavsa, A.S. Collins, J.F. Foden, L. Kropinski, M. Santosh, T.R.K. Chetty, C. Clark. D., 2012. Delineating crustal domains in Peninsular India: age and chemistry of orthopyroxene-bearing felsic gneisses in the Madurai Block Precambrian Research, 198-199. 77-93

Pophare, M.A. and Dewalkar, S.M. 2007. Groundwater quality in eastern and south eastern parts of Rajura Tehsil, Chendrapur district, Maharashtra. Gondwana Geol. Mag. Spec. 11, 119-129.

Rai, S.S., Srinagesh, D., Gaur, V.K., 1993. Granulite evolution in South India— a seismic tomographic perspective. Geological Society of India Memoir. 25, 235–263.

Raju, N.J., 2007. Hydrogeochemical parameters for assessment of groundwater quality in the upper Gunjanaeru River basin, Cuddapah District, Andhra Pradesh, South India. Environ Geol 52: 1067-1074.

Raith and Harley, J.G. Raith, S.L. Harley., 1998. Low-P/high-T metamorphism in the Okiep Copper district, western Namaqualand, South African Journal of Metamorphic Geology, 6, 281-305.

Rajmohan N, Elango L., 2004. Identification and evolution of hydrogeochemical processes in the groundwater environment in an area of the Palar and Cheyyar River Basins, Southern India. Environmental Geology, 46, 47–61.

Rammohan, H. S. 1984. A climatological assessment of water recourses of Tamil Nadu.Indian Journal of Power and River Valley Development. 34, 58–63.

Reddy, A.G.S., Niranjan, K.K., 2010. Identification of the hydrogeochemical processes in groundwater using major ion chemistry: a case study of Penna–Chitravathi river basins in Southern India November 2010. 170, 365–382.

Reddy, A.G.S., Niranjan, K.K., Subba, R.D., Sambashiva, R. S., 2009.Assessment of nitrate contamination due to groundwater pollution in north eastern part of Anantapur District, AP India. Environmental Monitoring and Assessment.148, 463–476.

Reddy, N.B.Y., Prasad, K.S.S., 2005.Hydrogeochemistry of groundwater in and around Tadpatri area, Anantapuir district, AP. Journal of Indian Association of Environmental Management. 32, 66–73.

Renie, Verweij, 2003. A new index for determining amount of Calcium carbonate scale formed by water. Journal of American Water Assn., 36,. 472-486.

Sajeev, K**.,** Windley, B.F., Connolly J.A.D., Kon Y., 2009. Retrogressed eclogite (20 kbar, 1020ºC) from the Neoproterozoic Palghat-Cauvery suture zone, southern India. *Precambrian Research.* 171, 23-

Sajeev, K., Osanai, Y., Kon Y., Itaya, T., 2009. Stability of pargasite during ultrahigh-temperature metamorphism: A consequence of titanium and REE partitioning? American Mineralogist, 94, 535–545.

Sami,K., 1992. Rechargemechanisms and geochemical processesin a semi-arid sedimentary basin, Eastern Cape, South Africa. Journal of Hydrology (Amsterdam). 139, 27–48.

Santosh, M., Sajeev, K**.,** Li, J.H., Liu, S.J., Itaya T., 2009. Counter clockwise exhumation of a hot orogen: The Paleoproterozoic ultrahigh-temperature granulites in the North China Craton. *Lithos* v. 110, p. 140–152.

Sarin, M. M., Krishnaswamy, S., Dilli, K., Somayajulu,B. L. K., Moore, W. S. 1989. Major ion chemistry of the Ganga-Brahmaputra river system: Weatheringprocess and fluxes to the Bay of Bengal. Geochimica et Cosmochimica Acta, 53, 997–1009.

Saxena, V.K., Ahamed S.,2001.Dissolution of fluoride in groundwater :water rock interaction study. Environmental geology. 40,1084-1087.

Schoeller, H., 1965. Qualitative evaluation of groundwater resources. In Methods and techniques of groundwater investigations and development. 54–83.UNESCO.

Schoeller, H., 1967. Geochemistry of groundwater—an international guide for research and practice . Chapter. 15. 1–18. UNESCO.

Shaji, E, Bindu, J.Viju and D.S.Thambi.,2007. High fluoride in ground water of Palghat District, Kerala. Current Science, 92, 240-245.

Simeonov,P.,Einax,J., Stanimirova., Kraft J., 2002. Environmetric modelling and interpretation of river water monitoring data Analytical and Bioanalytical Chemistry, 374 (5) 898-905.

Simões, C., Batista-Foguet, J.M., Matos, M.G. L. 2008, CalmeiroAlcohol Use and Abuse in Adolescence: Proposal of an Alternative Analysis. Child: HealthCare and Development, 34, 301-391.

Singh, P. K., Amrita, M., Dinesh, M., Vinod, K. S., and Singh, S. 2006. Evaluation of groundwater qualityin northern Indo-Gangetic alluvium region.EnvironmentalMonitoring and Assessment, 112, 211–230

Sridhar, S.G.D. Kanagaraj, G. Mahalingam, S and Amaladas, P., 2013. Hydro chemical analysis of groundwater between Sadras and Chinnakuppam, Kancheepuram District, Tamil Nadu, India. Journal of Academia and Industrial Research. 2,160-166.

Srinivasamoorthy K, Chidambaram S, Vasantavigar M, Prasanna.V., John. P., 2007. Geochemistry of Fluorides in groundwater of Salem district, Tamil Nadu, India, Indian Journal of Geochemistry. 22, 237-246.

Srinivasamoorthy, K,S.Chidambaram and M.Vasanthavigar.,2008. Geochemistry of fluorides in groundwater, Salem District, TamilNadu, India. Journal of .Environmental Hydrology. Volume.16: Paper 25.

Srinivasamoorthy, K.S., Chidambaram, V.S., Sarma, M., Vasanthavigar,K., Vijayaraghavan, Rajivgandhi, P., Anandhan, R. Manivannan., 2009. Hydrogeochemical characterization of groundwater in Salem District of Tamil Nadu, India. Research Journal of environmental of Earth Sciences. 1, 22-23.

Stallard, R. F., Edmond, J. M., 1983. Geochemistry of the Amazon, the influence of geology and weathering environment on the dissolved load. Journal of Geophysical Research, 88, 9671–9688.

Stoner, J. D. 1972 Determination of mass balance and entrainment in the stratified Duwamish River estuary, King County, Washington. United Stales Geological Survey Water Supply Paper 1873-C,74 .

SubbaRao, N., 2011. High-fluoride groundwater. Environ. Monit.Assess., 176, 637-645

SubbaRao N., 2003. Groundwater quality: focus on fluoride concentration in rural parts of Guntur districts, Andhra Pradesh, India. Hydrology Science Journal 48, 835–847.

SubbaRao, N. 2006. Seasonal variation of groundwater quality in a part of Guntur district, Andhra Pradesh, India. Environmental Geology. 49, 413–429.

Subramani, T, Elango, L., Damodarasamy, S.R., 2005. Groundwater quality and its suitability for drinking and agricultural use in Chithar River Basin, Tamil Nadu, India, International Journal of Environmental Geology. 47, 1099-1110

Subramani, T, Rajmohan, N., Elango, L., 2010. Groundwater geochemistry and identification of hydro geochemical processes in a hard rock region, Southern India', Environmental Monitoring Assessment.162, 123-137.

Subramani, T., 2005.Hydrogeology and identification of geochemical processes in Chithar River Basin, Tamil Nadu, India. Ph.D. Thesis, Anna University, Chennai, India.

Subramani, T., Elango, L., &Damodarasamy, S. R. 2005a. Groundwater quality and its suitability fordrinking and agricultural use in Chithar River basin,Tamil Nadu, India. Journal of Environmental Geology. 47, 1099–1110.

Subramani, T., Elango, L., Srinivasalu, S., Marikio, T.2005b. Geological setting and groundwater chemistry in Chithar River basin, Tamil Nadu, India. Journal of Indian mineralogist. 39, 108–119.

Thompson, S. E., Harman, C., Schumer, R., Wilson, J., Basu, N.,Brooks, P., Donner, S., Hassan, M., Packman, A., and Rao, P.:2011Patterns, puzzles and people: implementing hydrologicsynthesis, Hydrol. Process., 25, 3256–3266.

Tood D.K., 1980. Groundwater hydrology, 2nd edition, New York, John Wiley and sons.

Tweed, S.O., Weaver, T.R., Cartwright, I., and Schaefer, B., 2006. Behavior of rare earth elements in groundwater during flow and mixing in fractured rock aquifers: an example from the Dandenong Ranges, southeast Australia. Chemical Geology, 234, 291-307.

Tweed, S.O., Weaver, T.R., Cartwright, I., Schaefer, B., 2006. *Behaviour of rare earth elements in groundwater during flow and mixing in fractured rock aquifers: an example from the Dandenong Ranges, southeast Australia.* Chemical Geology, 234, 291-307.

WHO 1993 Drinking Water Quality Guidelines (3 volumes), Geneva: World Health Organisation• World Health Organization – World Water Day 2001 – Naturally Occurring Hazards.1-8.

WHO (World Health Organization) 1996. Guide lines for drinking water quality Geneva, 2, 231-237.

WHO .1994 Fluoride and oral health. Geneva: WHO Technical ReportSer 846

WHO 1996.Guideline for drinking water quality. Geneva World Health Organization.

WHO 2008.vGuidelines for drinking-water quality (3rd edition.). Geneva: World Health Organization.

WHO 2000. Fluoride in drinking water, Draft II.RetrievedAugust 26, 2002 from http:/www.who/int 190 /environmental information / information resources / htm does/ fluoride/ fluoride.html.

WHO 1970. Fluoride and Human Health, Monograph series, Geneva, World Health Organization. No. 59, 225-271.

WHO .1971. International drinking water standards, World Health Organizations.

Wilcox, L.V., 1955. Classification and use of irrigation waters.US.Department of Agriculture Circular No. 969. Washington, D.C.19.

World Health Organization, WHO 2004.―Guidelines for drinking water quality‖ Geneva.

WHO 1984. Guidelines for drinking water quality‖ Geneva Volume.1-30.

Yoshida, M., 1992. Precambrian tectonothermal events ineast Gondwana land crustal fragments and their correlation (IGCP-288), In R. Tsudhi (Edition.), Japan contribution to the IGCP 51–62. Osaka.

Zheng, J., Chai, F., Yang, F., Meng, Q., Li, Q., 2017. Geology, genesis, and geodynamic setting of Cihai: An Early Permian diabase-hosted skarn iron deposit in the eastern Tianshan, Northwest China: International Geology Review, 1–18.

Zhenghui et al., 2012. Groundwater and the environment: Applications for the global community, Boca Raton: Lewis. . 175

Annexure 2

Pie diagram of water geochemistry

1

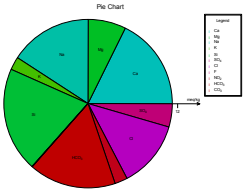
Pie Chart
Legend
Ca
Mg
Na
K
Br
SO_4
Cl
F
NO_3
HCO_3
CO_3
meq/lg
1
0

2

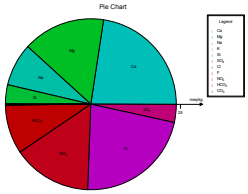
Pie Chart
Legend
Ca
Mg
Na
K
Br
SO_4
Cl
F
NO_3
HCO_3
CO_3
meq/lg
1
0.5

3

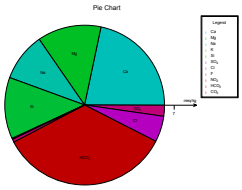
Pie Chart
Legend
Ca
Mg
Na
K
Br
SO_4
Cl
F
NO_3
HCO_3
CO_3
meq/lg
1
0

4

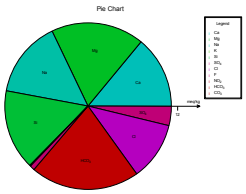
Pie Chart
Legend
Ca
Mg
Na
K
Br
SO_4
Cl
F
NO_3
HCO_3
CO_3
meq/lg
1
0

5

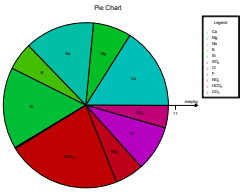
Pie Chart
Legend
Ca
Mg
Na
K
Br
SO_4
Cl
F
NO_3
HCO_3
CO_3
meq/lg
1
0.5

6

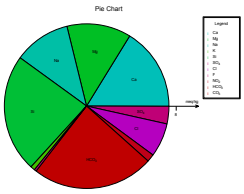
Pie Chart
Legend
Ca
Mg
Na
K
Br
SO_4
Cl
F
NO_3
HCO_3
CO_3
meq/lg
1
0

7

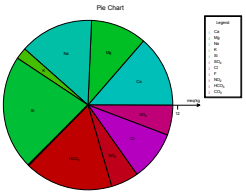
Pie Chart
Legend
Ca
Mg
Na
K
Si
SO4
Cl
F
NO3
HCO3
CO3
Na
Mg
Ca
Si
SO4
Cl
NO3
HCO3
CO3
mmol/kg
12

8

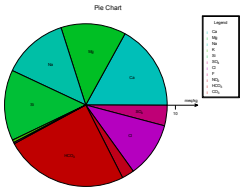
Pie Chart
Legend
Ca
Mg
Na
K
Si
SO4
Cl
F
NO3
HCO3
CO3
Na
Mg
Ca
Si
SO4
Cl
HCO3
mmol/kg
10

9

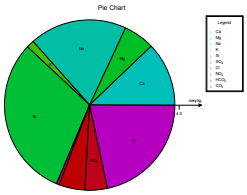
Pie Chart
Legend
Ca
Mg
Na
K
Si
SO4
Cl
F
NO3
HCO3
CO3
Na
Mg
Ca
Si
Cl
mmol/kg
4.5

10

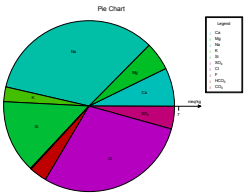
Pie Chart
Legend
Ca
Mg
Na
K
Si
SO4
Cl
F
NO3
HCO3
CO3
Na
Mg
Ca
K
SO4
Si
Cl
mmol/kg
1

11

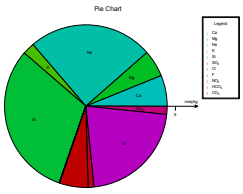
Pie Chart
Legend
Ca
Mg
Na
K
Si
SO4
Cl
F
NO3
HCO3
CO3
Na
Mg
Ca
Si
Cl
mmol/kg
6

12

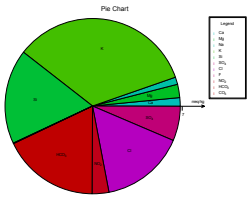
Pie Chart
Legend
Ca
Mg
Na
K
Si
SO4
Cl
F
NO3
HCO3
CO3
Na
Mg
Ca
Si
SO4
Cl
HCO3
NO3
mmol/kg
7

13

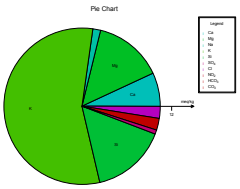

14

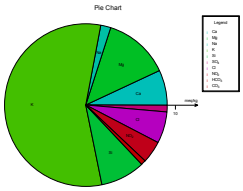

15

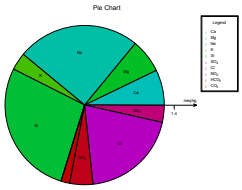

16

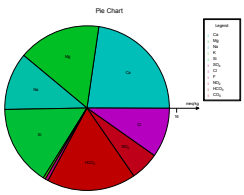

17

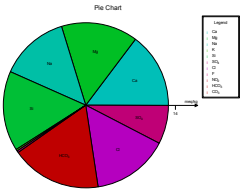

18

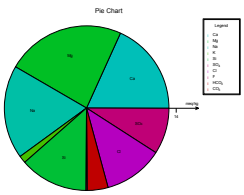

19

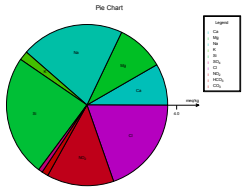

20

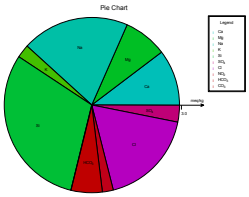

21

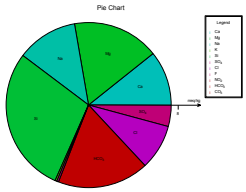

22

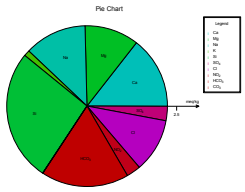

23

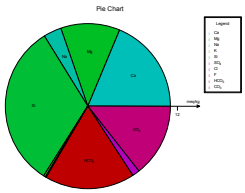

24

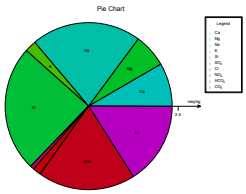

25

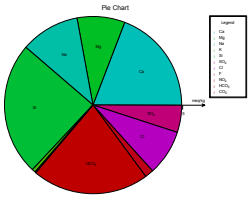

26

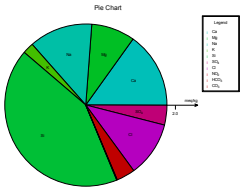

27

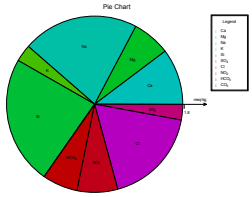

28

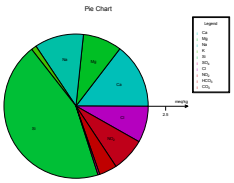

29

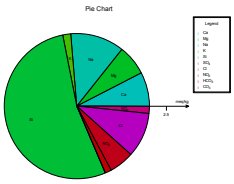

30

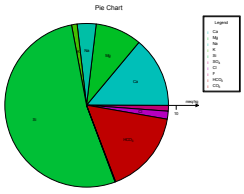

31

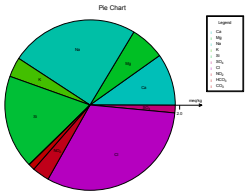

32

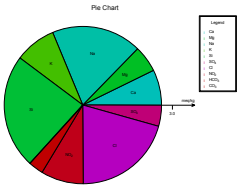

33

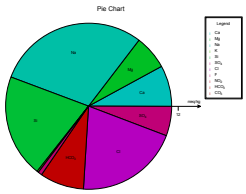

34

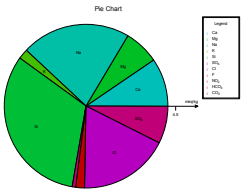

35

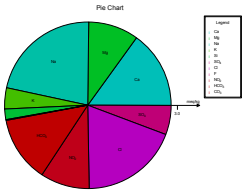

36

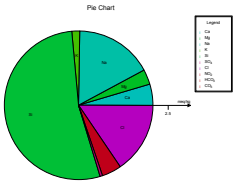

37

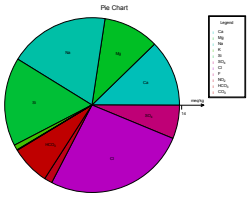

38

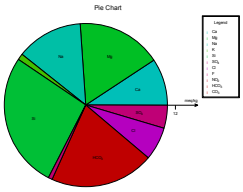

39

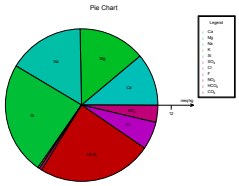

40

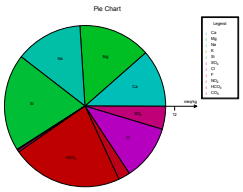

41

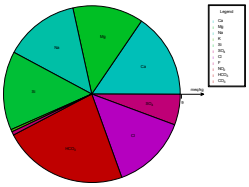

42

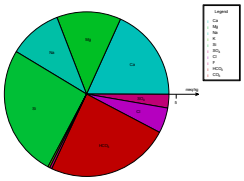

43

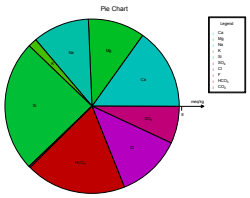

44

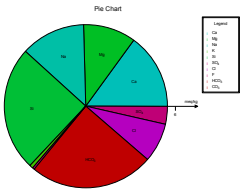

45

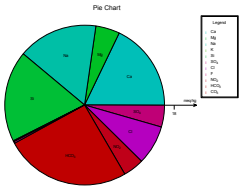

46

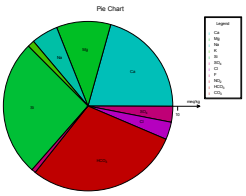

47

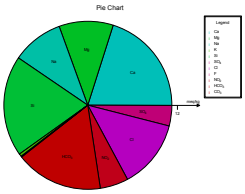

48

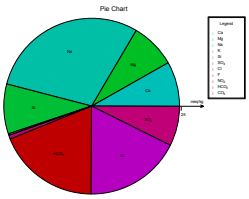

49

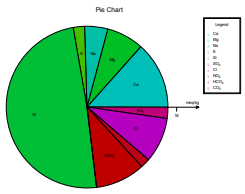

50

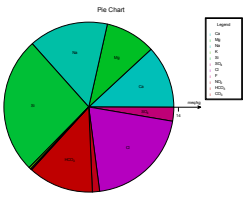

51

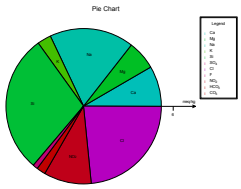

52

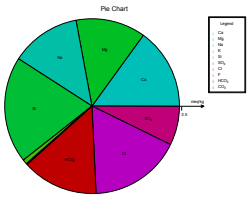

53

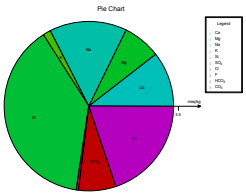

54

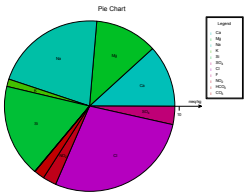

55

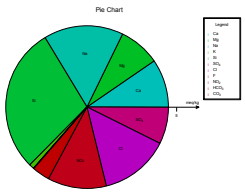

56

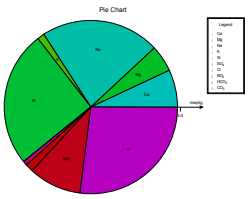

57

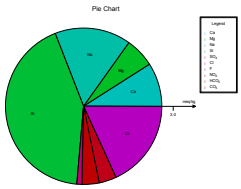

58

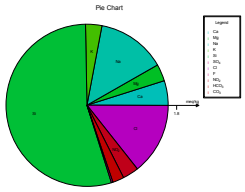

59

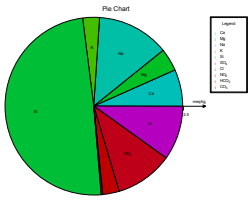

60

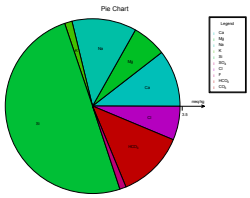

61

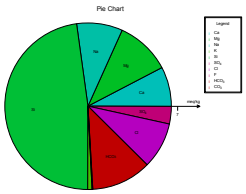

62

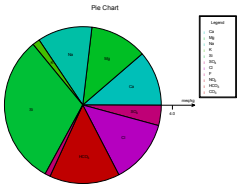

63

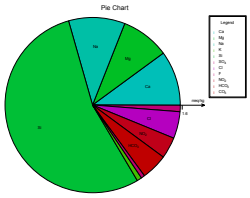

64

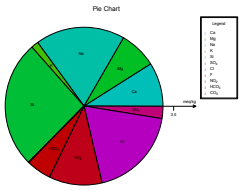

65

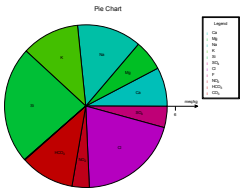

66

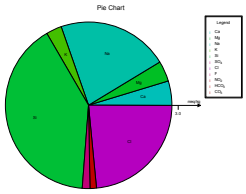

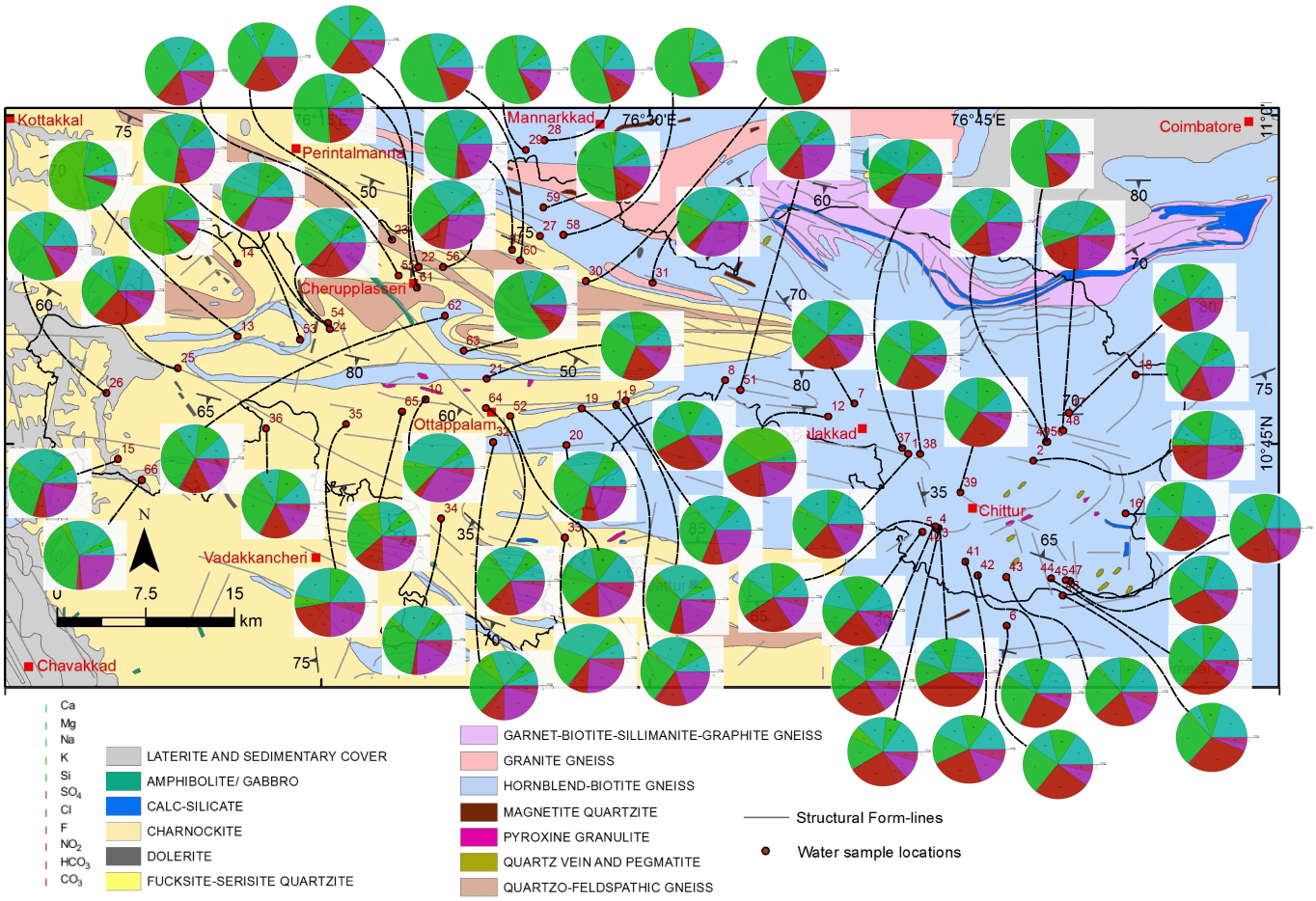
Kottakkal
Perintalmanna
Mannarkkad
Cherupplasseri
Ottappalam
Vadakkancheri
Chavakkad
Chittur
Coimbatore
76°30'E
76°45'E
10°45'N
11°0'N
N
0
7.5
15
km
Ca
Mg
Na
K
Si
SO4
Cl
F
NO2
HCO3
CO3
LATERITE AND SEDIMENTARY COVER
AMPHIBOLITE/ GABBRO
CALC-SILICATE
CHARNOCKITE
DOLERITE
FUCKSITE-SERISITE QUARTZITE
GARNET-BIOTITE-SILLIMANITE-GRAPHITE GNEISS
GRANITE GNEISS
HORNBLEND-BIOTITE GNEISS
MAGNETITE QUARTZITE
PYROXINE GRANULITE
QUARTZ VEIN AND PEGMATITE
QUARTZO-FELDSPATHIC GNEISS
Structural Form-lines
Water sample locations

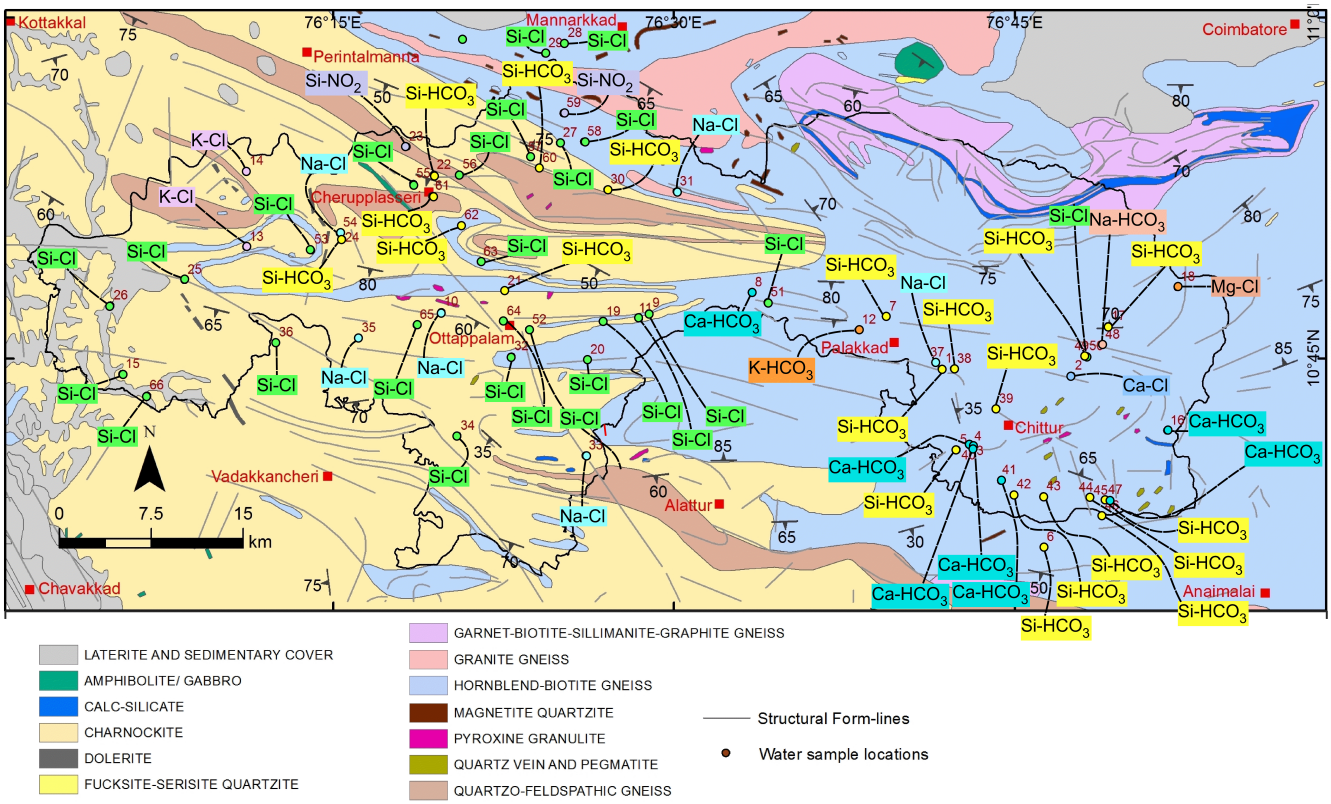
Kottakkal
Perintalmanna
Mannarkkad
Coimbatore
Cherupplasseri
Ottappalam
Palakkad
Chittur
Vadakkancheri
Alattur
Chavakkad
Anaimalai
76°15'E
76°30'E
76°45'E
11°0'N
10°45'N
0
7.5
15
km
N
LATERITE AND SEDIMENTARY COVER
AMPHIBOLITE/ GABBRO
CALC-SILICATE
CHARNOCKITE
DOLERITE
FUCKSITE-SERISITE QUARTZITE
GARNET-BIOTITE-SILLIMANITE-GRAPHITE GNEISS
GRANITE GNEISS
HORNBLEND-BIOTITE GNEISS
MAGNETITE QUARTZITE
PYROXINE GRANULITE
QUARTZ VEIN AND PEGMATITE
QUARTZO-FELDSPATHIC GNEISS
Structural Form-lines
Water sample locations